Pyroptosis and Pyroptosis-Like:

Two stories of macrophage death against bacterial invaders

A thesis submitted by

Beiyun C. Liu

in partial fulfillment of the requirements for the degree of

Ph.D.

in

Immunology

Tufts University

Sackler School of Graduate Biomedical Sciences

February 2018

Advisors: Ralph R. Isberg, Ph.D. & Alexander Poltorak, Ph.D.

Abstract

The re-discovery of caspase-11 led to the refinement of the functions of both caspase-11 and caspase-1. The current consensus is that caspase-11 is both the initiator and executioner caspase for cell death upon binding by bacterial lipopolysaccharide present in the cytosol. Caspase-1, on the other hand, is the executioner caspase for cleavage and activation of various IL-1 family of cytokines. The actions of both caspases complete the host defense mechanism of pyroptosis, defined as a necrotic cell death process with concomitant release of mature IL-1 cytokines. Upstream and downstream players in the caspase-11 cascade have also been elucidated in rapid succession. The activation of caspase-11 upon Gram-negative bacterial infection require a family of proteins known as the Guanylate Binding Proteins (GBPs). Downstream of caspase-11, the pore forming protein GasderminD (GsdmD) oligomerizes to form plasma membrane pores, resulting in cell death. Detailed in this dissertation are two projects that I investigated on macrophage pyroptosis against two different bacterial pathogens. In the first project, I built upon existing knowledge of GBPs to refine their role and placement in the initiation of cytosolic pathogen sensing. Here, I used a mutant of *Legionella pneumophila* that shows inadvertent cytosol permeability to model the initial response of a naïve macrophage to cytosol bacterial presence. I report that low levels of GBP expression are maintained by quiescent Interferon signaling, and is crucial for the timely release of bacterial contents to initiate downstream immune responses. In the second project, I explored the morphology of a rapid, necrotic cell death phenotype mediated by caspase-8 during *Yersinia* species infection. Using *Y. pseudotuberculosis* in conjunction with a small molecule inhibitor to mimic the virulence factor YopJ, I found that caspase-8 activation induced the cleavage of multiple gasdermins, resulting in a pyroptotic-like cell death morphology and IL-1 release. I am glad to have been able to first amend and then to add to our understanding of this rapidly evolving field of host defense known as pyroptosis.

Acknowledgments

Ralph and Sasha have both independently told me, more than once, that a number of my behaviors during grad school were unprecedented. It may be to their chagrin that their attempt at guilt functioned to vastly encourage me. In fact, their reluctance at having me be distracted from my first project resulted in my deep involvement in four projects, two of which you will read about in this document. Much like growing up in a divorced household, my experience lacked neither frustration nor freedom. Freedom since for the most part, I was able to convince at least one of the two to invest in what I wanted to work on. Frustration since for the most part, there was constant misunderstanding from one or both on what I was actually working on, as I was truly handicapped at staying interested in one thing at a time. And much like a rebellious child, I have both of my mentors to thank for my scientific traits.

The mentorship from Ralph during my formative years were irreplaceable. He was, and remains, constantly critical of a new finding, yet surprisingly encouraging of a null result. This balance, as I appreciated over time, is what promotes truth-seeking in scientific research. It was under those early years of Ralph's tutelage that I came to understand the concept of scientific stringency and to embrace it. Today, I want to believe that I can design a well-controlled experiment in my sleep.

As I became a scientific "teen", the freedom offered by Sasha enabled me to step into the next phase of my development. In fact, Sasha sponsored the project that initially was started as a distraction from paper writing. And what's a better way to get distracted than by receiving tantalizing pieces of experimental data from your best friend? This brings me to the next critical person in my training: my scientific twin Joseph Sarhan. Joe and I were constantly bouncing ideas off of each other in both of our original projects. We got so good at ideas juggling, that it is now impossible to separate who came up with what for the second story in this thesis. It is a true incarnation of equal contribution. Poor Sasha therefore had two unruly, unprecedented students rather than one. Nevertheless, he allowed our science to develop into the way it has. And when he resisted, we had Irina Smirnova as another pair of ears to hear our pleas for reagents, and to help us deter Sasha from taking the wrong students.

Speaking of younger students, I had the pleasure of training three promising younglings during my "tenure" at Tufts: Hayley Muendlein, Amy Tang, and Rachael Nilson. Experiencing their development has taught me valuable lessons on how to be an effective mentor, and I look forward to how each of them will grow. My involvement with their scientific progress was also one of the factors that convinced me to stay in academia at a time when I was seriously contemplating on jumping ship to industry. The other proponent came in the form of an unexpected conference. In November of 2016, Ralph took me to one of his last HHMI meetings. There, I had the opportunity to converse with many of the scientists whose work I follow, amongst them was Dr. Feng Shao. After seeing my work, Feng offered an opportunity of joint submission. I was deeply honored and encouraged by his offer, although I felt that my work would not have been able to live up to his. As it turns out, the story he was working on at the time is one that will usher in a new era: he had discovered, using *Shigella flexneri*, one of the first examples of cytosolic resident bacteria directly degrading GBPs to avoid capture.

If November 2016 was when I was coaxed back from jumping off the academia ledge, I had to very seriously figure out if academia is the right place for me. Two additional scientists solidified that choice. They were Dr. Robert Watson of Texas A&M and Dr. Doug Green of St. Jude Children's Research Hospital. Conversing with them was emboldening. They made me feel that if it's something I can think of, it's something I can do. My inner engine for the year of 2017 was thus revved by these three pillars of ambition, and then fueled by the insatiable drive from myself and Joseph for more data deeper into the unexplored. And here we are, at the end of 2017, with a project that was born less than a year ago that is now ready for the scrutinizing eyes of the scientific community. Working on this one together had enabled us to transcend our individual abilities, and we hope that this one would earn Feng's stamp of approval.

As I conclude my acknowledgements, I would like to thank those who have been steadfast in their support throughout this entire process. These include Dr. Debra Poutsiaka, Dr. Brigitte Huber, and Dr. Steve Bunnell, Dr. Joan Mecsas, and Dr. Stephen Schworer. Debbie, being my clinical mentor, allowed me to shadow her in the hospital multiple times during my training. Her mentorship exposed me to a different world and continues to remind me that whatever research I do, I should be doing it for humans.

Brigitte, with her resilient personality shows me that one can be tough and still be personable. I got the tough part, the personable part needs some work. Steve is an encyclopedia of scientific knowledge, skill, and whisperer of computers, always inspiring me to read more, think unconventionally, and geek out. Joan provides the calming influence to tamper the fiery forces that I had somehow managed to surround myself with, not denying that I'm quite adept at spreading fires too. And Steve Schworer was the senior student who pointed me to Ralph when I was a most pathetically lost first year in Sasha's lab. He took care of Joe and myself until we grew up enough to start testing our own strengths.

I am very grateful to the challenges and triumphs that I have experienced at Tufts. One makes their own training ground here, and mine had done more than I could have hoped for in preparing me for the next step of my maturation as a scientist.

Beiyun C. Liu

Boston, November 2017

Table of Contents

List of Figures

List of Abbreviations

5z7	(5Z)-7-Oxozeaenol
AIM2	absent in melanoma 2
ASC	apoptosis associated speck-like protein containing a CARD
ATP	adenosine triphosphate
BAL	bronchoalveolar lavage
BMDMs	Bone marrow derived macophages
CARD	Caspase activation and recruitment domain
cFLIP	cellular FLICE-inhibitory protein
cGAMP	cyclic [G(2',5')pA(3',5')p
cGAS	cyclic GMP AMP synthase
CMV	Cytomegalovirus
CXCL1	chemokine (C-X-C motif) ligand 1
dAdT	deoxyadenylic-deoxythymidylic
DD	Death Domain
DNA	Deoxyribonucleic Acid
ELISA	enzyme-linked immunosorbent assay
FACS	Fluorescence-activated cell sorting
FADD	Fas-associated protein with death domain
FBS	fetal bovine serum
FPKM	Fragment per kilobase mapped
GAPDH	Glyceraldehyde-3-Phosphate Dehydrogenase
GBP	Guanylate Binding Protein
GFP	Green Fluorescent Protein
GTP	Guanosine triphosphate
HSV	Herpes Simplex Virus
IAP	Inhibitors of Apoptosis
IFN	Interferon
IFNAR	Type I Interferon Receptor I
IL-1	Interleukin 1
ISG	Interferon Stimulated Genes
IU	International Units
JAK	Janus Kinase
L.pn	*Legionell pneumophila*
LCV	*Legionella* containing vacuole
LPS	Lipopolysaccharide
M-CSF	Macrophage colony stimulating factor
MAPK	Mitogen-activated protein kinases
MAVS	Mitochondrial antiviral-signaling protein

MDA5	Melanoma Differentiation-Associated protein 5
MDM	monocyte derived macrophages
MEF	Mouse embryonic fibroblast
MK2	MAPK-activated protein kinase 2
MLKL	Mixed Lineage Kinase Like
MOI	multiplicity of infection
MyD88	Myeloid differentiation primary response 88
Naip5	NLR family, apoptosis inhibitory protein 5
Nec-1	Necrostatin-1
NFkB	nuclear factor kappa-light-chain-enhancer of activated B cells
NLRC4	NLR Family CARD Domain Containing 4
NLRP3	NLR Family Pyrin Domain Containing 3
NOD	nucleotide-binding oligomerization domain
PARP	Poly (ADP-ribose) polymerase
PBMC	peripheral blood mononuclear cell
PI	Propidium Iodide
PITs	Pore induced intracellular traps
polyI:C	Polyinosinic-polycytidylic acid
PMA	phorbol 12-myristate 13-acetate
PYD	Pyrin
RIG-I	retinoic acid-inducible gene I
RIP	Receptor Interacting Protein
RNA	ribonucleic acid
ROI	Region of Interest
STAT	Signal Transducer and Activator of Transcription
STING	Stimulator of Interferon
TAB1	TGF-beta-activated kinase 1 and MAP3K7-binding protein 1
TAB2	TGF-beta-activated kinase 1 and MAP3K7-binding protein 2
TAK	TGF-beta activated kinase 1
TGFb	Transforming growth factor beta
TLR	Toll Like Receptor
TNF	Tumor Necrosis Factor
TRADD	Tumor necrosis factor receptor type 1-associated DEATH domain
TRIF	TIR-domain-containing adapter-inducing interferon-β
WGA	wheat germ agglutinin
WT	wild type
Y.p.	*Yersinia pseudotuberculosis*
YOP	*Yersinia* outer membrane protein
zVAD	carbobenzoxy-valyl-alanyl-aspartyl-[O-methyl]-fluoromethylketone

Chapter 1: Introduction

Cell death is no longer as simple as programmed or accidental. One of the speakers at a recent conference that I attended had a slide in which he enumerated more than 30 forms of cell death discovered to date. The field of cell death is growing rapidly, but as our techniques become finer, many of the existing definitions and names are likely to merge and change as we uncover the underlying molecular mechanisms (Green 2016). In the present dissertation, I describe two stories of macrophage cell death that result from bacterial infection, and the theme of changing definitions rings true for both.

1.1 The birth of pyroptosis

The term pyroptosis was first introduced in 2001 to distinguish this necrotic, inflammatory cell death from the immunologically silent apoptosis that occurs as part of homeostasis (Cookson & Brennan 2001). Specifically, the first descriptions of macrophage pyroptosis were bacterial or bacterial toxin-induced cell death that engage caspase-1, as demonstrated for anthrax lethal toxin, *Shigella flexneri* and *Salmonella typhimurium* infection (Friedlander 1986; Cordoba-Rodriguez et al. 2004; Hilbi et al. 1998; Brennan & Cookson 2000). Macrophage cell death elicited by these bacterial and their toxins displayed a rapid necrotic nature, distinct from the programmed cell death of physiology, which had been named apoptosis.

The mechanism of caspase-1 activation quickly followed with the identification and characterizations of numerous inflammasome structures that nucleate in response to cytosolic “danger” signals to recruit and activate caspase-1 via proximity-induced autocleavage (de Zoete et al. 2014; Vanaja et al. 2015; van de Veerdonk et al. 2011).

Interestingly, caspase-1 was originally named Interleukin-1β-Converting Enzyme, ICE, for its function in cleaving Interleukin-1β from its inactive 31kDa pro-form to its bio-active 17kDa fragment (Thornberry & Molineaux 1995; Black et al. 1989; Kostura et al. 1989). This was soon followed by the identification of Ich-3, present day caspase-11, as an upstream activator of ICE/caspase-1 in response to LPS-induced sepsis (Wang et al. 1996; Wang et al. 1998). Ich-3/caspase-11 was found to be lowly expressed in resting macrophages, but highly inducible with LPS or IFN stimulation (Wang et al. 1996; Schauvliege et al. 2002). In 1995, the generation of the *Casp1-/-* mouse ablated both cell death and IL-1 release (Kuida et al. 1995; Li et al. 1995). Coincidentally, caspase-11 upregulation in response to LPS was also lost in cells lacking caspase-1 (Kang et al. 2000), although the reason behind this loss of expression would not be known for another decade. In 2009, pyroptosis, defined as caspase-1 mediated necrotic cell death concurrent with IL-1 release, was officially recognized as a programmed cell death mechanism (Kroemer et al. 2009).

1.2 Caspase-11: the non-canonical inflammasome and defense against cytosolic bacteria

2011 was the year in which the re-discovery of an accidental genetic ablation changed the definition of pyroptosis (Kayagaki et al. 2011). That particular genetic ablation was the passenger mutation of a null-allele of *Casp4*, the gene encoding caspase-11, in the *Casp1-/-* mouse (Kuida et al. 1995). What followed was the naming of Caspase-11 as the non-canonical inflammasome in its ability to drive cell death directly, with secondary roles of activating caspase-1 for IL-1 cleavage (Yang et al. 2015; Broz & Monack 2013).

Caspase-1, accordingly, became the canonical inflammasome for its direct involvement in oligomeric structures that involved a NOD-like cytosolic "danger" sensor, a CARD-PYD containing adaptor, and multiple units of caspase-1 itself to cleave and activate the IL-1 family of cytokines (de Zoete et al. 2014). Several major gaps in knowledge remained surrounding the activation of caspase-11, and how caspase-11 in turn is able to activate caspase-1.

With its re-discovery, it was very quickly unveiled that caspase-11 can be activated by bacterial lipopolysaccharide (LPS) present in the cytosol (Kayagaki et al. 2013; Hagar et al. 2013), defining the caspase as a critical sensor for cytosolic bacterial presence (Aachoui et al. 2013; Broz et al. 2012). Furthermore, caspase-11 is unique in that its CARD domain can directly bind to the lipidA portion of LPS, thus positing the idea that caspase-11 may only need LPS presence for nucleation and auto-activation (Shi et al. 2014). Despite the finding the caspase-11 can bind directly to LPS, several other experimental evidences suggest a more complex picture to the activation of caspase-11. For example, caspase-11 activation in response to pure LPS transfection requires the macrophages to be pre-activated by an inflammatory stimulus (Kayagaki et al. 2013; Hagar et al. 2013). Second, caspase-11 activation can be achieved with a wide range of lipidA structures, including those that cannot stimulate TLR4, such as the lipidA of *L. pneumophila* (Case et al. 2013; Girard et al. 2003; Erridge et al. 2004; Fuse et al. 2007).

In terms of the macrophage priming step as a pre-requisite for caspase-11 activation, several explanations now exist. Caspase-11 itself is lowly expressed at resting state, but rapidly upregulated via a MyD88 signal or a JAK/STAT signal (Schauvliege et al. 2002). These signals also drive the upregulation of several Immune-regulated GTPases,

including a family of Guanylate Binding Proteins (GBPs) (Kim et al. 2011; Yamamoto et al. 2012).

1.3 Guanylate Binding Proteins in cell autonomous immunity

It is starting to emerge now that one of the key virulence factors of cytosolic-resident Gram-negative bacteria are effectors that can degrade sensors upstream of caspase-11, the Guanylate Binding Proteins (GBPs). For example, *Shigella flexneri*, a pathogen adapt at residing in the cytosol, encodes an effector IpaH9.8 which selectively targets various GBPs for ubiquitination and degradation to prevent capture by these anti-microbial proteins (Li et al. 2017; Wandel et al. 2017). Without such knowledge earlier in the decade, one had to resort to manipulating the infection system to expose normally vacuole-residing bacteria to the cytosol for detection. The tools were mixed between using bacterial mutants that cannot maintain vacuole stability, such as the *Salmonella typhimurium ΔsifA* and the *Legionella pneumophila ΔsdhA*, or pre-activating the macrophages to lend them the ability to disrupt bacterial vacuoles, such as with LPS or Interferon (IFN). The latter case led to the discovery that caspase-11 activation required a family of GTPases, the above mentioned Guanylate Binding Proteins (GBPs) (Kim et al. 2011; Finethy et al. 2015; Pilla et al. 2014a).

GBPs are a family of 65-73kDa GTPases shown to be inducible by both IFNβ and IFNγ in mouse macrophages (Kim et al. 2011). There are 11 murine GBPs encoded in two clusters on chromosome 3 and chromosome 5. Humans encode 7 GBPs, all located in a single cluster on chromosome 1. Deletion of the *Gbp* locus on chromosome 3, which

include *Gbp1, Gbp2, Gbp3, Gbp5,* and *Gbp7*, results in loss of caspase-11 dependent pyroptosis toward both *L. pneumophila* and *S. typhimurium* (Pilla et al. 2014b; Meunier et al. 2014). The exact placement of GBPs upstream of caspase-11 activation remains controversial. Initial studies involving the GBPs have found their upregulation to coincide with pathogen vacuole disruption (Meunier et al. 2014). This appeared to be consistent with their appearance in proximity to bacteria prior to caspase-11 activation (Haldar et al. 2013; Traver et al. 2011; Haldar et al. 2015; Feeley et al. 2017).

Gbp1, for example, has been shown to recruit to *Listeria monocytogenes* and *Mycobacterium bovis* containing vacuoles within 2 hours post infection (Kim et al. 2011). Gbp1 was found to bind p62/Sequestosome-1, suggesting its involvement in autophagosome formation around intracellular bacteria. In addition to intracellular bacteria, Gbp1 has also been shown to be recruited to parasitophorous vacuoles of less virulent strains of *Toxoplasma gondii*, contributing to pathogen restriction (Selleck et al. 2013). Similarly, Gbp2 has been shown to localize to pathogen-containing vacuoles such as that of *S. typhimurium*, with colocalization with galectin-8 and LC3(Meunier et al. 2014), suggesting Gbp2 may elicit disruption of *S. typhimurium* vacuoles preceding the recruitment of autophagic or pyroptotic machinery. Supporting the idea that GBPs act to disrupt pathogen vacuoles include the finding that several GBPs, GBP2 included, can be isoprenylated for membrane insertion. Interactions with IRGs may further determine the localization of GBPs, with IRGM shown to differentially mark self and non-self vacuoles upstream of GBP recruitment (Haldar et al. 2013; Traver et al. 2011; Tiwari et al. 2009).

However, despite the seemingly robust evidence for GBPs as vacuole-disrupting factors, later studies were unable to re-capitulate a direct action of GBPs in either vacuole

lysis or bacterial killing. Instead, recent findings are shifting to support a model whereby GBPs mediate the release of bacterial components post pathogen vacuole disruption, a critical step for the activation of cytosolic immune sensors (Meunier et al. 2015; Man et al. 2015; Man et al. 2016). Key pieces of work that support this model are based in studies using *Francisella tulerensis,* an intracellular bacterium that gains cytosolic exposure and activates the AIM2 inflammasome. Absent in Melanoma 2 (AIM2) is one of several cytosolic nucleic acid sensors (Wu & Chen 2014; Barber 2011). AIM2 recognizes double stranded DNA, whereby activated AIM2 recruits the adaptor ASC, which in turn recruits pro-caspase-1, resulting in the formation of the AIM2 inflammasome (Hornung et al. 2009). Activation of the AIM2 inflammasome results in caspase-1 mediated pyroptosis and IL-1 maturation (Rathinam et al. 2010). During *F. tulerensis* infection of macrophages, chromosome-3 encoded GBPs were found to be critical for AIM2 activation (Meunier et al. 2015; Man et al. 2015). Follow-up study implicate GBP-mediated recruitment of Irgb10 as the mechanism for the release of bacterial contents for AIM2 and caspase-11 activation (Man et al. 2016).

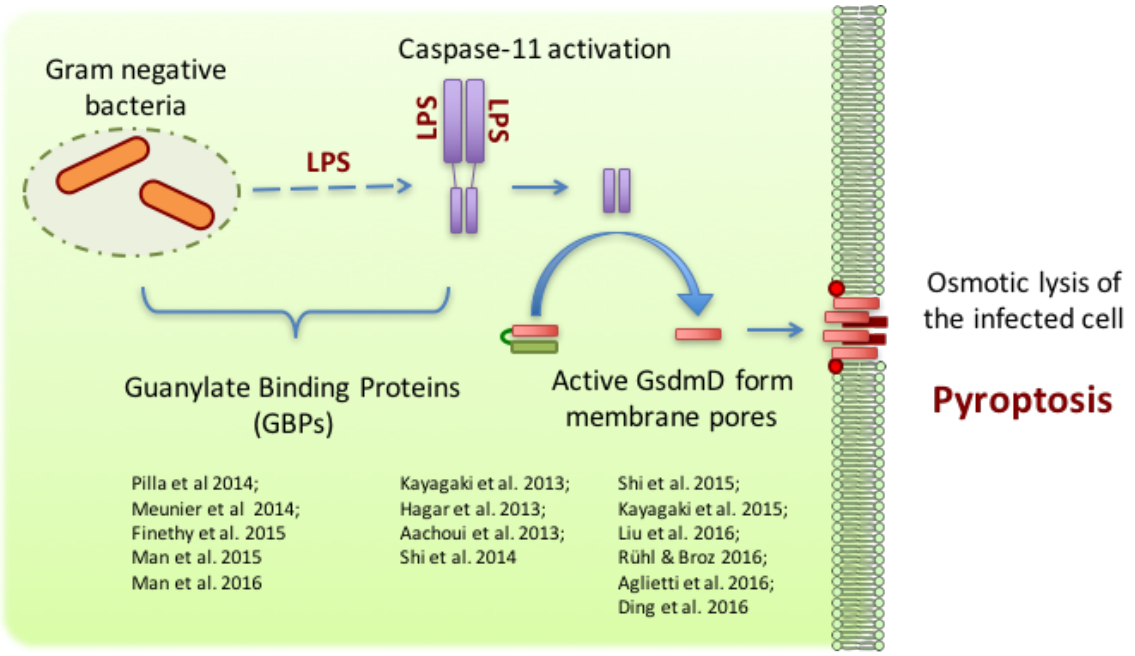

Figure 1.1. Schematic of Caspase-11 pyroptosis
Intracellular Gram-negative bacteria releases LPS in a manner depedent on Guanylate Binding Proteins. Released LPS is able to bind directly to caspae-11, inducing oligomerization and auto-cleavage, generating a 33kDa fragment active caspase. Active caspase-11 cleaves GasderminD, generating a cytotoxic N-terminal fragment of 31kDa in size. Multiple units of 31kDa GasderminD fragments oligomerize at the plasma membrane, resulting in pore formation, loss of osmotic gradient across the plasma membrane, and pyroptosis.

1.4 Cytosolic Legionella pneumophila activates caspase-11

As alluded to above, the vast majority of caspase-11 investigations were conducted in experimental systems where the macrophages were pre-activated with LPS or IFN prior to infection. This is in part due to the low expression of pro-caspase-11 and the GBPs at steady-state. Whereas the method was effective in identifying key players in the caspase-11 cascade, it does not address how a naïve macrophage detects invading pathogens. We therefore adopted the less used infection model of challenging naïve macrophages with bacterial mutants that are defective for maintenance of the cytosolic replication vacuole. The pathogen of choice was the SdhA-defective mutant of *L. pneumophila* (Laguna et al. 2006).

Legionella pneumophila is a Gram-negative intracellular bacteria and the causative agent of Legionnaires' disease (Roy & Tilney 2002). The environmental host of *L. pneumophila* include various species of fresh water amoeba. Human contact with the bacterium is usually via inhalation of aerosolized bacteria, whereby *L. pneumophila* infect and replicate within alveolar macrophages in the lungs (Roy & Tilney 2002; Albert-Weissenberger et al. 2007; Nash et al. 1984; Horwitz 1983). The bacteria replicates to vast numbers within 14-16 hours post infection, eventually lysing the host cell and proceeding to infect neighboring macrophages. The bacteria encodes a type IV secretion system (T4SS) called the Dot/Icm complex, which secretes over 200 effector proteins into the host cytosol, enabling the survival and replication of the bacteria in host membrane-derived vacuoles. These effectors perform various functions including the

recruitment of host ER-derived membrane to establish a peptide-rich replicative vacuole, inhibition of phagolysosomal fusion, and selective blockade of host cell protein translation. The *L. pneumophila dotA-* mutant that lacks the type IV secretion system is avirulent and cannot replicate in macrophages (Shin & Roy 2008; Ivanov & Roy 2013; Fontana et al. 2011; Vance 2010; Asrat, de Jesús, et al. 2014).

Integrity of the replicative vacuole is critical for successful replication of *L. pneumophila*. In the early 2000s, the Isberg lab identified a mutant of *L. pneumophila* that is defective for intracellular replication, with induction of macrophage cell death (Laguna et al. 2006). Subsequent studies elucidated that the mutant, *ΔsdhA,* became cytosolically exposed within 3 hours of infection, hence activating caspase-11 in infected cells (Creasey & Isberg 2012; Aachoui et al. 2013). Notably, despite cytosolic exposure of the bacteria, chromosome-3 encoded GBPs are nevertheless required for optimal caspase-11 activation and cell death (Pilla et al. 2014b). In addition to caspase-11 activation, the *ΔsdhA* mutant of *L. pneumophila* also trigger multiple cytosolic nucleic acid sensing pathways. Ge *et al.* (2012) showed that loss of SdhA enhanced the amount of bacterial DNA released into the host cytosol by measuring the amount of a non-secretable plasmid that is released by the bacteria. This heightened release of bacterial DNA was shown to activate the AIM2 inflammasome, resulting in IL-1 maturation (Ge et al. 2012). This finding is similar to the triggering of the AIM2 inflammasome by *F. novicida* upon pathogen vacuole to cytosol escape. As mentioned above, although the role of chromosome-3 encoded GBPs in AIM2 activation during *F. novicida* infection was shown (Meunier et al. 2015; Man et al. 2015; Man et al. 2016), it remains unclear

whether GBPs are similarly needed for AIM2 inflammasome activation during challenge with vacuole unstable *L. pneumophila.*

1.5 Type I IFN response during L. pneumophila challenge

Despite the Gram-negative cell wall structure of *Legionella* species, TRIF signaling is minimal during *L. pneumophila* challenge. The lipidA moiety of *Legionella* lipopolysaccharide is a weak agonist for TLR4, where several bulky hydrocarbon tails sterically hinders the binding of *Legionella* lipidA to the TLR4/MD2 complex (Girard et al. 2003; Erridge et al. 2004). Instead, surface TLR signaling triggered by *L. pneumophila* stems mostly from TLR2, which activates both the MAPK and NFκB pathways via the adaptor MyD88 (Shim et al. 2009; Fuse et al. 2007). MyD88 signaling is crucial for infection-induced cytokine production and contributes to control of bacterial replication *in vivo* (Archer et al. 2009). Amongst the virulence factors of *L. pneumophila* is the secretion of effectors that block protein synthesis in the infected cell. This block in protein synthesis is partially alleviated when infected with *L. pneumophila* missing five effectors secreted via the Dot/Icm: Lgt1, Lgt2, Lgt3, SidI, SidL (Fontana et al. 2011; Fontana & Vance 2011). Only a handful of highly expressed cytokines have been shown to escape (Fontana et al. 2011; Ivanov & Roy 2013). Cytokines that show escape of infection-induced translation inhibition include TNF, IL-6, pro-IL-1α, and pro-IL-1β, all of which show a dependency on MyD88 (Asrat, Dugan, et al. 2014).

Just as the Dot/Icm secretion system is important for bacterial growth within host cells, it is also a conduit for triggering of various cytosolic immune surveillance

pathways. Bacterial components that are translocated into the cytosol by the Dot/Icm include DNA, RNA, and peptidoglycan. These translocated species activate cytosolic PAMP sensors such as STING, RIG-1/MAVS, and NOD1/2 to result in activation of MAPK, NFκB, and IRF signaling and gene transcription (Fontana & Vance 2011; Lippmann et al. 2011). Both RNA and DNA species translocated via the Dot/Icm are able to induce a type I IFN transcriptional upregulation (Lippmann et al. 2011; Monroe et al. 2009). It is worth noting here that despite the transcriptional upregulation of type I IFNs during *L. pneumophila* macrophage challenge, evidence of IFN protein synthesis and a role for IFNAR signaling during infection is scarce. In fact, when Coers *et al.* developed a highly sensitive luciferase bio-assay to detect IFN protein production during infection, it was only with 20 hours of infection that IFN proteins from infected macrophage cultures showed an accumulation over unstimulated cultures (Coers et al. 2007). It is worth considering these data in light of the fact that TLR-stimulated macrophages survive for longer periods of time in culture compared to unstimulated macrophages, due to upregulation of pro-survival factors downstream of MAPK and NFκB activity. Corroborating the low levels of IFNs made during infection, experiments with *Ifnar-/-* macrophages are inconsistent in their restriction of *L. pneumophila* intracellular growth (Creasey & Isberg 2012; Plumlee et al. 2009). It is therefore unclear whether 1) if type I IFNs are able to bypass translational block, and 2) whether pathogen-induced IFNAR signaling contribute to infection outcome.

As mentioned above, the *ΔsdhA* mutant of *L. pneumophila* show enhanced release of bacterial DNA into the host cytosol (Ge et al. 2012). This mutant has also been shown to hyperinduce type I IFN transcriptionally (Monroe et al. 2009). The mechanism by which

ΔsdhA induces hyperinduction of type I IFN is still unclear and the specific function of the SdhA protein remains elusive. Recent identification of STING as a cytosolic DNA sensor has led to the discovery that STING is crucial for the sensing of *L. pneumophila* DNA inadvertently translocated via the Dot/Icm, leading to transcriptional induction of Type I IFN (Lippmann et al. 2011). Knockdown of STING using siRNA abolished transcriptional induction of *Ifnb* toward T4SS sufficient *L. pneumophila*. Similarly, *Ifnb* expression is diminished in *Irf3-/-* macrophages. Yet, despite the hyperinduction of *Ifnb* transcriptionally, *Ifnar-/-* macrophages remain restrictive to replication of the *ΔsdhA* mutant (Creasey & Isberg 2012).

1.6 Baseline signaling tuning macrophage responses: tonic Interferons

Constant low levels of IFN receptor (IFNAR) signaling have long been observed, although understudied. The answer lies in the presence of constitutive or tonic IFN during homeostasis. Amongst the 2000 ISGs that are responsive to IFN receptor signaling, the expression of 200-300 genes in resting B cells and macrophages depend on IFNAR presence (Mostafavi, Yoshida, Moodley, LeBoité, et al. 2016), attesting to a role of constitutive IFN at baseline. Notably, the concept that IFNs exist at steady-state first surfaced in the early 1980s. With the IFN protein products being elusively small in quantity and too dilute to be detectable in healthy animals and humans, early studies turned to the hybridization of mRNA transcripts of *Ifn* genes to measure steady-state expression. These studies found varying degree of expression in type I IFN genes in the spleen, kidney, liver, and peripheral blood leukocytes from healthy humans (Hiscott et al.

1984; Tovey et al. 1987). Indeed, when neutralizing antibodies against IFNγ or pan IFNα/β were injected into whole animals, blockade of these proteins enhanced tolerance to tumor grafts (Gresser et al. 1983; Gresser et al. 1985), indicating that *in vivo* levels of IFNs, although under the limit of protein detection, remains capable of conferring protection against malignant cells.

One of the earliest proposed sources for constitutive IFN production stems from triggering of low-levels of immune activation by commensal microorganisms. Macrophages from C3H/HeJ mice, which are hyporesponsive to LPS due to a mutation in TLR4, were found to be more supportive of vascular stomatitis virus (VSV) replication (Vogel & Fertsch 1987). In contrast, the restriction to VSV replication by macrophages from the LPS-responsive mouse strain C3H/OuJ can be partially lifted by neutralizing antibodies against IFNα/β. Recently, oral antibiotic treatment of C57BL/6J mice was found to increase susceptibility to LCMV and influenza virus. Disruption of commensal bacterial population was associated with severe reduction in expression of *Ifn* genes as well as genes in the IFN signaling pathway including *Stat1/2* and *Irf3/7*, and crucial ISGs involved in antiviral immunity including *Mx1/2* and *Oas* genes (Abt et al. 2012). Commensal microbiota is thus one source of constitutive IFN production that has a protective effect against pathogens.

In 2009, an *Ifnb*-promoter driven luciferase reporter *in vivo* revealed the thymus as a tissue with high *Ifnb* activity in the absence of any known perturbations to the animal (Lienenklaus et al. 2009). Since the thymus is a site of rapid cellular turnover where T cells undergo positive and negative selection, high transcriptional activity of *Ifnb* in the thymus supports the hypothesis that cellular damage provides a signal for IFN induction.

Notably, in healthy humans, amniotic fluid was one of the first sites found to harbor detectable amount of IFNα protein (Lebon et al. 1982; Chow et al. 2008), further supporting the notion that sites of high cellular or tissue turnover may trigger IFN production *in vivo*. Self-derived signals, in addition to microbiota, can thus drive intrinsic IFN production in healthy animals to establish a low, possibly protective, IFN status.

1.7 Sting: a cellular source of tonic Interferons

In recent years, the discovery of cytosolic DNA sensing pathways has revolutionized our understanding of how intracellular pathogens can elicit an IFN response. Cyclic GMP-AMP synthase (cGAS) is a nucleotidyl transferase that, upon binding to double-stranded DNA, produces a second messenger 2'3'cGAMP, which then activates the adaptor protein STING to elicit TBK1/IRF3 activation and *Ifn* induction (Sun et al. 2013; Jiaxi Wu et al. 2013; Zhang et al. 2013). STING is an ER-anchored protein that exists naturally as a dimer with the ligand sensing domain protruding into the cytoplasm (Ouyang et al. 2012). Various bacterial cyclic-di-nucleotide species, such as cyclic-di-AMP and cyclic-di-GMP, have been shown to bind directly in the groove located between the STING dimers, leading to activation. Mammalian cGAMP produced by the enzyme cGAS binds to STING with a higher potency than microbial cyclic-dinucleotides (Xiao & Fitzgerald 2013). Activation of STING results in recruitment of TBK1 and subsequent phosphorylation and activation of IRF3. Activated IRF3 dimers translocate into the nucleus where they facilitate the transcription of IFN family of genes. Thus, during infection, transfer of pathogen-derived DNA to the cytosol of the host cell, either intentionally or inadvertently, will trigger the activation of cGAS and STING, resulting in *Ifn* induction.

In 2012, homozygous deletion of *Sting* rescued the embryonic lethality of mice that lacked *DnaseII*, a nuclease necessary for the proper digestion of DNA in lysosomes (Ahn et al. 2012). *DnaseII*$^{-/-}$*Ifnar*$^{-/-}$ animals are also rescued from embryonic lethality, indicating that in the absence of proper DNase activity, excessive self-DNA activates STING, resulting in IFN-driven lethality (Ahn et al. 2012; Yoshida et al. 2005). Similarly, deficiency in TREX, a 3' exonuclease that digests cytosolic DNA, results in autoimmune disease marked by IFN over-production via the cGAS/STING pathway (Stetson et al. 2008; Gray et al. 2015).

STING mediated *Ifn* induction was also seen in models of radiation-induced DNA damage and defects in DNA repair (*Atm*$^{-/-}$). Using macrophages lacking ATM (a crucial component of DNA repair machinery) or subjected to γ-irradiation to induce DNA damage, the investigators showed that DNA-damage-accumulated macrophages showed heightened steady-state expression of *Ifnb, Ifna4, Mx1, Irf7*. The same study showed that cells experiencing low-levels of DNA damage were protected against VSV and HSV infections along with enhanced innate Pattern Recognition Receptor responses toward *L. monocytogenes* (Härtlova et al. 2015). Aberrant exposure of mitochondrial DNA provides an additional source for cGAS/STING activation and heightened cellular IFN signature that is associated with protection against viral infections (West et al. 2015; Rongvaux et al. 2014). The cGAS/STING pathway, originally discovered for their IFN-inducing role during infection, thus appear to be more commonly engaged during homeostasis to establish and maintain steady-state IFN production.

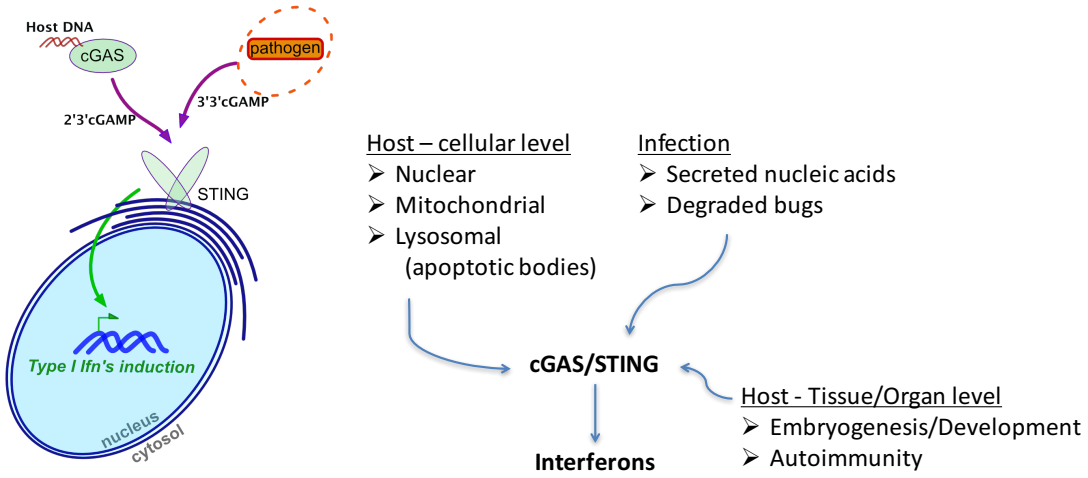

Figure 1.2. Mechanism of STING activation and the various signals that feed into STING signaling
Left: STING is an ER-anchored protein that exists as a dimeric form of two monomers. The binding groove of STING for cyclic-dinucleotides is formed at the interface of the two monomers, facing the cytosol. It is capable of binding bacteria cyclic-dinucleotides such as cyclic-di-AMP, cyclic-di-GMP, as well as the eukaryotic product cyclic-di-AMP-GMP (cGAMP). Upon binding of ligand, STING serves as a adaptor molecule for the recruitment of TBK1 and IRF3, encouraging proximity induced phosphorylation of IRF3 by TBK1. Phosphorylated IRF3 then undergoes dimerization, and dimerized IRF3 is responsible for transcriptional induction of type I IFNs as well as other ISGs.
Right: Various endogenous as well as exogenous sources of STING activation are shown, many of which have been postulated to act during homeostasis, driving tonic IFN signaling. See text for details.

1.8 Interleukin-1 and the organismal control of L. pneumophila

There are several laboratory strains of *L. pneumophila* used to interrogate the various host immune responses. Environmental *L. pneumophila* is a flagellated bacterium. During infection, flagellin monomers are secreted through the Dot/Icm into the host cell cytosol. Human alveolar macrophages do not recognize flagellin (Kofoed & Vance 2011), allowing for bacterial intracellular replication. In contrast, certain laboratory mouse strains encode NAIP5 alleles that does recognize bacterial flagellin, leading to NLRC4 inflammasome activation and caspase-1 activation (Fortier et al. 2009; Halff et al. 2012; Lightfield et al. 2011). Rapid caspase-1 inflammasome activation thus terminates bacterial intracellular replication via macrophage pyroptosis, resulting in a restrictive bacterial growth phenotype in macrophage culture. Laboratory mouse strains that are restrictive to bacterial growth in a flagellin dependent manner include C57BL/6, P/J, and MOLF/Ei (Losick et al. 2009). Mouse strains whose NAIP5 alleles do not recognize flagellin include A/J, C3H/HeJ [C3H], BALB/cJ [BALB], 129S1, and FvB/N (Wright et al. 2003).

On the organismal level, early studies showed that A/J animals, whose macrophages are absent for flagellin-driven NAIP5/NLRC4/Caspase-1 activation, are permissive to higher bacterial replication in the lungs, thus mimicking the human pathology more than the B6 animal (Brieland et al. 1994). Eventual clearance of the bacteria requires the action of CXCL1 and neutrophil recruitment to the site of infection (Tateda et al. 2001).

Similarly, B6 mice deficient for genes encoding the IL-1 receptor and IL-1α showed severe delay in bacterial clearance, defect in granulocyte recruitment to the site of infection, and heightened disease (Barry et al. 2013). The NAIP5 response by B6 animals is thus able to curtail *Legionella* growth *in vivo* by generating a robust IL-1 response at the site of infection, which then elicits a strong systemic CXCL1 upregulation, resulting in rapid neutrophil influx. Recent work on the caspase-11 inflammasome further suggest that pyroptosis, whether it be caspase-1 or caspase-11 mediated, plays a dual function of trapping the bacterium inside the cellular corpse while simultaneously releasing mature IL-1 to facilitate the rapid recruitment of neutrophil to the site of infection. The recruited neutrophils then facilitate the clearance of the bacterium by engulfment of the macrophage corpses with its bacterial load (Jorgensen et al. 2016; Miao et al. 2010).

Mutants of *L. pneumophila* harboring a deletion of the bacterial flagellin (*ΔflaA*) are able to evade detection by NAIP5 and replicate to high numbers in B6 macrophages (Ren et al. 2006). The *ΔflaA* mutant therefore is used to mimic the human macrophage response and allow for investigations to be done on a B6 background, where various genetic models exist. It is on the flagellin-deficient bacteria that the vacuole instability of the *ΔsdhA* mutant was generated for the study of cytosolic sensing pathways and caspase-11 activation.

1.9 Manuscript I summary

In manuscript I, Chapter 2, I use the vacuole unstable *L. pneumophila ΔsdhA* to investigate the role of GBPs in sensing of cytosolic pathogen by macrophages. I found

that since GBPs are Interferon stimulated genes, that their baseline expression is maintained by constitutive Interferon both in macrophage culture and in various tissue sites in the animal. Upon encountering bacteria with unstable vacuoles, GBP presence is crucial for the early recognition and disruption of cytosol-exposed bacterium, resulting in DNA and LPS release. The presence of cytosolic LPS is then able to engage caspase-11, leading to pyroptosis. The released bacterial DNA triggers two parallel pathways, the cGAS/STING pathway for IFN induction, and the AIM2 inflammasome pathway for IL-1 maturation. Systemically, both IFN and IL-1 play non-redundant roles in alarming other immune cells. IFN upregulates factors, independently of GBPs, that are able to degrade vacuoles of healthy, virulent bacteria upon second round of macrophage-bacteria encounter. Systemic IL-1 is critical for inducing Cxcl1 and the recruitment of neutrophils to limit infection.

1.10 Gasdermins are the downstream effectors of inflammatory caspases

As upstream activators of caspase-11 are being uncovered, the substrate of caspase-11 was revealed to be Gasdermin D (GsdmD), one of several Deafness family of proteins initially identified where gain of function mutation were linked to hereditary hearing loss (Chai et al. 2017; Nishio et al. 2014), and loss of function associated with gastric and other cancers (Saeki et al. 2009). During pyroptosis, caspase-1 and caspase-11 both can cleave the 55kDa GsdmD at Asp275 in human, Asp276 in mouse, to generate a cytotoxic N-terminal 31kDa fragment that is membranous, with a C-terminal 22kDa fragment that remains cytosolic (Kayagaki et al. 2015; Shi et al. 2015; He et al. 2015). Active p31

GsdmD forms multimeric pores of 10-14nm in diameter in the plasma membrane, resulting in non-selective ion fluxes and loss of osmotic pressure in the cell (Aglietti et al. 2016; Sborgi et al. 2016; Ding et al. 2016; Liu et al. 2016). As part of its functionality, the p31 subunit of GsdmD was found to have affinity for several phospholipids on the plasma membrane that faces the cytosolic side, explaining the movement of the active protein to the membrane. Amongst the lipids recognized by GsdmD is cardiolipin, a constituent of bacteria and mitochondrial membranes (Aglietti et al. 2016; Ding et al. 2016; Liu et al. 2016). The Shao and Lieberman labs simultaneously showed that in addition to being cytotoxic to mammalian cells, the N-terminal p31 GsdmD was also able to reduce the viability of bacteria upon co-incubation (Ding et al. 2016; Liu et al. 2016), thus expanding the functionality of GsdmD as not only a mammalian cell killer, but a plausible mechanism of bacterial attack that is unleashed during cellular demise.

The discovery of GsdmD also provided a clue to the missing link between caspase-11 and caspase-1 for the generation of mature IL-1 cytokines. GsdmD was found to be critical for IL-1β release during pyroptosis (He et al. 2015). Recently, MLKL, the effector of necroptosis which also generates membranous pores upon activation by RIP1 and RIP3 kinases, was shown to induce ion-flux induced activation of the NLRP3 inflammasome (Conos et al. 2017; Gutierrez et al. 2017). As GsdmD pores are larger and more non-specific than MLKL pores (Chen et al. 2016), it becomes very likely that potassium efflux during GsdmD pore formation constitutive the primary mechanism of caspase-1 inflammasome activation during caspase-11 mediated pyroptosis.

GsdmD is one of 6 genes in the human Gasdermin/Deafness family, one of 10 in mouse (Kovacs & Miao 2017). The only other gasdermin expressed in resting murine bone marrow derived macrophages (in house RNA-sequencing data) is GsdmE, or DFNA5. GsdmE was recently discovered to drive necrotic death when activated by one of the apoptotic caspases, caspase 3 (Rogers et al. 2017; Yupeng Wang et al. 2017). Since then, all 6 gasdermin family proteins have been shown to have pore-forming capabilities, and a roughly similar structure and activation mechanism, where the C-terminal auto-inhibitory fragment folds onto the N-terminal cytotoxic fragment until cleaved by a caspase (Shi et al. 2017; Kovacs & Miao 2017).

Interestingly, the presence of gasdermins is a critical determinant of whether a cell will undergo pyroptosis or apoptosis given a death-inducing stimulus. For example, when macrophages deficient for GsdmD are given a caspase-1 trigger, pyroptosis can transition back to an apoptotic morphology (He et al. 2015). In these cases, it was shown that ASC oligomers can recruit caspase-8, thus making apoptosis the back-up to pyroptotic cell death (Mascarenhas et al. 2017; Pierini et al. 2012; Sagulenko et al. 2013). Similarly, an apoptotic stimulus can manifest as pyroptosis in cells expressing high abundance of GsdmE, cleavable by caspase-3 (Yupeng Wang et al. 2017). The discovery of gasdermins thus uncovers a novel facet of plasticity between apoptosis and pyroptosis.

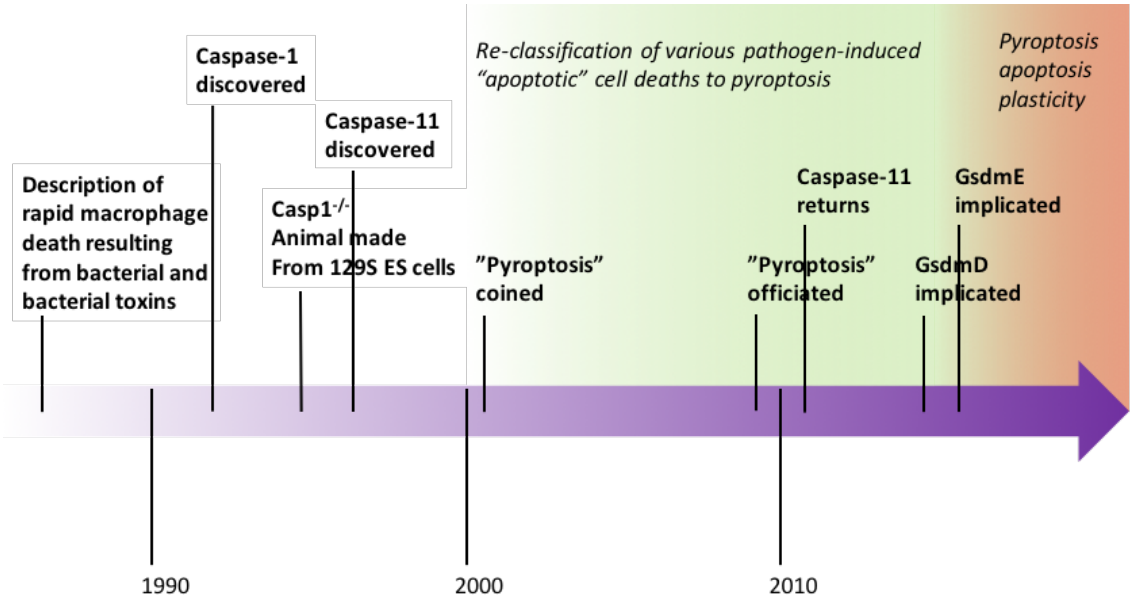

Figure 1.3. Chronological timeline for advances in the field of pyroptosis
Timeline details the events described in the text from the first published description of bacterial induced lytic cell death, at the time known as apoptosis, to discovery of the inflammatory caspases, to the recent discovery of the Gasdermin family of pyroptotic effectors. Several shifts in paradigms have occurred, first with the naming of pyroptosis in 2001, to distinguish this form of cell death from the immunologically silent apoptosis. With the recent findings in gasdermin biology, the field of cell death is in the midst of another conceptual advance.

1. 11 Necroptosis is the backup cell death mechanism upon block of apoptosis

Plasticity amongst cell death pathways is not itself a new concept. In fact, it is one of the basic tenets underlying the study of necroptosis, a necrotic cell death mechanism that can be engaged when apoptotic caspases are blocked. Necroptosis is most well studied in a model of Tumor Necrosis Factor (TNF) induced death. TNF receptor signaling engages the TNF receptor associated adaptor TRADD (Hsu et al. 1995) to recruit Receptor Interacting Protein kinase 1 (RIP1) via death domain (DD) interactions (Hsu et al. 1996). RIP1 is ubiquitinated at lysine 63, providing a scaffold for the recruitment of TAK1/TAB1/TAB2 complex and downstream activation of MAP kinases and NFκB, driving the production of inflammatory cytokines and pro-survival factors (Kelliher et al. 1998). In cases in which MAP kinases and/or NFκB signaling is blocked, RIP1 can dissociate from TNF receptor and interact with FADD and pro-Caspase-8, leading to caspase-8 activation and cell death (Micheau & Tschopp 2002). It is at this stage that if caspase activity is blocked, RIP1 kinase activity will be engaged, phosphorylating RIP3 to activate the pseudokinase mixed lineage kinase like (MLKL). Phosphorylation of MLKL results in its trimerization and insertion into the plasma membrane, leading to cell death (Feltham et al. 2017; Li et al. 2012; Murphy et al. 2013; Cai et al. 2013). The laboratory tool for pan-caspase inhibition is a tri-peptide inhibitor designed based on commonalities shared in caspase substrate cleavage sites: Benzyloxycarbonyl-val-ala-asp fluoromethylketone, or z-VAD-FMK (colloquially shortened to zVAD) (Talanian et al. 1997). It acts as a noncleavable pseudosubstrate for caspases that bind irreversibly to the caspase activation site cysteine.

In recent years, necroptosis has similarly been shown to occur downstream of TLR signaling during caspase inhibition (Kaiser et al. 2013; He et al. 2011). In this case, RIP1 is recruited to TLRs that utilize the adaptor TRIF. TLR3 and TLR4 engage the adaptor TRIF, where TRIF interacts with RIP1/RIP3 via RHIM domains. Again, recruitment of RIP1 is necessary for inflammatory signaling. However, if zVAD is used to inhibit caspases upon TLR3 or TLR4 signaling, necroptosis is engaged in a manner dependent on RIP1 and RIP3 kinase activity and MLKL activation (Meylan et al. 2004; Kaiser et al. 2008; Kaiser et al. 2013). The other protein identified in recent years to encode a RHIM domain and can interact directly with RIP1 is DAI/ZBP1 (Rebsamen et al. 2009). In this case, ZBP1 was found to engage necroptosis in response to RNA virus infection (Upton et al. 2012).

While the virus inhibits Caspase-8 activity to subvert apoptotic cell death, necroptosis is thought to engage as a secondary mode of cell death that benefits the host by limiting viral replication in infected cells (Cho et al. 2009; Upton et al. 2010; Huang et al. 2015). However, recent findings are starting to challenge this idea that necroptosis only has a role during infections by pathogens that inhibit apoptosis. One finding is that the embryonic lethality of caspase-8 deficiency can be rescued by the additional loss of RIP3 (Kaiser et al. 2011; Günther et al. 2011), suggesting that necroptosis can be engaged during development and has to be checked by caspase-8. ZBP1 has also been shown to spontaneously interact with RIP3 to drive necroptosis during embryonic development, plausibly contributing to lethality in the absence of RIP1 (Kim Newton et al. 2016; Lin et al. 2016). In these studies, RIP1 was found to interfere with ZBP1/RIP3 interactions,

which corroborates previous findings that RIP1 deficiency results in perinatal lethality of the animal (Kelliher et al. 1998; Berger et al. 2014).

Additionally, RIP kinases play a role during hypoxia-induced tissue damage, such as ischemic reperfusion injuries that can occur during kidney transplant and severely reduce the success of the transplanted kidney (Linkermann et al. 2013; Lau et al. 2013). The small-molecular inhibitor of RIP kinases, necrostatin-1, has been shown to be effective in preventing ischemia-reperfusion based tissue injury (Xie et al. 2013; Degterev et al. 2008; You et al. 2008). However, whether the effect of Nec-1 is blocking the necroptosis arm of RIP kinases or the inflammatory arm of MAP kinases and NFκB signaling that requires RIP1 scaffolding function is an area of ongoing investigation. Several studies have shown that tissue injury ensues in a RIP-kinase dependent, MLKL independent manner, suggesting that inflammatory cytokines may be at play in the absence of necroptotic cell death (K Newton et al. 2016). Additionally, RIP3 kinase may also play a role in inflammatory cytokine production in addition to cell death (Gong et al. 2017).

1.12 Inhibition of inflammatory signaling leads to macrophage death

As mentioned above, RIP1 is needed for activation of MAP kinases and NFκB signaling by serving as a ubiquitination scaffold for the recruitment of TGFβ-associated kinase (TAK1). TAK1 interacts with TAB1 and TAB2, where it experiences constitutive phosphorylation and baseline activity (Omori et al. 2012; Mihaly et al. 2014). Genetic ablation of *Map3k7,* the gene encoding TAK1, results in embryonic lethality (Sato et al. 2005). In monocytes and macrophage-like cell cultures, *Map3k7* deletion sensitizes the

cells to TNF induced cell death via autocrine signaling (Lamothe et al. 2013; Morioka et al. 2014; Wang et al. 2015). In an infection setting, bacteria that inhibit MAPK and NFκB signaling has similarly been shown to induce cell death, such is the case for *Bacillus anthracis* and *Yersinia* species (Park et al. 2002; Monack et al. 1997).

In the case of *Yersinia* induced macrophage death, the effect has been narrowed down to the *Yersinia* outer protein YopJ (*Y. pestis* and *Y. pseudotuberculosis*) or YopP (*Y. enterocolitica*), which inhibits TAK1 phosphorylation via acetylation of the kinase on several residues within the activation loop (Paquette et al. 2012). The cell death mechanism driven by *Yersinia* YopJ was recently shown to be caspase 8 dependent, RIP3 independent (Philip et al. 2014; Weng et al. 2014), suggestive of apoptosis. However, *Yersinia* induced macrophage cell death does show partial dependency on RIP1 kinase activity (Peterson et al. 2017), which has traditionally been associated with necroptosis and thought to be unnecessary for caspase-mediated apoptosis. Further complicating the classification of *Yersinia* induced cell death is the rapidness of cellular necrosis, which takes a semblance to necroptosis rather than the slower secondary necrosis that occurs as the last stage of apoptosis (Galluzzi et al. 2015; Vanden Berghe et al. 2010).

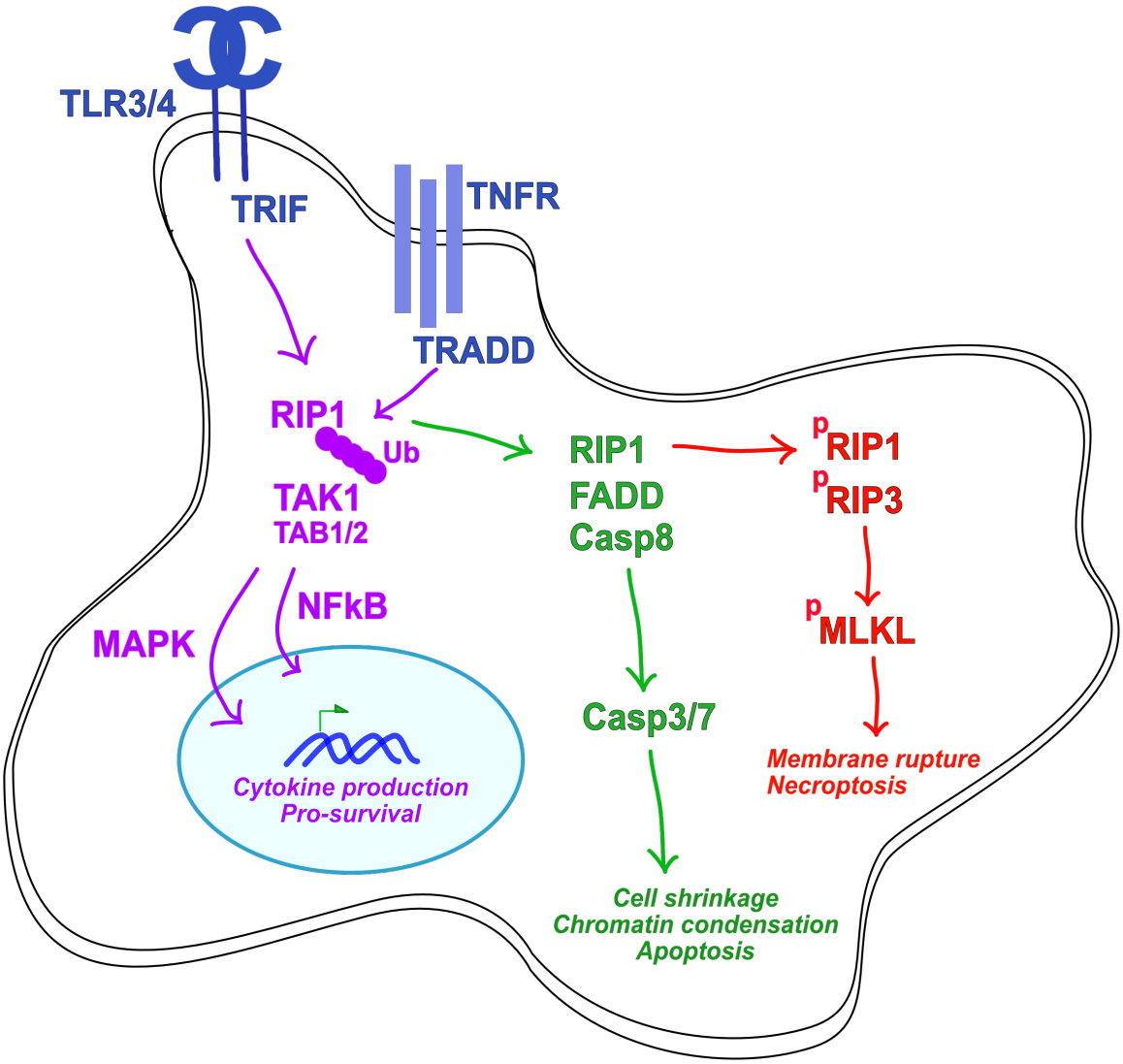

Figure 1.4. Inhibition of inflammatory signaling switch cells to apoptosis and necroptosis
Three branches of signaling downstream of inflammatory cell surface receptors result in vastly different cellular outcomes. TLR3/4 and TNF receptor signaling drives a pro-inflammatory, pro-survival cellular program that depends on the success of TAK1 driven MAPK and NFkB signaling (magenta). RIP1is recruited to adaptors located at plasma membrane receptors, and serves as an inflammatory signaling scaffold, where its K63 ubiquitination recruits the TAK1/TAB1/TAB2 complex for MAPK and NFkB activation. Success of this pathway generates inflammatory cytokine production as well as synthesis of pro-survival factors, including cFLIP and varous Inhibitors of Apoptotic Proteins (IAPs). If TAK1 signaling is unsuccessful, RIP1 dissociate from signaling complexes at these plasma membrane receptors and forms Complex IIa along with FADD and Caspase-8. Complex IIa drives caspase-8 function, leading to activation of executioner caspases 3 and 7, resulting in apoptosis (green). If caspases are inhibited, RIP1 kinase activity is engaged, which phosphorylates RIP3. RIP3 then phosphorylated MLKL, which forms oligomeric structures that disrupt the plasma membrane, leading to necroptosis (red).

1.13 Lipopolysaccharide of Yersinia species are TLR4 evasive at mammalian body temperature

The three *Yersinia* species that induce pathology in mammals are *Y. pestis, Y. pseudotuberculosis,* and *Y. enterocolitica* (Viboud & Bliska 2005). One common immunoevasive strategy shared amongst these three species is their ability to modify the lipid A structure of LPS in a temperature dependent manner (Knirel & Anisimov 2012; Rebeil et al. 2004). The general composition of LPS are the O antigen, the core oligosaccharide, and lipid A. The lipid A portion of LPS confers most of the immunostimulatory activites, with the prototypical lipid A exemplified by that of *E.* coli, which is composied of six acylated lipid chains with a carbon length of 12 to 16 (Tan & Kagan 2014). Mammalian TLR4 complexes with MD2 to form a binding pocket for five out of the six lipid A acyl chains to fit into. The interaction of MD2 with LPS is direct and with high affinity. The last acyl chain of lipid A extends along the surface of MD2, where its positioning facilitates the bound TLR4/MD2 complex to dimerize with another TLR4/MD2 complex to initiate signaling of the TIR domains on the cytoplasmic tail of TLR4 (Park et al. 2009). Lipid IVa, the precursor to lipid A, only contains four acyl chains and varies in its capacity to bind TLR4/MD2 from different species. For example, lipid IVa acts as an antagonist for TLR4 activation in human macrophages, but is weakly stimulatory against TLR4 of murine macrophages (Golenbock et al. 1991). Preventing the conversion of lipid IVa to lipid A is a common evasive strategy used by bacteria, especially in the case of pathogenic *Yersinia* species.

Y. enterocolitica and *Y. pseudotuberculosis* cause enteric diseases from contaminated food and water. *Y. pestis* is transmitted via a flea bite, leading to bubonic plague. In all three cases, transmission from the environmental source to mammals encompasses a temperature shift on the bacterium. At temperatures of lower than 28°C, all three species predominantly express hexa-acylated lipid A. However, at 37°C, LPS with hexa-acylated lipid A is shed, and the majority of progenitor lipid IVa fail to be processed to its hexa-acylated form (Rebeil et al. 2004). As eluded to above, hypo-acylated LPS is a poor stimulant of human TLR4, but does retain some activity in stimulating murine TLR4 (Golenbock et al. 1991). The reason for the species discrepancy was recently shown to be due to changes in two amino acids between human and murine MD2, which enables murine MD2, but not human MD2, to interact with hypo-acylated LPS and activate TLR4 for downstream signaling (Oblak & Jerala 2015). Consistently, *Y. pestis* can be attenuated by forced expression of hexa-acylated LPS to become immune-stimulatory to human macrophages (Montminy et al. 2006).

1. 14 Yersinia induced cell death and concomitant IL-1 secretion

With the discovery that *Yersinia* induced cell death occurred due to YopJ inhibition of level three MAP kinase TAK1, the study of *Yersinia* driven cell death quickly converged with the older field of caspase-8 mediated cell death that resulted from MAPK and NFκB inhibition. The critical pro-survival role of TAK1 was well established both genetically, as discussed above, and pharmacologically, with the advent of the small-molecule inhibitor 5Z-7-Oxozeaenol (5z7) (Jiaquan Wu et al. 2013). In fact, 5z7 was also

used to mimic the cell death induced during *Yersinia* infection (Philip et al. 2014). It therefore appears consistent that *Yersinia* is utilizing several immune evasive strategies to generate an immunologically silent infection, by modifying it LPS for lower stimulatory activity, dampening cytokine production via the inhibition of a critical kinase upstream of both MAPK and NFκB pathways, and by inducing the death of macrophages via caspase-8 driven apoptosis. Just as necroptosis was not as simple as an arms race against viruses that block host cell apoptosis to benefit viral replication, *Yersinia's* attempt at immune-evasion by inhibiting TAK1 also has a twist.

Paradoxically, despite that both YopJ and the synthetic TAK inhibitor 5z7 are efficient at blocking inflammatory cytokine production, *Yersinia* infections both in cell culture and *in vivo* elicit robust IL-1 responses, with IL-1 receptor signaling playing a crucial role in the survival of the animal (Ratner et al. 2016). The IL-1 family of cytokines is unique in its activation and secretion. They lack canonical secretory sequences, therefore are not secreted upon synthesis as is the case for most other cytokines. Additionally, IL-1β and IL-18 are synthesized as zymogens, where a cleavage event is required to cleave the pro-peptides into the bioactive fragment. The synthesis of pro-IL-1 require NFκB signaling, and generally occur downstream of TLR activation (Cogswell et al. 1994). The IL-1 maturation event requires the formation of the inflammasome and caspase-1 activation, cleaving pro-IL-1β and pro-IL-18 (Franchi et al. 2009). IL-1α does not require a cleavage step for activation. Nevertheless, it is also not secreted upon synthesis, and require the activation of caspase-1 or caspase-11 for release (van de Veerdonk et al. 2011; Li et al. 1995; Thornberry & Molineaux 1995). In terms of the caspase-1 inflammasome, many upstream cytosolic "danger" sensors exist that is able

to sense bacterial components including flagellin (NAIP5), toxins (NALP1), DNA (AIM2), and the most promiscuous being NLRP3 which can be activated by high ATP, nigericin, and drop in cellular potassium levels (Sutterwala et al. 2014; Franchi et al. 2009). The model for IL-1 maturation and release is thus interconnected with events surrounding plasma membrane rupture and pyroptosis (Bergsbaken et al. 2009).

Recently, activation of the NLRP3 inflammasome has also been observed during necroptosis (Conos et al. 2017). During caspase-11 mediated pyroptosis, NLRP3 inflammasome was found to activate as a consequence of GsdmD pore formation and the efflux of potassium ions, thus providing a link between caspase-11 activation and caspase-1 activation (He et al. 2015). Potassium efflux induced inflammasome activation may be a commonality shared amongst various necrotic modes of cell death (Wallach et al. 2016). The GsdmD pore additionally provide a conduit for mature IL-1 cytokine release. With the discovery of the membrane patching activities of the ESCRT complex during necroptosis, it has also been suggested that transient GsdmD pores may be formed, releasing small amounts of IL-1, then patched to prevent total demise of the cell (Kovacs & Miao 2017). Transient GsdmD pores may thus explain the phenomenon in which IL-1 release has been observed in the absence of cell death (Zanoni et al. 2016; Zanoni et al. 2017).

The conundrum still remains, however, on how a *Yersinia* infected cell that is undergoing YopJ induced TAK inhibition is able to synthesize pro-IL-1. This question is starting to be addressed with single-signal cytokines such as TNF, where TNF synthesis was found to localize in cells that not not sufficiently intoxicated by YopJ (Peterson et al. 2016a; Lemaître et al. 2006). Given this finding, and that *Yersinia* species have been

reported to secrete immune-stimulatory outer membrane vesicles (Eddy et al. 2014), non-YopJ intoxicated macrophages may also be the ones synthesizing pro-IL-1. The follow-up question therefore becomes, what is the mechanism of pro-IL-1 activation? In the absence of YopJ, YopM has been shown to induce the activation of the PYRIN inflammasome, caspase-1 activation, and IL-1 maturation (Ratner et al. 2016). The loss of YopJ here presumably releases the block of cytokine synthesis, allowing for more pro-IL-1 to be made in the first place. It is unclear whether or not YopM has a physiological role in inflammasome activation in the presence of YopJ.

1. 15 Manuscript II summary

In manuscript II, Chapter 3, my co-author Joseph Sarhan and I report that caspase-8, during Yersinia infection as modeled by Y. pseudotuberculosis, can induce the cleavage of both GsdmD and GsdmE, resulting in pyroptotic cell death and IL-1 secretion. Our findings lie at an intersection between a core immunological/developmental phenomenon with a pathogen-induced host cell defense mechanism. The immunological phenomenon is that during blockade of MAP kinase and NFκB signaling, cell death ensues in a caspase-8 dependent manner, frequently described as apoptosis (Günther et al. 2011; Feltham et al. 2017). During Yersinia infection, the Yersinia effector YopJ acetylates and inhibits level three MAP kinase TAK1 (Paquette et al. 2012), resulting in a cell death that depends on caspase-8 (Weng et al. 2014; Philip et al. 2014). Our investigations focused on the morphology of macrophage death with TAK1 inhibition and its downstream consequences. In accordance to the appearance of GsdmD/E active fragments, loss of

GsdmD prolongs the death phase, converting its morphology from pyroptosis to apoptosis. Notably, due to TAK-inhibition in blocking pro-IL-1 synthesis, we found that successful IL-1 maturation during Yersinia infection required two populations, a population of TAK-inhibited dying cells as platforms for inflammasome formation, as well as a population of cells that are not intoxicated by YopJ to provide pro-IL-1. The absence of either components will compromise the overall effectiveness of the immune response, such as in humans. Using human macrophages from three independent sources, we found that human macrophages do not readily respond to TAK inhibition by cell death, with severely compromised IL-1 production.

Chapter 2: Constitutive Interferon signaling maintains GBP expression required for the release of bacterial components to elicit pyroptosis and anti-DNA responses[1]

[1] Beiyun C Liu, Joseph Sarhan, Alexander Panda, Hayley I Muendlein, Jörn Coers, Masahiro Yamamoto, Ralph R Isberg, Alexander Poltorak. To be submitted to *Cell Host and Microbe*

2.1 Background

When challenged with intracellular pathogens, the ability of the macrophage to mount rapid responses is crucial for the success of cell-autonomous immunity. To this end, numerous cytosolic surveillance pathways exist to drive immune responses on the transcriptional level, such as cytokine gene expression, as well as post translationally, including inflammasome activation and host cell death (Randow et al. 2013). Cytosolic presence of bacterial lipopolysaccharide (LPS) has been shown to activate Caspase-11, resulting in a lytic form of host cell death known as non-canonical inflammasome-mediated pyroptosis (Kayagaki et al. 2011; Yang et al. 2015; Meunier & Broz 2014). Vacuolar pathogens such as *S. typhimurium* and *L. pneumophila* predominantly bypass caspase-11 activation by maintaining pathogen replication vacuoles that protect the bacterium from cytosolic sensing (LaRock et al. 2015; Isberg et al. 2009). Caspase-11 activation in response to vacuole-resident bacteria requires Interferon (IFN) pre-activation of macrophages (Broz et al. 2012; Case et al. 2013). Recently, a family of Guanylate Binding Proteins (GBPs) encoded on chromosome 3 have been implicated upstream of caspase-11 (Pilla et al. 2014a; Meunier et al. 2014). The mechanistic step(s) in which GBPs function remains controversial.

GBPs belong to a family of IFN-inducible GTPases that interact with phagocytic oxidases and initiators of autophagy (Kim et al. 2011). The GBP proteins are undetectable by standard immunoblot probing procedures at cellular resting state, but are highly upregulated by IFNγ and, to a lesser extent, IFNα/β (Kim et al. 2011; Yamamoto et al. 2012). In IFN-activated macrophages, a number of GBPs localize to pathogen containing vacuoles (Kim et al. 2011; Meunier et al. 2014; Yamamoto et al. 2012), and

have been functionally associated with either pathogen vacuole rupture and bacterial killing or both (Meunier et al. 2014; Meunier et al. 2015; Man et al. 2015). Additionally, induction of an IFN response during infection (Broz et al. 2012; Man et al. 2016; Meunier et al. 2014) has resulted in a model postulating that infection-driven IFN signaling is required for GBP synthesis and function (Meunier & Broz 2014).

During *L. pneumophila* challenge, bacterial DNA/RNA trigger cytosolic sensors to induce *Ifnb* transcription within 4-6 hours of infection (Monroe et al. 2009; Lippmann et al. 2011), although secreted IFNβ protein is not detected until 20 hours post infection (Coers et al. 2007). The disconnection between *Ifnb* gene transcription and protein accumulation is presumably due to inhibition of host cell protein translation as a consequence of *Legionella* infection (Ivanov & Roy 2013; Asrat, Dugan, et al. 2014; Fontana et al. 2011). In line with these findings, caspase-11 activation in response to vacuolar-resident *L. pneumophila* requires IFN priming. Interestingly, the need for IFN priming for cell death can be bypassed by a *L. pneumophila* mutant lacking the SdhA protein (*ΔsdhA*) (Monroe et al. 2009; Aachoui et al. 2013). This mutant strain forms an unstable vacuole that exposes the bacterium to the host cytosol (Laguna et al. 2006; Creasey & Isberg 2012). Despite the cytosolic exposure of *L. pneumophila ΔsdhA*, caspase-11 activation remains dependent on GBPs encoded on chromosome 3 (Pilla et al. 2014a). The differential requirement of IFN priming for pyroptosis when challenged with vacuole-stable or cytosol-accessible bacteria calls for a re-evaluation of the function of GBPs upstream of caspase-11.

In this work, we investigated the initiation of antimicrobial responses that result in caspase-11 activation. We show that in the absence of infection, host-intrinsic

constitutive IFN signaling sustains GBP expression both *in vitro* and *in vivo,* and that endogenous levels of GBPs are sufficient for the release of LPS from cytosolic bacteria, resulting in rapid pyroptosis. Notably, GBPs are required for the release of DNA as well to activate two major cytosolic DNA sensing pathways: the cGAS/STING pathway to generate an IFN response, and the AIM2 inflammasome pathway for caspase-1 activation and IL-1 maturation. During *Legionella* pneumonia, chromosome-3 GBP mediated IL-1 signaling is a crucial determining factor in early clearance of vacuole unstable *L. pneumophila* bacteria. Our findings indicate that downstream from vacuole lysis, endogenous GBP activity controls the release of bacterial components, driving immune activation. Similar results in human macrophages support the concept that host-intrinsic cytokine signaling determines antimicrobial responses at the onset of infection.

2.2 Results

2.2.1 Infection-driven IFN signaling is dispensable for pyroptosis

To mimic cellular responses in human macrophages, all *L. pneumophila* strains used in the present study are deficient for flagellin (*ΔflaA*) to bypass the Naip5/NLRC4/caspase-1 cell death pathway that occurs on the C57BL/6J (B6) genetic background (Ren et al. 2006). Flagellin-deficient *L. pneumophila* bacteria reside within *Legionella*-containing vacuoles (LCV) that protect the bacterium from cytosolic sensing. *L. pneumophila*(*ΔsdhA*) mutants are unable to maintain the integrity of the replicative vacuole, resulting in death of infected macrophages (Laguna et al. 2006; Creasey & Isberg 2012). Using macrophage incorporation of propidium iodide as a read-out for cell death over time, we found that maximal macrophage pyroptosis toward *L. pneumophila ΔsdhA* was observed by 6 hours post infection (hpi) (Fig 1A). Cell death induced by both the WT and *ΔsdhA* strains largely depended on caspase-11, as macrophages from *Casp11*$^{-/-}$ showed enhanced survival (Fig 2.1A). Using *L. pneumophila*-GFP^{+} to distinguish infected and bystander cells based on GFP signal, we confirmed that the majority of cell death observed in the whole population was occurring in the subpopulation that harbored bacteria, and was dependent on caspase-11 (Fig 2.8A, Fig 2.8B). To rule out the contribution of necroptosis, another form of necrotic cell death that is driven by RIP1/RIP3 (Wallach et al. 2016), we used Necrostatin-1 (Nec1) to inhibit RIP1/RIP3 activity. Inhibition of RIP1/RIP3 did not affect cell death during *L. pneumophila ΔsdhA* infection, further arguing for a caspase-11 pathway (Fig. S1C).

L. pneumophila infection of macrophages results in robust *Ifnb* transcription via cytosolic DNA and RNA sensing pathways STING and RIG-I/MDA5, respectively

(Monroe et al. 2009; Lippmann et al. 2011). Since *Legionella* translocates effectors that selectively block host cell protein translation, it is unclear if Type I IFNs bypass the *L. pneumophila*–elicited translational block (Ivanov & Roy 2013; Asrat, Dugan, et al. 2014; Fontana et al. 2011). In spite of the fact that transcriptional induction of *Ifnb* in response to the *L. pneumophila ΔsdhA* mutant was similar in magnitude to that of LPS (Fig. 2.8D), there was no accumulation of the IFNβ protein in the supernatants of cells by 8 hours post infection, even though abundant IFNβ protein was detected in cells stimulated with LPS, cytosolic cGAMP, and cytosolic polyI:C (Fig 2.1B, Fig. 2.8D). To determine if infected macrophage populations were experiencing IFN signaling, we probed for STAT1 phosphorylation downstream of IFN receptors. We were unable to detect any increase in STAT1 phosphorylation during the first 6 hours of *L. pneumophila* infection, in contrast to that observed in the presence of LPS, cGAMP, and polyI:C (Fig 2.1C, D). To dismiss the possibility of missed STAT1 phosphorylation in dying cells, STAT1 phosphorylation was measured in *Casp11*$^{-/-}$ cells or B6 cells treated with pan-caspase inhibitor zVAD (Fig 2.1D). We were unable to detect any increase in STAT1 phosphorylation in macrophages from either *Casp11*$^{-/-}$ or B6 mice treated with zVAD (Fig 2.1D).

IFN feedback is proposed to drive *de novo* synthesis of GBPs and pro-caspase-11 (pro-caspase-11), so we investigated if these proteins were produced prior to cell death. We were unable to detect accumulation of GBP2 by 4 and 6 hours post infection (Fig 2.1E), although we did see clear accumulation of GBP2 protein in response to the avirulent *L. pneumophila dotA*$^{-}$ mutant by 10 hours post infection, consistent with its inability to block protein synthesis (Fig. 2.8E; Ivanov & Roy 2013). We observed an

increase of pro-caspase-11 within 6 hours of infection (Fig 2.1E). To determine if pro-caspase-11 was synthesized by infected or bystander cell populations, macrophages challenged with *L. pneumophila*-GFP strains were sorted to separate infected GFP^+ from bystander GFP^- cells. We found no detectable increase in pro-caspase-11 in the infected GFP^+ population, with the majority of pro-caspase-11 accumulation contained within the bystander GFP^- population (Fig 2.1F). The lack of accumulation of both GBP2 and pro-caspase-11 protein in infected cells indicates that *de novo* synthesis of these effectors is not needed for caspase-11 activation, and that the low protein abundance present in resting macrophages is sufficient for functional output.

To determine if IFN signaling concurrent with infection is able to stimulate pyroptotic death, cells were incubated with 100U/ml of recombinant IFNβ at various times leading up to bacterial challenge and cell death was monitored (Fig 2.1G-I). We found that despite robust IFNAR signaling in response to exogenous IFNβ (Fig. 1H), IFNβ stimulation simultaneous with, or 1 hour prior to, infection had no effect on cell death induced by either the *ΔsdhA* mutant (Fig 2.1I, left) or WT (Fig. 2.8G). IFNβ pre-treatment at least 4 hours prior to infection was needed to significantly increase the rate of cell death, as demonstrated by a reduction in the time to 50% of maximal cell death (Fig 2.1I, middle). Extensive IFN treatment did not significantly increase the maximal cell death in response to the *ΔsdhA* mutant (Fig 2.1I, right). This contrasts strongly with cells challenged with the WT strain in which 4 hours of IFN pre-treatment significantly augmented the cell death response (Fig. 2.8F). In both cases, at least 4 hours of pre-activation with IFNβ was necessary to enhance the cell death phenotype, suggesting that

cell death depends on pre-established IFN status and, in the case of *L. pneumophila ΔsdhA,* does not require infection-induced IFN.

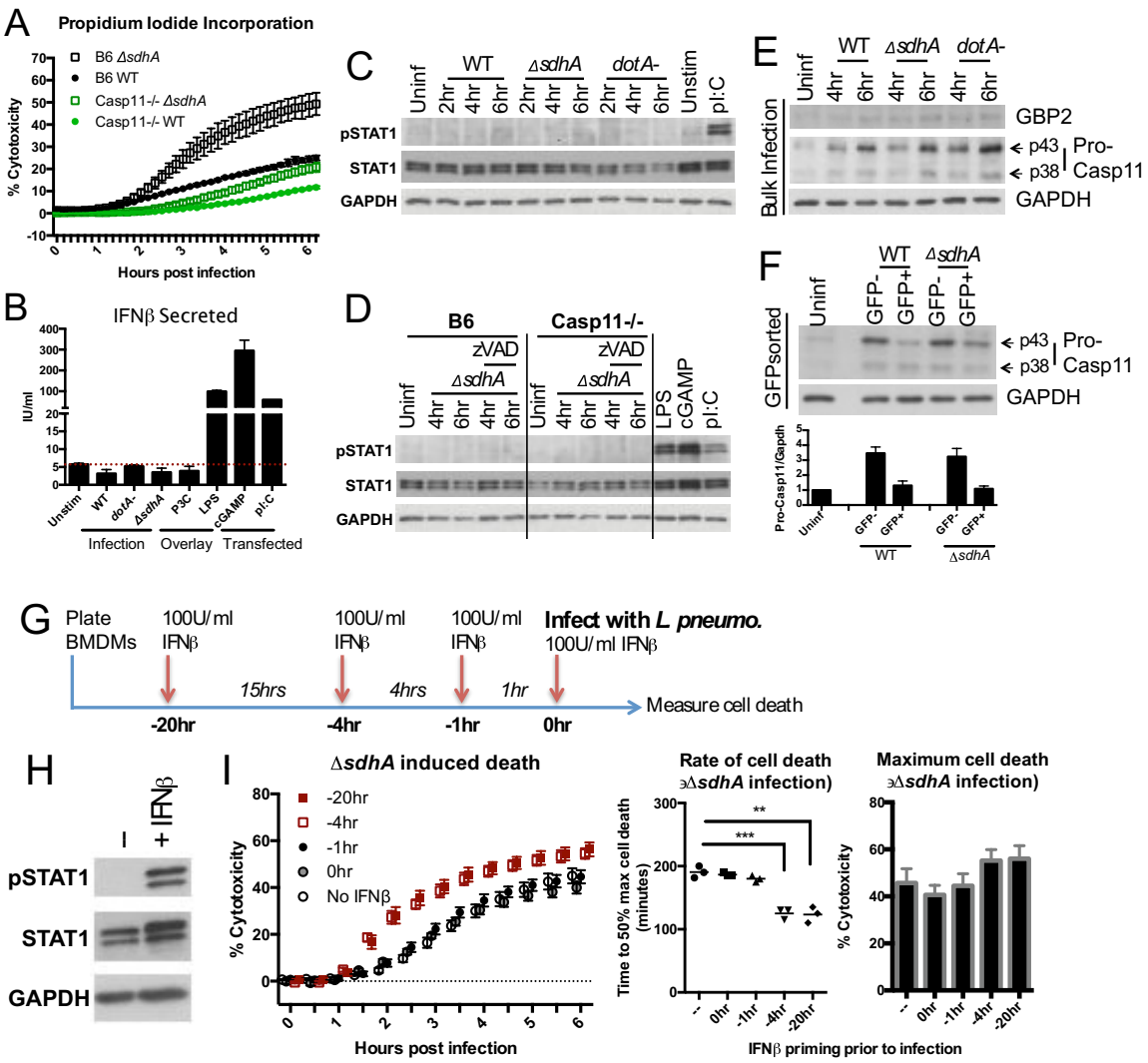

Figure 2.1. Infection-driven IFN signaling is dispensable for pyroptosis

(A) Macrophages were infected with *L. pneumophila* WT and *ΔsdhA* strains, propidium iodide (PI) incorporation used to monitor death.

(B) B6 macrophages were infected with WT, *dotA*-, or *ΔsdhA* strains. At 8 hours post infection (hpi), supernatants were collected and measured by ELISA for IFNβ protein. Control stimulations (8 hours) included TLR2 agonist P3C (Pam3Cysk4), TLR4 agonist LPS, STING agonist cGAMP (transfected) and RIG1/MDA5 agonist polyI:C (transfected).

(C) B6 macrophages were challenged with WT, *dotA*-, or *ΔsdhA* strains for the indicated times. Whole cell lysates were probed by immunoblot. 2 hours challenge with polyI:C (TLR3 agonist, overlay) used as control.

(D) Macrophages were challenged with the *ΔsdhA* mutant for the indicated times in the absence or presence of zVAD (pan-caspase inhibitor). Whole cell lysates were probed by immunoblot. 6-hour transfection with polyI:C (RIG1/MDA5 agonist) and cGAMP (STING agonist) as controls.

(E) B6 macrophages were challenged with WT, *dotA*-, or *ΔsdhA* strains for the indicated times. Whole cell lysates were probed by immunoblot.

(F) Macrophages challenged for 6 hours with WT or *ΔsdhA* strains were FACS sorted into GFP+ (infected) and GFP- (bystander) populations and probed by immunoblotting. Blot shows one representative experiment. Bar graph is quantified from n=3 experiments, normalized to pro-caspase-11 levels in unstimulated macrophages.
(G) Timeline applies to panels H-I, Fig S1F. B6 macrophages were pre-treated with 100U/ml of IFNβ at the indicated time prior to, or concurrent with challenge by *L. pneumophila ΔsdhA*.
(H) Immunoblot of whole cell lysates from unstimulated or 1 hour IFNβ stimulation.
(I) PI incorporation as function of time after challenge of B6 macrophages by *L. pneumophila ΔsdhA* in the presence of IFNβ at noted time frames (left). Rate of cell death displayed as time to 50% of maximal cell death (middle). Maximum cell death measured at 6 hpi (right).

2.2.2 Constitutive IFNAR signaling controls the rate of macrophage cell death

Sub-threshold amounts of IFNα/β are thought to maintain expression of a set of Interferon Stimulated Genes (ISGs) required for cellular responses against infectious threats (Gough et al. 2012). To determine the impact of constitutive IFN signaling on caspase-11 activation, we treated macrophages continuously with an IFN receptor (IFNAR)-blocking antibody (clone MAR1-5A3) starting at 1hr or 20hrs prior to infection, respectively (Fig 2.2A-D). Blocking IFNAR 1hr prior to infection did not affect cell death kinetics toward the *ΔsdhA* mutant (Fig. 2.2C, D) despite the fact that the antibody efficiently blocked STAT1 phosphorylation in response to exogenous IFNβ (Fig. 2B). However, 20-hour-blockade of IFNAR prior to infection depressed cell death in response to the *ΔsdhA* mutant (Fig 2.2C, D). Macrophages from mice lacking Type I IFN receptor (*Ifnar*$^{-/-}$) also exhibited reduced cell death (Fig 2.2E). This reduction was due to a delay in onset of death, with a significant increase in time to 50% maximal cell death in *Ifnar*$^{-/-}$ macrophages compared to those from B6 mice (Fig 2.2F). Prolonged inhibition of IFNAR signaling in *Casp11*$^{-/-}$ macrophages did not reduce death further, indicating that death in macrophages lacking constitutive IFN signaling remained caspase-11 dependent (Fig. 2.9A).

We next determined if loss of constitutive IFN signaling perturbed basal levels of proteins in the caspase-11 pathway. STAT1 is an ISG whose protein abundance is sustained *via* constitutive IFNAR signaling (Gough et al. 2012; Gough et al. 2010) as can be demonstrated by a 20-hour antibody block of IFNAR reducing total STAT1 protein levels (Fig 2.2G). Similarly, 20 hours of IFNAR block resulted in reduced mRNA expression for several ISGs such as *Irf7, Isg15, and Mx1* (Fig. 2.9B). We did not observe

a reduction in baseline expression of pro-caspase-11 protein or *Casp11* mRNA under any conditions in which constitutive IFN signaling is lost (Fig 2.2H, I). Therefore, delayed cell death in the absence of IFNAR signaling is likely not due to a deficit in pro-caspase-11 abundance. Looking upstream at GBP expression, consistent with published literature, we were unable to detect GBP2 protein in B6 macrophages in the absence of IFN priming (Fig 2.2I). Since the available antibodies against other GBPs have not been stringently tested for specificity, we measured GBP expression by qRT-PCR (Fig 2.2J, Fig 2.9C-D). Of the 5 *Gbps* encoded on the chromosome 3 locus, only *Gbp2, Gbp3,* and *Gbp7* were expressed in macrophages at steady-state (Fig 2.9C), with expression of *Gbp2* and *Gbp3* reduced in *Ifnar*$^{-/-}$ and *Ifnb*$^{-/-}$ macrophages. Consistent with macrophages from the genetic knock-outs, expression of *Gbp2* and *Gbp3* were significantly reduced when antibody was applied to block constitutive IFNAR signaling (Fig 2.2J). Interestingly, not all GBPs were equally affected by constitutive IFNAR signaling status in macrophages, such as the case of *Gbp7* on chromosome 3 as well as *Gbps* encoded on the chromosome 5 locus (Fig 2.2J, Fig 2.9D).

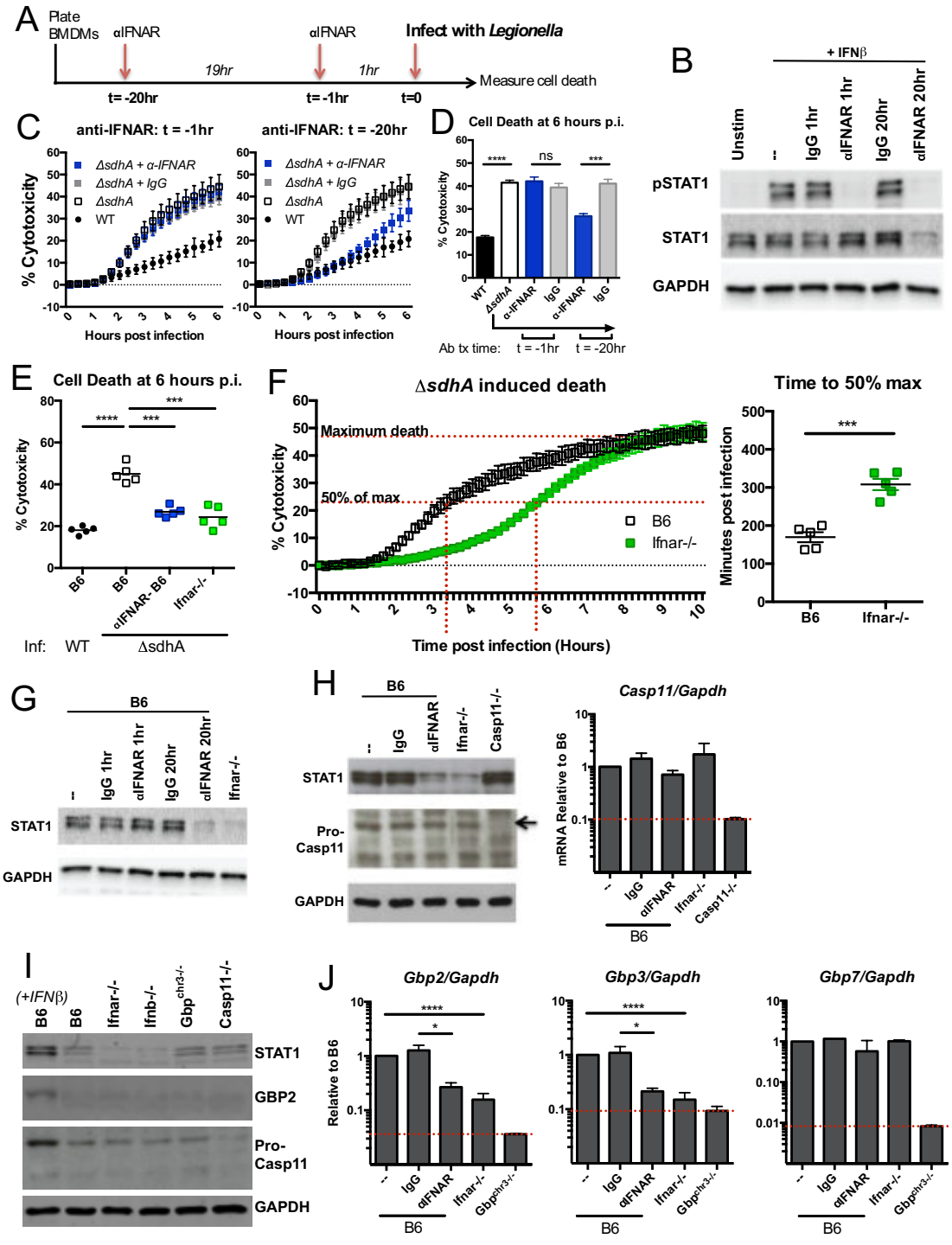

Figure 2.2. Constitutive IFNAR signaling controls the rate of macrophage cell death
(A-D) IFN receptor blocking antibody (αIFNAR) or IgG control were added for various times before or concurrent with bacterial inoculation. **(A)** Antibody block and inoculation schematics. **(B)** Immunoblot of macrophages in response to 1hr treatment with 100U/ml of exogenous IFN, in the presence of noted antibodies for 1 hour or 20 hours prior to IFNβ addition. **(C)** *L. pneumophila ΔsdhA* infection driven PI incorporation of macrophages that were treated with control IgG or αIFNAR antibody for 1 hour or 20 hours prior to infection. **(D)** PI uptake by 6 hpi; n=3.

(E) Cell death of macrophages from noted strains 6 hpi with ΔsdhA mutant, as measured by PI incorporation. αIFNAR: 20 hr pre-treatment. Triplicate averages from n=5 shown with each marker representing one experiment.
(F) Left: death of macrophages inoculated with ΔsdhA as a function of time. Red dotted lines indicate maximum death and time to 50% maximal death. Right: time to 50% maximal death plotted for triplicate averages from cells from 5 animals.
(G) Total STAT1 protein in presence of αIFNAR blocking antibody or in untreated *Ifnar-/-* macrophages were assessed by immunoblotting.
(H) Immunoblot (left) and mRNA (right) of caspase-11 expression in the presence or absence of IFN signaling. Left: arrow marks the p43 subunit of Pro-caspase-11. Caspase-11 antibody also shows a non-specific band at 37kDa (very close to the published p38 subunit). Right: dotted red line marks background amplification by qPCR from *Casp11-/-* macrophages.
(I) Steady state protein levels determined by immunoblotting of macrophages from various mouse strains probed with noted antibodies. Lysate in the first lane is from B6 macrophages treated with 100IU/ml of IFNβ for 8 hours. Other samples were unstimulated macrophages.
(J) qRT-PCR of noted genes as labeled. Dotted red line marks background amplification by qPCR from $Gbp^{chr3-/-}$ macrophages.

2.2.3 Endogenous GBP expression and rate of cell death are controlled by a narrow window of low-dose IFN signaling

Pyroptosis of *Ifnb*$^{-/-}$ macrophages exhibited delayed onset after challenge with *L. pneumophila ΔsdhA* compared to B6, consistent with reduced *Gbp2* and *Gbp3* expression (Fig 2.3A). To determine the amount of IFN needed to rescue this defect, *Ifnb*$^{-/-}$ BMDMs were treated with increasing amounts of IFNβ 20hrs prior to challenge with bacteria (Fig 2.3B). Cell death in response to challenge with the *ΔsdhA* mutant was restored with an IFNβ dose as low as 0.5U/ml (Fig 2.3B). 0.5U/ml or 1U/ml of IFNβ was enough to restore expression of STAT1 protein (Fig 2.3C), *Gbp2* and *Gbp3* (Fig 2.3D), as well as several other ISGs (*Isg15, Mx1, Irf7,* Fig 2.10) to levels observed in B6 macrophages in absence exogenous IFN addition.

We found that even a dose as low as 4U/ml of IFNβ added to *Ifnb*$^{-/-}$ macrophages was sufficient to induce a cytotoxic response that was equivalent to cells stimulated with 100U/ml of IFNβ, which is a standard dose used for IFN activation (Fig 2.3B). This parallels the amount necessary to mimic STAT1 phosphorylation levels in B6 macrophages (Fig 2.3C). Of particular interest is that for detection of GBP2 protein by immunoblotting, at least 10-50U/ml of IFNβ stimulation was needed (Fig 2.3E, F). These findings indicate that constitutive IFN signaling can be achieved with intermittent release of undetectable amount of Type I IFNs.

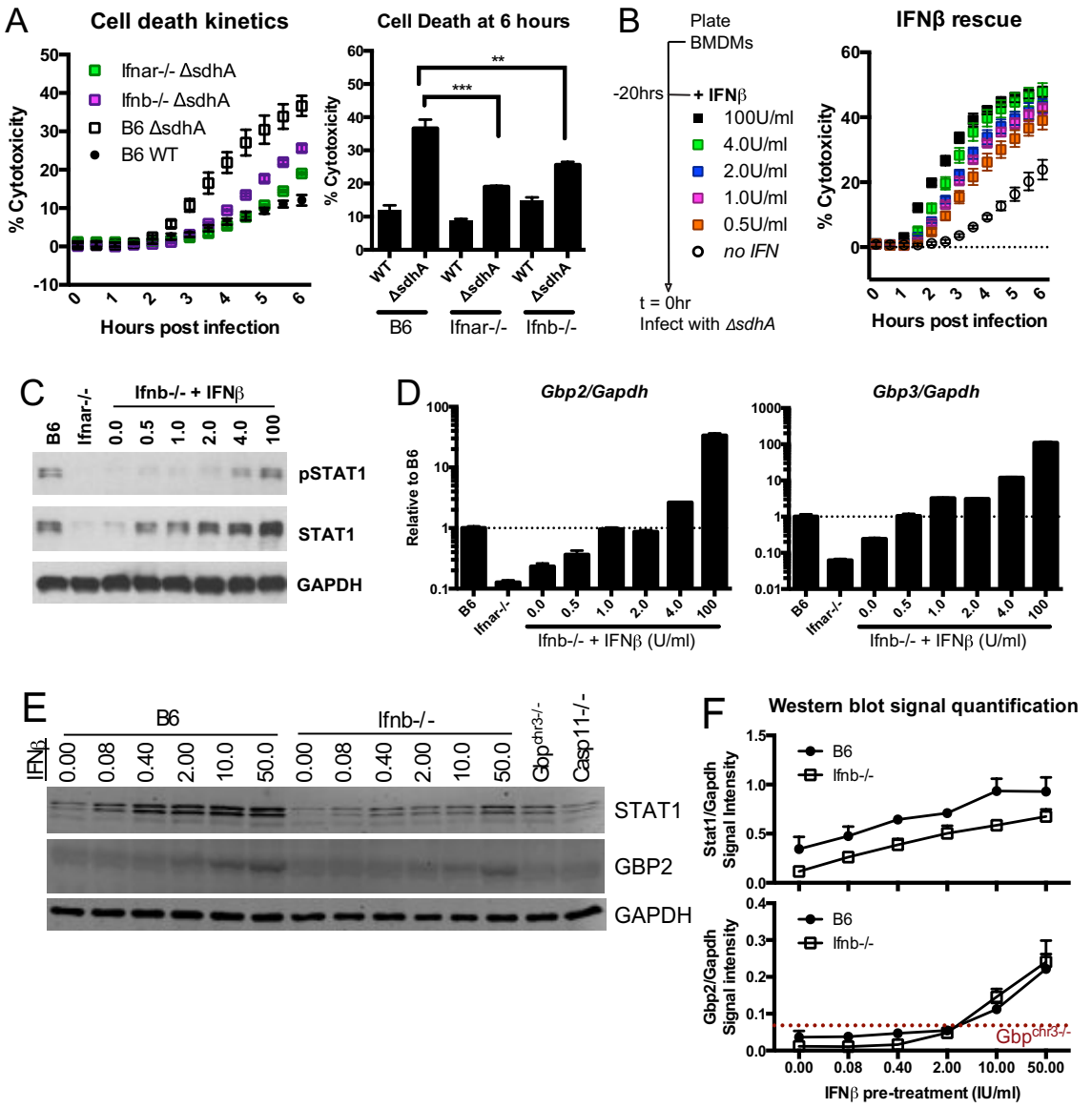

Figure 2.3. Endogenous GBP expression and rate of cell death are controlled by a narrow window of low-dose IFN signaling

(A) Macrophages from noted strains were challenged with *L. pneumophila ΔsdhA* and macrophages death measured by PI incorporation. Left: representative experiment showing kinetics of cell death. Right: Cell death determined by PI incorporation at 6 hpi. N = 3.

(B) *Ifnb*$^{-/-}$ macrophages were treated for 20 hours with noted doses of recombinant IFNβ. Cells were then challenged with *L. pneumophila ΔsdhA* and macrophages death measured by PI incorporation.

(C) Immunoblot and **(D)** qRT-PCR after 20hr treatment of *Ifnb*$^{-/-}$ macrophages with low-dose IFNβ. Dotted black line indicates steady-state expression of genes of interest in B6 macrophages.

(E, F) B6 and *Ifnb*$^{-/-}$ BMDMs were stimulated with various doses of recombinant IFNβ for 8 hours. Immunoblot shown in **(E).** Quantification of band intensity over GAPDH in **(F)**. Dotted red line indicate threshold of antibody detection on the LiCOR; representative of 3 experiments.

2.2.4 GBPs are required for cytosolic bacterial disruption

The localization of GBPs around pathogen-containing vacuoles has been associated with bacterial death (Meunier et al. 2014; Meunier et al. 2015; Man et al. 2016), although this association has not been demonstrated during restriction of either *L. pneumophila* or *Chlamydia muridarum* (Pilla et al. 2014a; Finethy et al. 2015). In addition, there is disagreement on the exact step(s) promoted by GBPs , with earlier studies suggesting a role of GBPs in pathogen vacuole disruption, and later studies seeing GBPs as functioning downstream of pre-destroyed vacuoles (Meunier et al. 2015; Man et al. 2016; Meunier et al. 2014; Man et al. 2015). We therefore sought to determine the role of GBPs in the disruption of *Legionella* containing vacuole (LCV).

The loss of LCV integrity can be assayed by immunofluorescent probing of bacteria in the absence of membrane permeabilization with detergents (Creasey & Isberg 2012). In mouse macrophages having intact innate immune function, cytosolic *L. pneumophila* assumes an aberrant morphology after breakdown of the LCV, which can be detected as the normally rod-shaped organism assuming a swollen, frayed or truncated morphology (Fig 2.4A) (Laguna et al. 2006; Creasey & Isberg 2012). We found that in macrophages lacking IFNAR ($Ifnar^{-/-}$), chromosome-3 encoded GBPs ($Gbp^{chr3-/-}$), and Caspase-11 ($Casp11^{-/-}$), loss of integrity of the *L. pneumophila ΔsdhA* vacuole was indistinguishable from that observed for B6 macrophages, indicating that constitutive IFN signaling and GBPs plays no role in vacuole disruption (Fig 2.4B). However, when challenged with *L. pneumophila ΔsdhA,* $Gbp^{chr3-/-}$ macrophages exhibited delayed and reduced maximal cell death (Fig 2.4C). Within the cytosol-accessible bacterial population, we observed

that cytosolic *L. pneumophila* retained their rod shape in *Gbp*$^{chr3-/-}$ macrophages up to 10 hours post infection, indicating that GBP function was required for inflicting damage on cytosolic bacteria (Fig 2.4D, E). In *Ifnar*$^{-/-}$ macrophages, cytosolic bacteria retained their rod-shaped morphology at early time points post-vacuole disruption (Fig 2.4F). The percentage of bacteria that exhibited aberrant morphology eventually approached levels seen in B6 macrophages by 8 to 10 hours post infection (Fig 2.4G).

WT *L. pneumophila* triggers pyroptotic cell death only when macrophages were pre-activated with IFNs, in contrast to the *ΔsdhA* mutant (Fig 2.11A, B; Fig 2.8G) (Case et al. 2013). This process requires the chromosome-3 encoded GBPs (Pilla et al. 2014a). To determine whether GBPs acted at the step of vacuole destabilization or bacterial degradation in IFN activated macrophages, WT *L. pneumophila-GFP*$^{+}$ was examined microscopically for cytosol accessibility as well as bacterial morphology (Fig 2.11C-E). 100U/ml of IFNβ pre-activation rapidly destabilized the vacuoles of WT *L. pneumophila,* increasing cytosolic accessibility by 1.5 hours post infection approximately 2.5-3 fold, irrespective of GBP or caspase-11 presence (Fig 2.11C). Notably, the percentage of cytosolic accessible bacteria declined rapidly in B6 macrophages, but was retained in *Gbp*$^{chr3-/-}$and *Casp11*$^{-/-}$ macrophages, consistent with the notion that B6 cells harboring cytosolic bacteria were lost due to rapid pyroptotic response (Fig 2.11A). Morphologically, IFN-activation resulted in the loss of rod-shaped appearance in 80-90% of cytosolic accessible *L. pneumophila* within 3 hours of infection in B6 and *Casp11*$^{-/-}$ macrophages. Almost all bacteria within the cytosolic accessible sub-population retained

their rod-shaped morphology in *Gbp*$^{chr3-/-}$ macrophages, despite IFN pre-activation (Fig 2.11D, E).

We therefore conclude that IFN pre-activation drives the synthesis of factors other than GBPs that can destabilize an intact bacterial vacuole. While GBPs were dispensable for vacuole disruption under all conditions tested, they were required for the disruption of bacteria exposed to the cytosol, a crucial event upstream of caspase-11 activation and cell death.

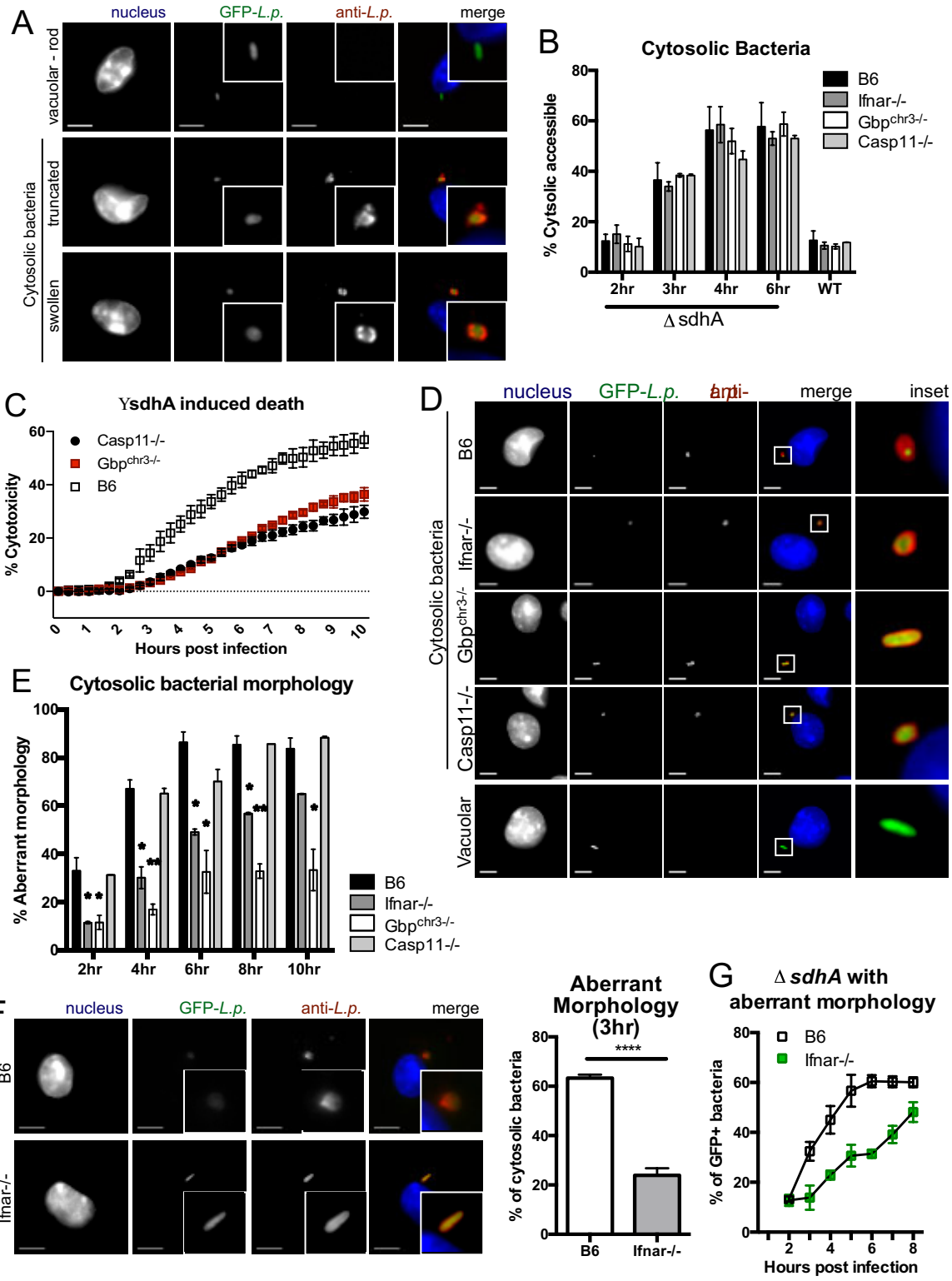

Figure 2.4. Constitutive IFN signaling hastens bacterial degradation post vacuole disruption
(A) Representative images of vacuolar and cytosolic bacteria in B6 macrophages to demonstrate various morphologies. 100x lens, scale bar = 5μm.

(B) At the indicated time points, macrophages challenged with *L. pneumophila*-GFP WT and *ΔsdhA* strains were fixed and stained with an antibody against *Legionella* with no detergent permeabilization. Percentage of antibody-stained bacteria relative to GFP^+ bacteria plotted as cytosolic bacteria.
(C) Noted macrophages were inoculated with *L. pneumophila ΔsdhA,* and macrophages death was measured by PI incorporation kinetically and quantified from n=3
(D) Representative images of cytosolic bacteria at 8 hpi. 63x lens, scale bar = 5μm.
(E) Percentage of bacteria with aberrant morphology in the cytosolic fraction at indicated time points.
(F) Left: representative images of cytosolic *ΔsdhA* in noted macrophages at 3 hpi. Images were taken with 100x lens, scale bar = 5μm. Right, percentage of bacteria with aberrant morphology quantified at 3 hpi.
(G) Percentage of cytosol-accessible bacteria with aberrant morphology, quantified by microscopy at the indicated time points.

2.2.5 Human macrophages require JAK/STAT signaling for constitutive antimicrobial responses

Caspase-4 and caspase-5 are human orthologs of mouse caspase-11 that drive activation-induced cell death in response to intracellular LPS (Shi et al. 2014; Casson et al. 2015). Similar to our observations with mouse macrophages, both human bronchoalveolar lavage (BAL) cells and human peripheral blood monocyte derived macrophages (MDM) challenged with *L. pneumophila ΔsdhA* exhibited cell death in the absence of an IFN priming event (Fig 2.5A-D, Fig 2.12). In fact, they executed pyroptosis at a faster rate than mouse BMDMs, exhibiting maximal death by 4 hours post infection (Fig 2.5A, 2.5C).

Due to the lack of reliable human IFNβ neutralizing and IFNAR blocking antibodies, we elected to use JAK/STAT inhibitors to block IFNAR signaling (Mostafavi, Yoshida, Moodley, Leboité, et al. 2016; Zurney et al. 2007; Jackson et al. 2016). Human MDMs were treated with JAK1/2 inhibitor Ruxolitinib (JAKi) for either 40 hrs prior to infection (pre-infection block), or exclusively during infection (co-infection block) (Fig 5E). Treatment of human MDMs with JAKi abolished all IFNβ-stimulated STAT1 phosphorylation, independent of treatment protocol (Fig 2.5F). Treatment with JAKi for 40 hrs also led to a drastic reduction of Stat1 protein levels (Fig 2.5F) and *hISG15* and *hMX1* mRNA expression (Fig 2.5G), indicating that there was loss of important ISG signatures. The long-term block with JAKi prior to infection significantly reduced *L. pneumophila ΔsdhA*-induced cell death in human MDMs (Fig 2.5H, 2.5I), mimicking the results we observed with antibody blockade of IFNAR in murine macrophages (Fig. 2.2A-D, G).

Examining steps upstream of cell death, we observed that LCVs within human MDMs challenged with *L. pneumophila ΔsdhA* showed loss of integrity that was similar to that observed in mouse macrophages, with 8 fold more of the *ΔsdhA* mutant becoming cytosolically exposed within 4 hours of infection (Fig 2.5J). Long term Jak1/2 inhibition prior to infection with *L. pneumophila ΔsdhA* did not reduce cytosol-permeability (Fig 2.5J). In contrast, within the cytosol-exposed *ΔsdhA* population, long term Jak1/2 inhibition prior to infection significantly decreased the percentage of bacteria with aberrant morphology (Fig 2.5K, L). These results point to the global importance of this host-derived constitutive signaling pathway in protecting against cytosolic Gram-negative pathogen.

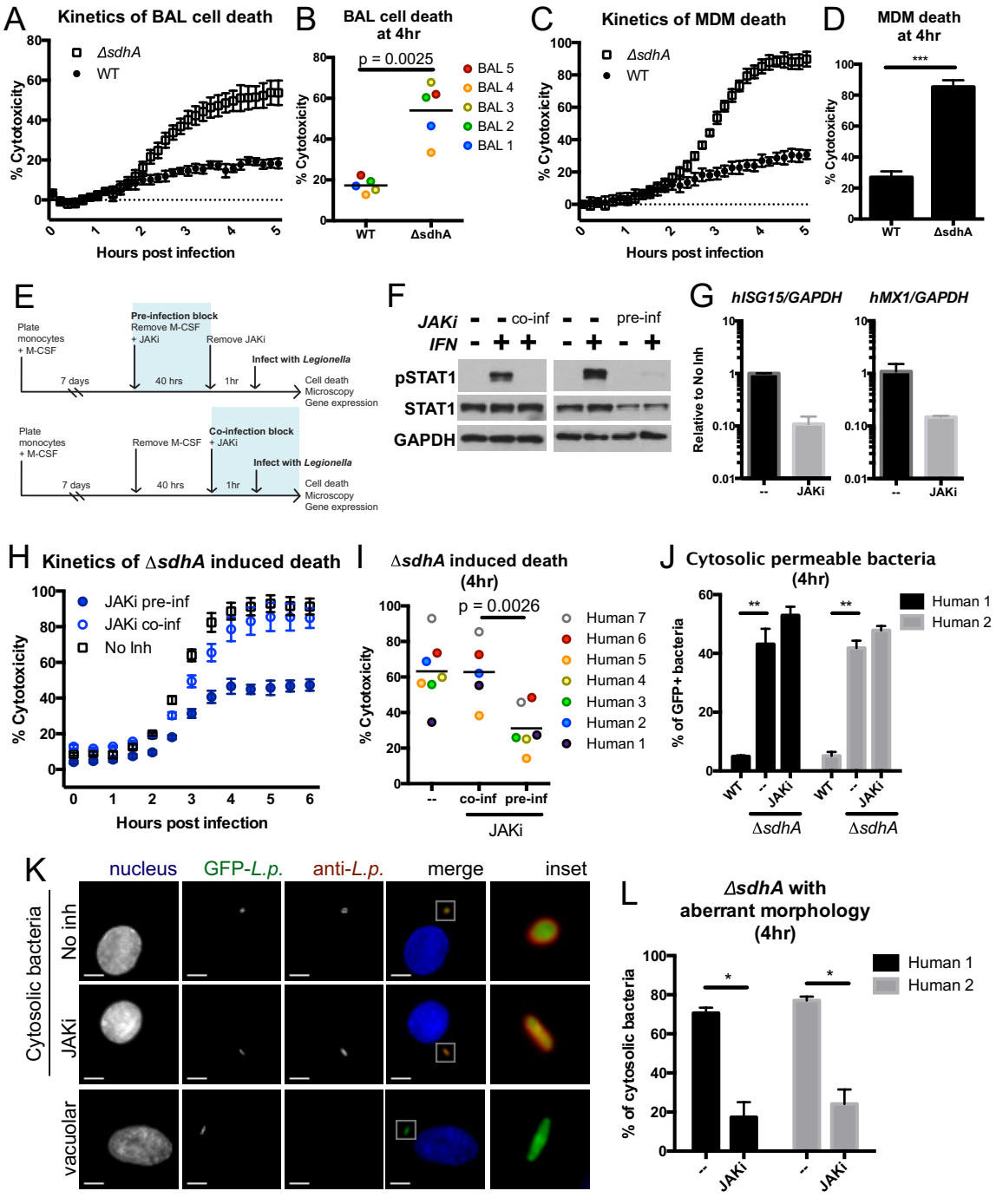

Figure 2.5. Human macrophages require JAK/STAT signaling for constitutive antimicrobial responses

(A, B) Human bronchoalveolar lavage (BAL) cells were challenged with *L. pneumophila* WT or *ΔsdhA* strains. **(A)** Cell death as a function of time assayed by PI uptake, compiled from 5 patients with mean +/- SEM plotted. **(B)** Magnitude of cell death in individual BAL samples by 4 hpi, represented as one marker per patient.

(C, D) Human peripheral blood monocyte derived macrophages (MDM) were challenged with *L. pneumophila* WT or *ΔsdhA* strains with kinetics of PI incorporation in **(C)** and maximal cell death by 4 hours post infection (representative of 3 experiments) in **(D)**.

(E) Experimental set-up for panels F-L, where human MDMs treated with JAKi prior to or concurrent with inoculation with *L. pneumophila ΔsdhA*.
(F) 200IU/ml of recombinant human IFNβ was used to stimulate human MDMs, incubated for the indicated times with JAKi. At 1 hour post IFN stimulation, lysates were collected and probed by immunoblot.
(G) Gene expression in human MDMs with or without JAKi for 40 hrs.
(H, I) PI incorporation of human MDMs in response to *L. pneumophila ΔsdhA* in presence of pretreatment or simultaneous treatment with JAKi. Representative kinetics of death in **(H),** maximum cytotoxicity from 7 individual donors in **(I).**
(J) Percentage of cytosolic accessible *L. pneumophila ΔsdhA* based on antibody staining without detergent permeabilization. Data shown from 2 individual donors.
(K) Representative images, and **(L)** quantification of cytosolic *L. pneumophila ΔsdhA* in human MDMs in presence or absence of 40hr JAKi pretreatment. Images taken with 63x lens, scale bar measures 5μm.

2.2.6 GBPs mediate the release of DNA to activate cytosolic DNA sensing pathways

To examine whether the observed bacterial morphological changes resulted in release of intracellular bacterial content into the macrophage cytosol, we probed for the presence of bacterial DNA in the cytosol of the host cell. Using *L. pneumophila* carrying the non-transferable pJB908 plasmid, the presence of pJB908 in the macrophage cytosol provides a measure of DNA resulting from loss of bacterial membrane integrity (Ge et al. 2012). We found that in B6 macrophages challenged with *L. pneumophila ΔsdhA*(pJB908), there was 2.5-3 times more plasmid detected in cytosolic extracts than in extracts from WT infected cells (Fig 2.6A), consistent with previous reports (Ge et al. 2012). In contrast, cytosolic extracts from *Ifnar*$^{-/-}$ macrophages and *Gbp*$^{chr3-/-}$ macrophages infected with the *ΔsdhA* mutant harbored significantly lower amounts of plasmid than from similarly infected B6 macrophages (Fig 2.6A). During WT *L. pneumophila* challenge, the release of pJB908 plasmid into the macrophage cytosol was enhanced by IFN pre-activation in B6 and *Casp11*$^{-/-}$ macrophages (Fig 2.6B). This enrichment is lost in *Gbp*$^{chr3-/-}$ macrophages, consistent with the retention of intact cytosolic bacterial morphology (Fig 2.6B, Fig 2.11D-E).

The passive release of bacterial DNA into the host cytosol is postulated to drive cGAS/STING activation and *Ifnb* induction. As predicted by this model, we found significantly reduced *Ifnb* induction in *Gbp*$^{chr3-/-}$ macrophages in response to *L. pneumophila ΔsdhA* (Fig 2.6C). Of interest, we found significantly heightened *Ifnb* induction in *Casp11*$^{-/-}$ macrophages, consistent with reports that Caspase 1/11 activation curtails cGAS/STING activation (Corrales et al. 2016; Wang et al. 2017).

In addition to *Ifnb* induction, GBP function has been shown to be upstream of AIM2 inflammasome activation in response to *Francisella* (Meunier et al. 2015; Man et al. 2016; Man et al. 2015). *Legionella* DNA in the host cytosol can also activate AIM2, although GBP involvement in this process is unclear (Ge et al. 2012).To examine the role of GBPs in AIM2 activation, we assayed for ASC oligomerization microscopically (specks) and IL-1β cleavage during *L. pneumophila ΔsdhA* challenge (Fig 2.6D-F). We saw peak enrichment of ASC specks in *L. pneumophila ΔsdhA*-infected B6 macrophages at 7 hours after challenge (Fig 2.6D, E; Fig 2.13). This enrichment of ASC in proximity to bacteria is best visualized in cells lacking both Caspase 1 and Caspase 11 (*Casp1*$^{-/-}$ *Casp11*$^{-/-}$) or B6 macrophages treated with zVAD to block caspase activation (Fig 2.6E left, Fig 2.13). Total numbers of macrophages harboring ASC specks also showed significant enrichment in the absence of Caspase 1 and Caspase 11 (Fig 2.6E right), consistent with pyroptosis curtailing ASC oligomerization. Of note, we observed no enrichment of ASC specks in *Gbp*$^{chr3-/-}$ macrophages in response to *L. pneumophila ΔsdhA* challenge compared to WT bacteria, either by percentage of cells harboring ASC specks, or by the presence of ASC specks near bacteria (Fig 2.6D, E). Lastly, *L. pneumophila ΔsdhA* infection resulted in the cleavage of pro-IL-1β into the 17kDa mature IL-1β fragment in B6 macrophages. This cleavage event is significantly reduced in *Casp11*$^{-/-}$ macrophages, and further reduced in *Gbp*$^{chr3-/-}$ macrophages (Fig 2.6F).

Our findings argue that the levels of GBPs in resting macrophages was sufficient for disruption of cytosol-exposed bacteria, releasing LPS and DNA, with resulting host cell death and activation of the cytosolic DNA sensing pathways respectively.

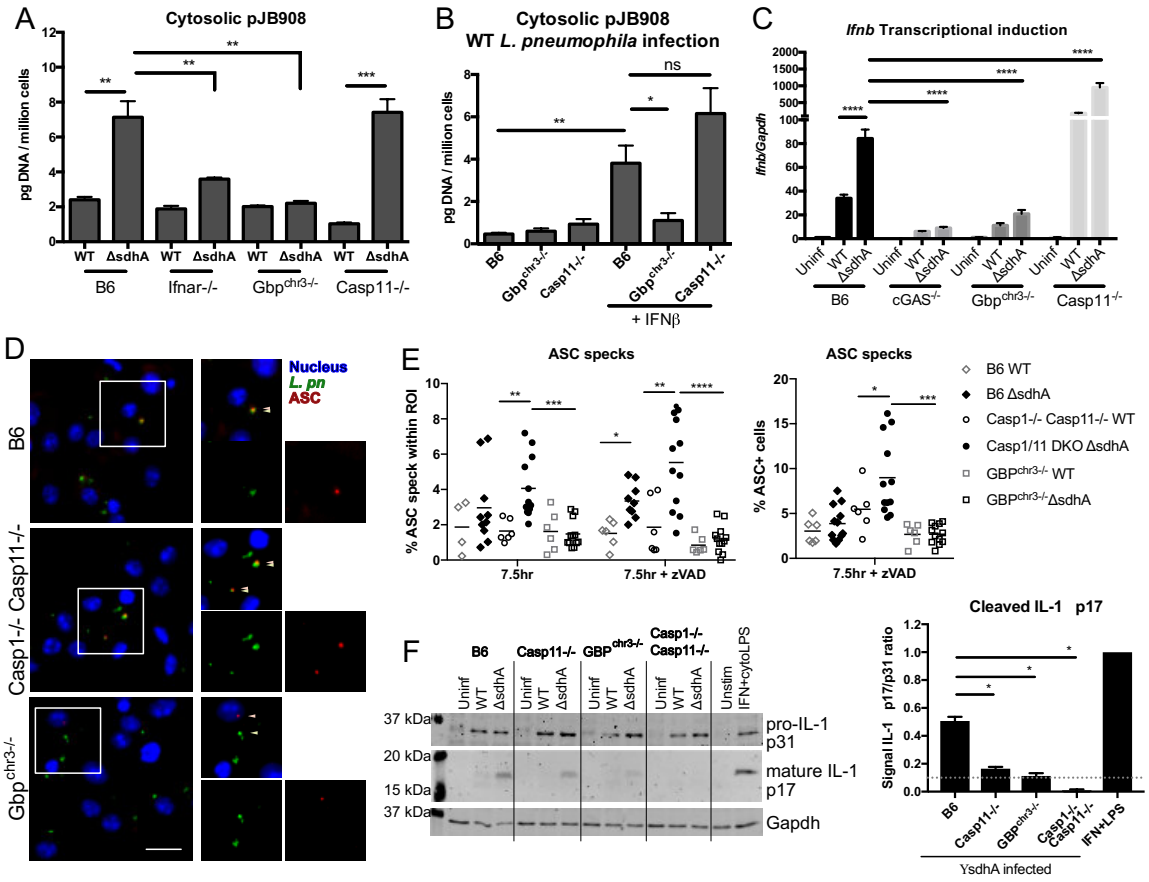

Figure 2.6. GBPs mediate bacteriolysis to release DNA and LPS for immune activation
(A) Amount of pJB908 plasmid (pg/million cells) extracted from cytosolic fractions of macrophages challenged with *L. pneumophila* (pJB908) strains, 6 hpi.
(B) pJB908 plasmid (pg/million cells) extracted from cytosolic fractions of noted macrophages that were inoculated with WT *L. pneumophila* (pJB908) 3 hpi in presence or absence of IFNβ 20 hr pre-treatment.
(C) *Ifnb* transcriptional induction from WT and *L. pneumophila ΔsdhA* infected macrophages of the indicated strains measured by qRT-PCR at 4 hpi.
(D) Representative images of *ΔsdhA L. pneumophila* and ASC co-staining at 7 hpi. Images were taken with 20x lens, scale bar = 10μm.
(E) Left: quantification of ASC positive staining gated within ROI, where ROI is defined as regions of positive anti-*L.pn.* signal. Right: quantification of ASC positive cells from total number of cells enumerated via Hoescht staining. See detailed image analysis in supplemental experimental methods. Each symbol is a technical replicate. One representative experiment out of three are shown.
(F) Whole cell lysate and precipitated supernatant from *L. pneumophila* infected cells were probed by western blot for p17 cleavage product of IL-1β. Representative western blot on the left, quantification from n=3 on the right.

2.2.7 Chromosome-3 GBPs are required for IL-1-mediated CXCL1 response during Legionella pneumonia

In *Legionella* pneumonia models utilizing flagellated bacteria, the NLRC4 inflammasome elicits a robust IL-1 response in the lungs. IL-1 receptor signaling was shown to be crucial for the induction of CXCL1 to recruit neutrophils, ultimately resulting in clearance of the bacteria (Barry et al. 2013; Tateda et al. 2001). Recently, pyroptotic macrophage corpses have been shown to retain bacteria at the site of infection. In conjunction with IL-1-mediated CXCL1 response, the influx of neutrophils engulfs the macrophage carcasses along with the trapped bacteria to facilitate clearance (Jorgensen et al. 2016). The IL-1 amplification loop leading to CXCL1 production thus appear to be crucial for clearance of bacteria that illicit inflammasome activation.

To examine the role of GBPs during *Legionella* pneumonia, B6, $Gbp^{chr3-/-}$, and $IL\text{-}1r^{-/-}$ mice were infected with $1x10^7$ of *L. pneumophila ΔflaA* or *L. pneumophila ΔflaA ΔsdhA* bacteria. We observed an acute drop in body temperature of B6 mice within the first 7 hours post *ΔsdhA L. pneumophila* infection (Fig 2.7A). These mice recovered their temperature by 20 hours post infection and did not show overt signs of illness thereafter. In contrast to B6 mice, $Gbp^{chr3-/-}$ and $IL\text{-}1r^{-/-}$ mice do not exhibit a *ΔsdhA L. pneumophila-specific* temperature drop early post infection. Temperature recovery is also delayed in $Gbp^{chr3-/-}$ and $IL\text{-}1r^{-/-}$ mice (Fig 2.7A).

Systemically, B6 animals harbor a robust, and acute increase in serum CXCL1 that coincides with the dip of body temperature (Fig 2.7B). This spike in serum CXCL1 was absent in $Gbp^{chr3-/-}$ mice and $IL\text{-}1r^{-/-}$ mice (Fig 2.7B). Looking into the inflammatory

responses localized to the site of infection, we observed a *ΔsdhA*-specific increase in IL-1α and IL-1β in the lungs of B6 and *IL-1r*$^{-/-}$ animals as early as 4-6 hours post infection (Fig 2.7C). This IL-1α and IL-1β production is further amplified during the next 10 hours post infection in B6, in a manner dependent on the presence of IL-1 receptor (Fig 2.7D). Interestingly, we did not observe the *ΔsdhA*-specific increase in IL-1α and IL-1β in the lungs *Gbp*$^{chr3-/-}$ mice at any time post infection (Fig 2.7C, D). We conclude that the loss of chromosome-3 encoded GBPs hindered IL-1 responses in the lungs, resulting in an inability to rapidly upregulate a systemic CXCL1 response during the early phase of infection.

To determine whether the perturbations in cytokine production impacted rate of bacterial clearance, we measured bacterial CFU in the lungs of B6, *Gbp*$^{chr3-/-}$, and *IL-1r*$^{-/-}$ mice. At the sub-lethal dose of $1x10^7$ bacteria, C57BL/6 mice show replication restriction toward both strains of *L. pneumophila* used, with more severe restriction with bacteria lacking SdhA. Clearance of the *ΔsdhA* mutant can be observed as early as 1 day post infection, and complete by 5 days post infection (Fig 2.7E). Compared to B6 and *IL-1r*$^{-/-}$ mice, *Gbp*$^{chr3-/-}$ mice retained significant higher loads of *ΔsdhA* mutant in the lungs at 48 hours post infection (Fig 2.7F). This prolonged persistence of bacteria in *Gbp*$^{chr3-/-}$ mice is consistent with GBP functioning upstream of IL-1 production. At 5 days post infection, although we can no longer reliably detect the *ΔsdhA* mutant, we did observe significantly higher bacterial burden for SdhA-sufficient *L. pneumophila* in both *Gbp*$^{chr3-/-}$ and *IL-1r*$^{-/-}$ mice (Fig 2.7G).

Lastly, to determine whether tonic Interferon signaling plays a role in the expression of GBPs *in vivo*, we performed RNA-sequencing in various tissue sites to assess global gene expression in uninfected B6 and *Ifnar*$^{-/-}$ animals (Fig 2.7H). Genes with higher than 2 fold expression difference between B6 and *Ifnar*$^{-/-}$ tissues are highlighted in yellow. Blue circles depict *Gbps*, and magenta circles representing classic ISGs including *Stat1, Isg15, Isg20, Irf7, Mx1, and Mx2.* In whole lungs of resting B6 animals, a few *Gbps* are skewed toward higher expression in B6 as opposed to *Ifnar*$^{-/-}$ animals. However, *Gbp* expression does not appear to be influenced by IFNAR presence in extracted alveolar macrophages, despite an overall gene expression profile that leans toward greater expression in B6. Of note, in resident peritoneal macrophages and kupffer cells, the expression of *Gbps* and classical ISGs are significantly higher in B6 than *Ifnar*$^{-/-}$. We were able to validate our RNA sequencing results from the lungs and resident peritoneal macrophages of B6, *Ifnar-/-* and *Ifnb-/-* animals (Fig 2.14). We observed reduction of varying degrees in baseline expression of *Gbp2, Gbp3,* and *Gbp7* from whole lung and peritoneal cells of *Ifnar-/-* and *Ifnb-/-* animals (Fig 2.14A, B). Interestingly, whereas all of these genes show a reliance on IFN receptor for baseline expression, IFNβ does not appear to be always required, suggesting a role for various IFNα's *in vivo* (Fig 2.14C, D).

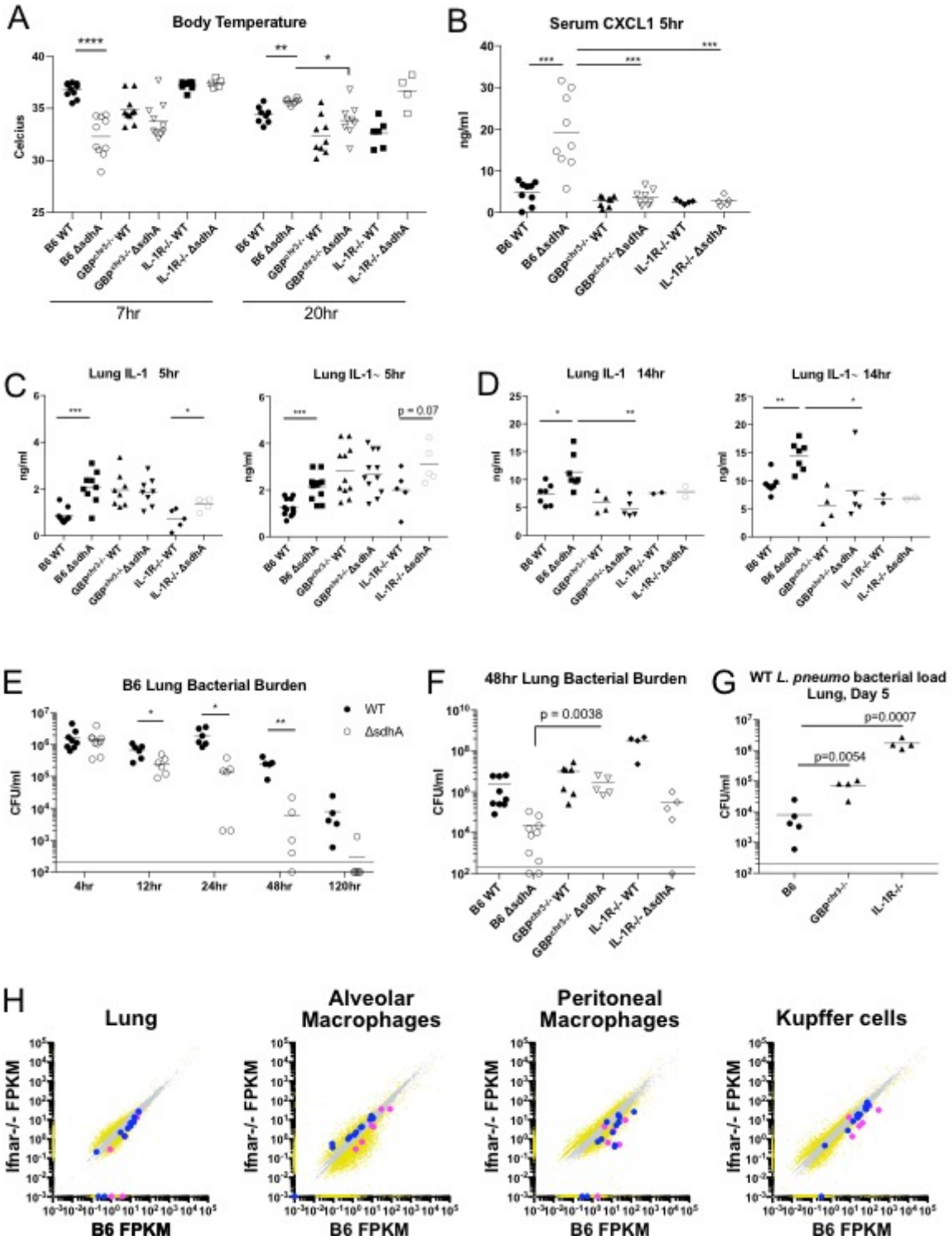

Figure 2.7. Chromosome-3 encoded GBPs are required for IL-1-mediated CXCL1 response during *Legionella* pneumonia

(A) Mice were infected with $1x10^7$ *L. pneumophila* bacteria oropharyngeally. Body temperature of mice at various timepoints post infection. Results are pooled from 2 experiments, each dot represents an animal. **(B)** Serum CXCL1 was measured by ELISA. Each dot represents an animal, results are pooled from 3 experiments in which tissues were harvested within a 4-6 hour window post infection.

(C, D) Lung IL-1α and IL-1β were measured by ELISA. Each dot represents an animal, results are pooled from 3 experiments in which tissues were harvested at the indicated time post infection.
(E, F, G) *Legionella* colony forming units from whole lung tissue from the indicated mouse strains.
(H) Whole genome RNA-sequencing was performed on the indicated tissue and cellular populations. Fragments per kilobase mapped (FPKM) is plotted. Each dot is an individual gene. Gray dots represent genes where the expression difference between B6 and *Ifnar-/-* tissue is less than 2 fold. Yellow dots represent genes in which the expression difference between B6 and *Ifnar-/-* tissue is more than 2 fold. Blue dots represent the 11 *Gbp* genes encoded on the mouse genome. Magenta represent classical ISGs *Stat1, Irf7, Isg15, Isg20, Mx1, Mx2*.

2.3 Discussion

Macrophage upregulation of an Interferon response is a common strategy against intracellular pathogens to facilitate anti-microbial activities including autophagy, pathogen recognition and attack, and host cell death (Schneider et al. 2014; Randow et al. 2013). Many recent studies have uncovered the mechanism of hyper-IFN-mediated protection (MacMicking 2012; Pilla-Moffett et al. 2016). However, in the absence of disease and infection, an immunocompetent host is quiescent for cytokine responses, with intermittent spikes of IFN occurring only during infection or immune dysregulation (Bocci 1985; Gough et al. 2012; Taniguchi & Takaoka 2001). Little is known about the initial host-pathogen encounter at the onset of infection, prior to the infection-driven IFN spike. In this work, we set out to investigate the mechanisms by which naïve macrophages respond to vacuolar and cytosolic bacteria while simulating a physiologically relevant host-pathogen initial encounter.

Using the cytosol-accessible bacteria *L. pneumophila ΔsdhA*, we found that caspase-11 action occurred independently of infection-driven IFN feedback. Instead, constitutive IFN signaling in the absence of infection maintained adequate GBP expression to mediate an attack against cytosol-accessible bacteria. We propose that upon challenge with vacuole-resident bacteria, a small percentage of mutants that are unable to maintain a stable replication vacuole engage endogenous GBPs, resulting in the release of bacterial components into the cytosol, such as DNA and LPS. Both bacterial components activate subsequent host-cytosolic pathogen recognition pathways. LPS activates caspase-11 (caspase 4/5 in humans), resulting in pyroptotic cell death and caspase-1 cleavage of IL-1 family of cytokines. The downstream executioner of pyroptosis was recently shown to be

GsdmD (Shi et al. 2015; Kayagaki et al. 2015; He et al. 2015). Simultaneously, cytosolic bacterial DNA activates the cGAS/STING pathway for initiation of *Ifna/b* induction, thus showing that GBPs act upstream of infection-induced IFN. In the absence of protein translation block, this IFN response would in turn activate neighboring bystander cells, generating an IFN-activated phenotype in yet uninfected macrophages. These IFN-activated macrophages would thus be able to lyse pathogen vacuoles in a GBP-independent manner. However, the GBPs are again needed post vacuole-disruption. In the absence of functional caspase-11, GBP-mediated release of bacterial DNA can additionally engage the AIM2 inflammasome, as previously shown (Meunier et al. 2015; Ge et al. 2012).

On a systemic level, IL-1 receptor signaling on endothelial cells amplifies the CXCL1 response to recruit neutrophils to the site of infection. Recent work by Jorgensen and colleagues showed that pyroptotic macrophage corpses can trap cytosolic bacteria, increasing the efficiency by which neutrophils can uptake and degrade the invading pathogen (Jorgensen et al. 2016). In our *Legionella* pneumonia model, we found that chromosome-3 encoded GBPs are necessary for heightened IL-1α and IL-1β produced locally in the lungs. With the absence of IL-1α and IL-1β, $Gbp^{chr3-/-}$ mice are unable to elicit a robust systemic CXCL1 response, resulting increased bacterial burden and course of illness resembling that of defective IL-1 signaling.

Upstream of endogenous GBP expression, there exists a sensitive balance in which constitutive cytokine signaling primes the system for critical immune responses to occur upon infection. This concept was best represented in $Ifnb^{-/-}$ macrophages, where the loss of ISG expression can be restored with a single low dose of IFNβ. This indicates that

even small, intermittent triggering of the IFN receptor can be effective in maintaining ISG steady-state levels. Several studies now show support for the model by which constitutive IFN production can be triggered by cell-intrinsic DNA damage via the cytosolic cGAS/STING pathway (Härtlova et al. 2015; Ahn et al. 2012; Rongvaux et al. 2014; West et al. 2015). Interestingly, we have recently shown that cGAS/STING mediated constitutive IFN signaling is crucial for macrophages to undergo necroptosis, a necrotic cell death pathway driven by RIP1/3 kinases in the presence of caspase inhibition (Sarhan, *et al*., in revision). One can speculate that *in vivo,* multiple signals may converge to maintain the homeostatic transcriptome networks downstream of IFNAR and other JAK/STAT pathways, and these signals can be derived from a number of different sources – microbiota components (Abt et al. 2012), DNA damage from tissue turnover (Lienenklaus et al. 2009), or even reactivation of endogenous retroelements (Stetson et al. 2008). Low levels of circulating cytokines can then play critical roles in conditioning innate immune cells during their maturation process, determining the rate and mechanism of response during infection. In support of this view, our RNA-sequencing efforts reveal that depending on the tissue site, different sets of genes may be responding to tonic IFN signaling. The implication of this data is beyond the scope of this current work, but may inform future studies, especially pertaining to pathogens that naturally reside at various tissue sites. Notably, the response to low levels of cytokines is conserved in humans, as macrophages from both the human and mouse respond very similarly to cytosol-resident *L. pneumophila*.

2.4 Author Contributions

B.C.L. designed and conducted experiments. B.C.L. and R.R.I. interpreted results and wrote the paper. J.S. provided experimental support and discussion. A. Panda provided human BAL cells. H.I.M. provided laboratory support. J.C., R.R.I., and A.P. provided guidance and reagents. M.Y. generated *Gbp*$^{chr3-/-}$ mice.

2.5 Supplemental Figures (2.8-2.14) and Legends

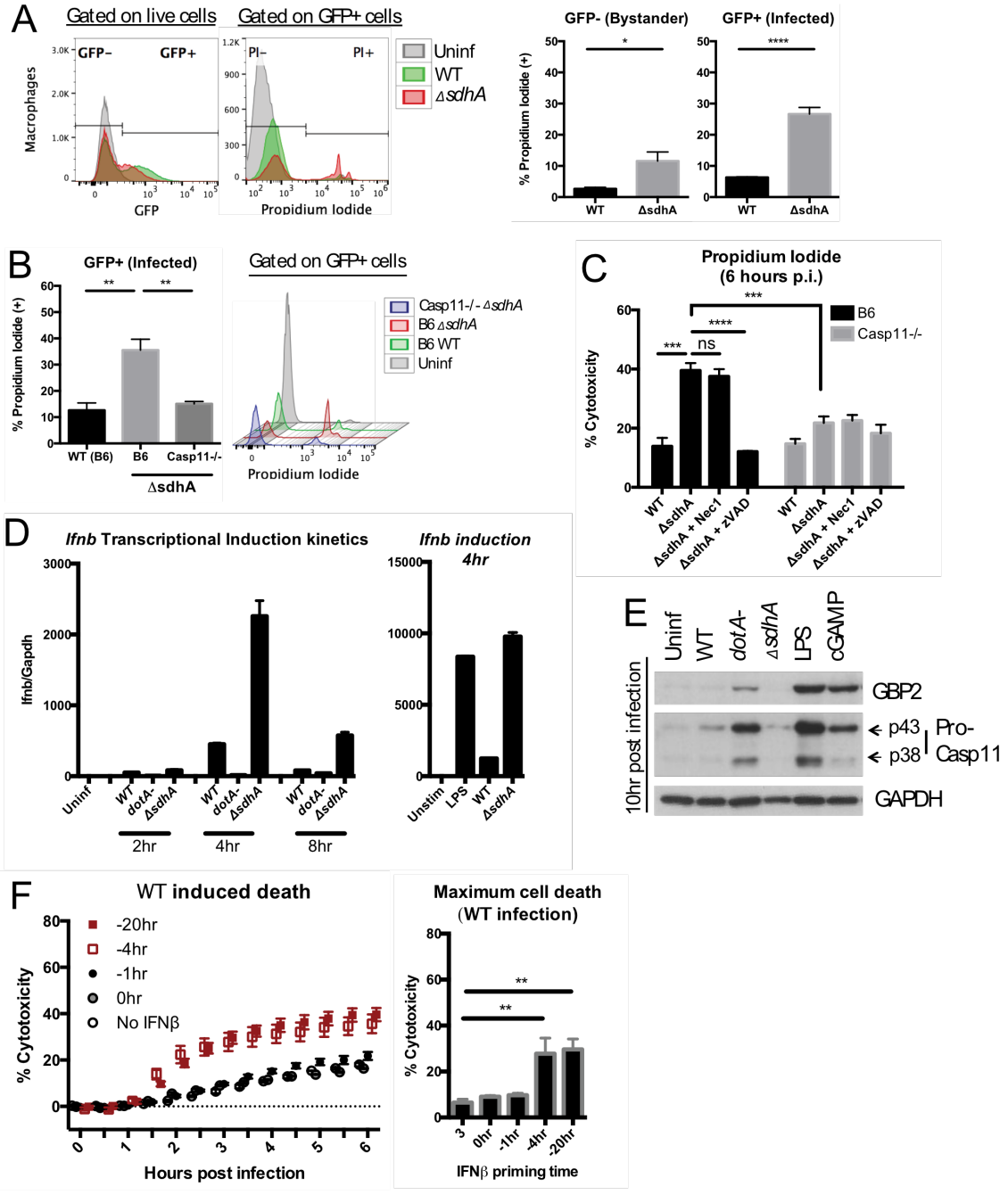

Figure 2.8.
(A, B) Macrophages were inoculated with *L. pneumophila* GFP and at 6 hpi **(A)** or 8 hpi **(B)**, cellular GFP-associated signal and propidium iodide (PI) incorporation were measured by flow cytometry. Histograms show one representative experiment. Bar graphs show compiled data from n>3 experiments of PI incorporation in the indicated gates after challenge of either B6 or *Casp11*$^{-/-}$ macrophages

(C) B6 and *Casp11*$^{-}$ macrophages were challenged with the *L. pneumophila* WT and *ΔsdhA* strains in the presence of Nec1 (RIPK1/3 inhibitor) or zVAD (pan-Caspase inhibitor). PI incorporation at 6 hpi is shown
(D) B6 macrophages were challenged with WT, *dotA*$^{-}$ mutant, or *ΔsdhA* mutants for the indicated times and *Ifnb* mRNA was measured by qRT-PCR.
(E) B6 macrophages were challenged with WT, *dotA*$^{-}$, or *ΔsdhA* strains for 10 hours. Whole cell lysates were probed by Western blot for Gbp2, pro-Casp11 and GAPDH. 10 hour LPS incubation and cGAMP transfection are displayed.
(F) B6 macrophages were pre-treated with 100U/ml of IFNβ at the indicated times points prior to, or concurrent with *L. pneumophila* WT challenge (see timeline in Fig 2.1G). Displayed is PI incorporation as a function of time (left), and maximum cell death measured at 6 hpi (right).

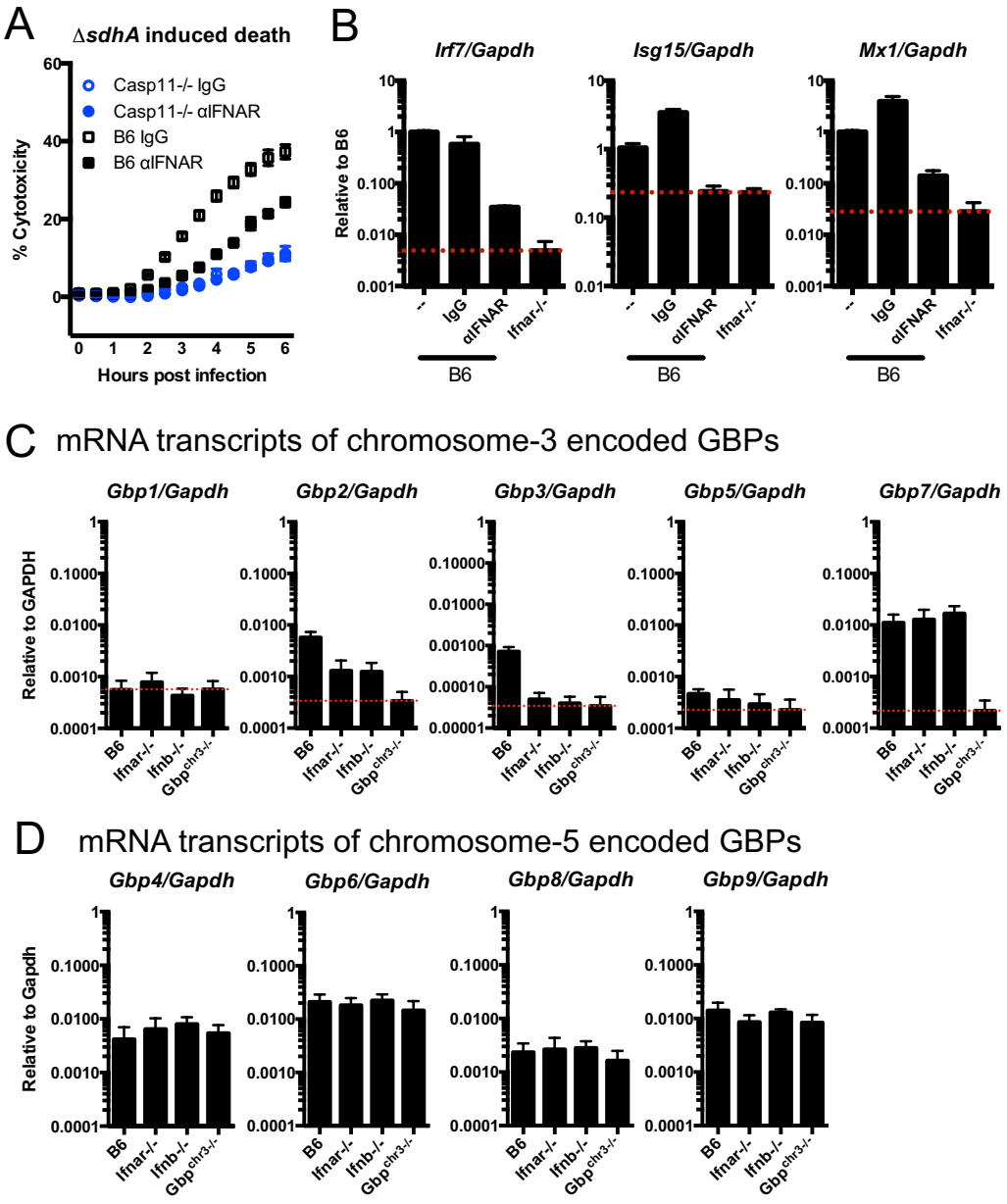

Figure 2.9.
(A) B6 and *Casp11*- Macrophages inoculated with *L. pneumophila ΔsdhA* after 20 hr treatment with noted antibodies. PI incorporation used to measure cell death.
(B) qRT-PCR of *Irf7, Isg15, Mx1* expression in the presence or absence of constitutive IFN signaling.
(C, D) qRT-PCR showing the baseline expression of noted genes in macrophages from various mouse strains. The CT values of genes of interest are normalized to sample-intrinsic *GAPDH* CT values. Dotted red line indicates background amplification from knock-out macrophages.

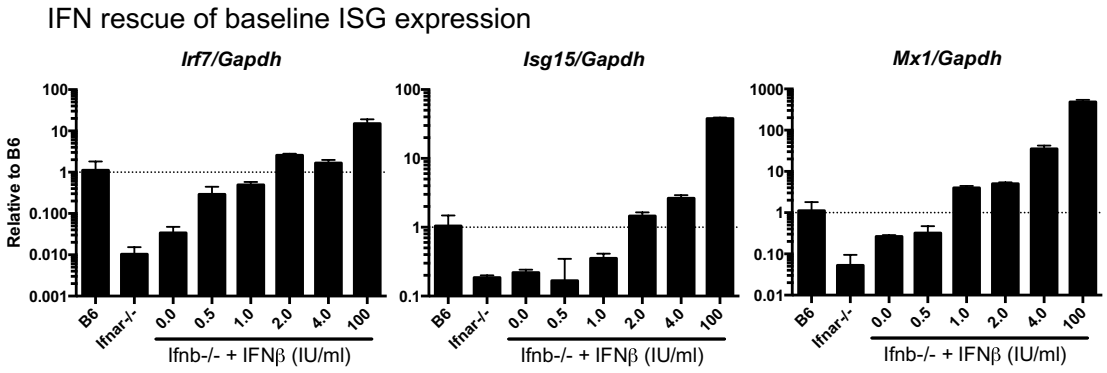

Figure 2.10.
Ifnb⁻ macrophages were treated for 20 hours with various doses of recombinant IFNβ as in Fig 2.3B, C, D). Transcript levels were measured by qRT-PCR. Dotted black line indicates steady-state expression of genes of interest in B6 macrophages.

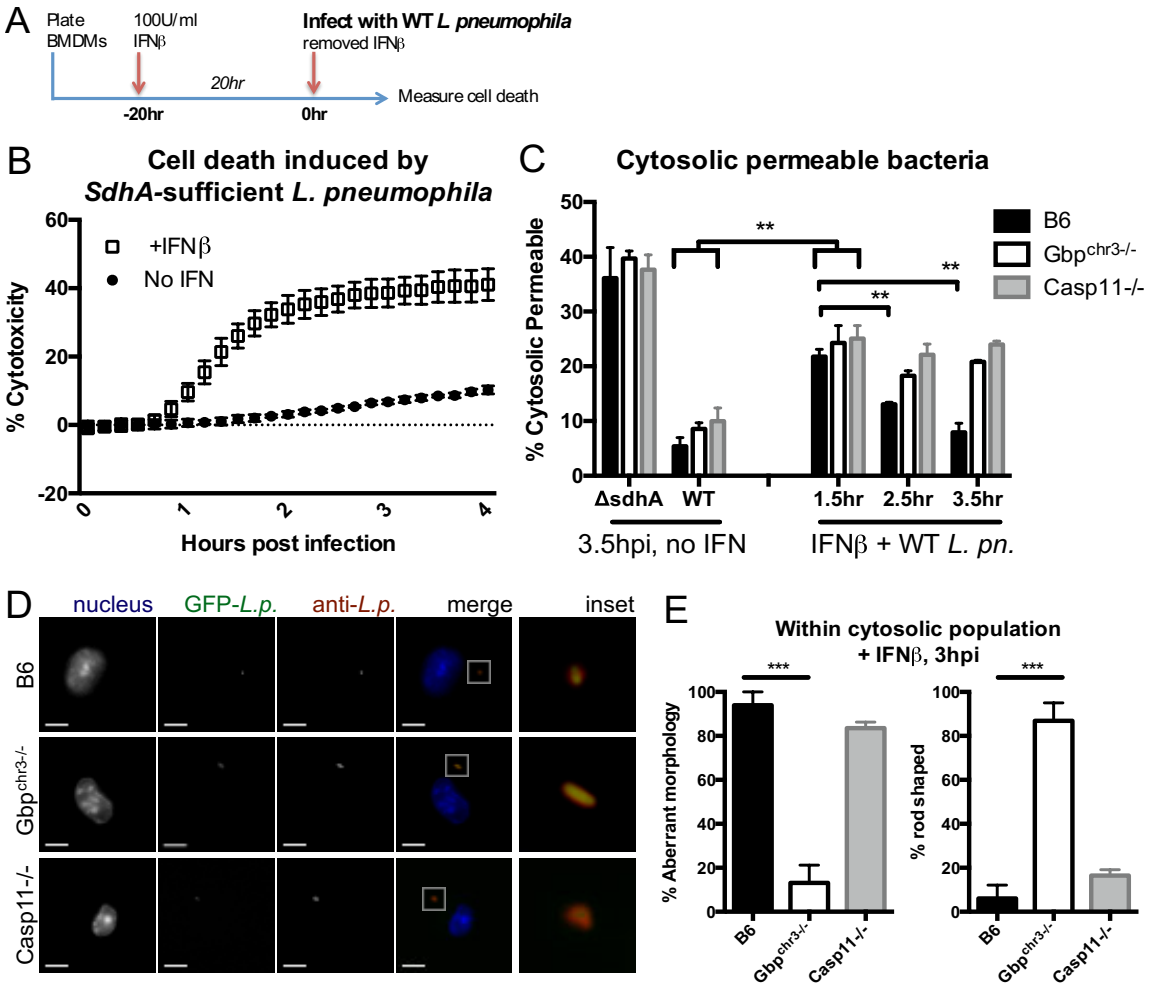

Figure 2.11.
(A) Macrophages were pre-treated for 20 hrs with 100U/ml of IFN prior to inoculation with WT L. pneumophila.
(B) Kinetics of WT L. pneumophila-induced cell death in the absence and presence of IFN pre-activation.
(C) Percentage of cytosolic-accessible L. pneumophila based on antibody staining without detergent permeabilization.
(D) Representative images of cytosolic WT bacteria in noted macrophages at 3 hpi. Images were taken using 63x lens, scale bar = 5m.
(E) Quantification of cytosolic accessible WT bacteria scored for aberrant (left) or rod-shaped (right) morphologyat 3 hpi.

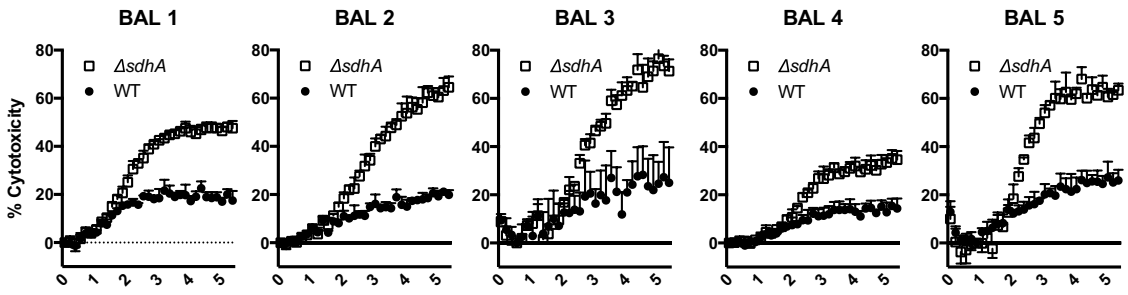

Figure 2.12.
Individual kinatics of *ex vivo* human bronchoalveolar lavage (BAL) cells infected with *L. penumophila*, 5 different donors.

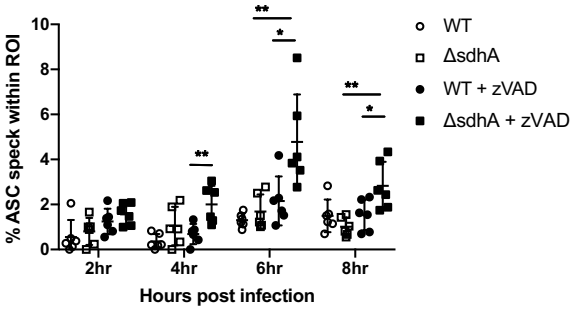

Figure 2.13.
B6 macrophages were challenged with the indicated strains of *L. pneumophila* in the presence of zVAD as indicated. ASC signal positivity was quantified within areas positive for anti-*Legionella* antibody (ROI).

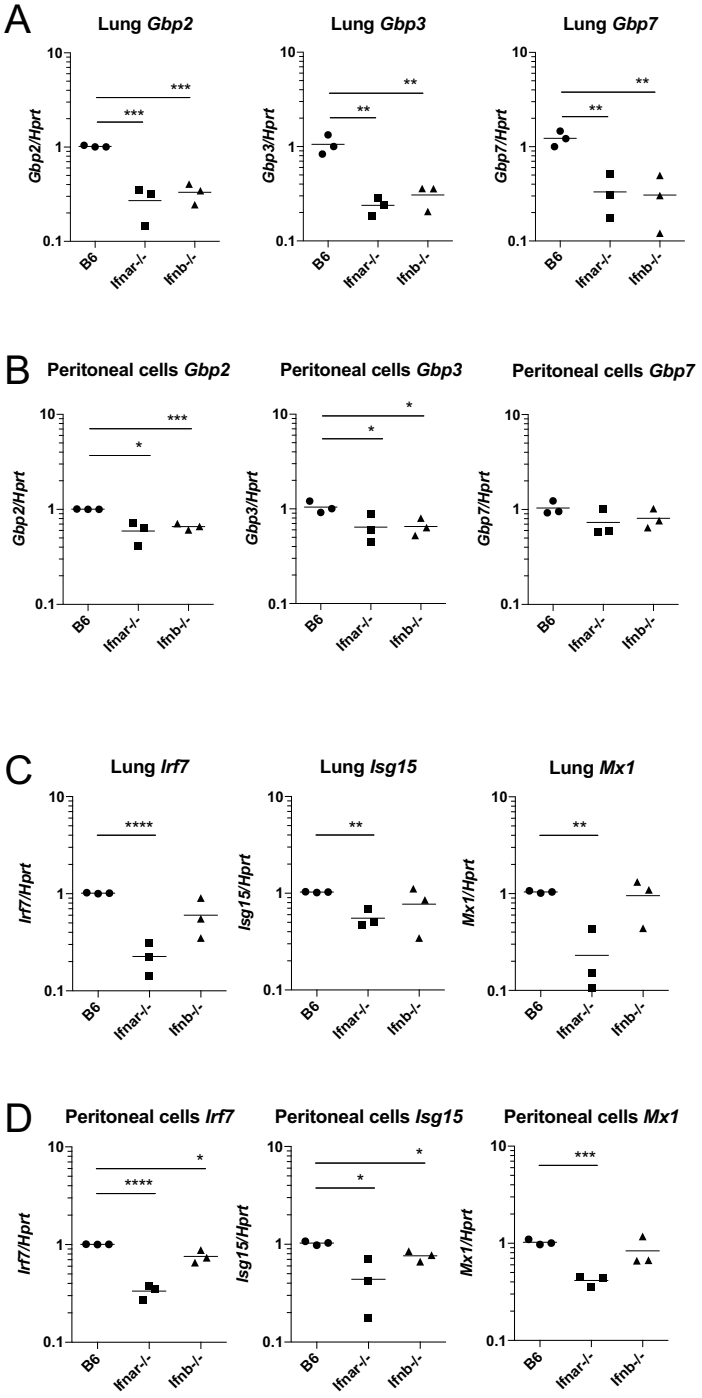

Figure 2.14.
(A-D) Whole lung tissue and resident peritoneal cells were extracted from uninfected animals of B6, *Ifnar-/-*, and *Ifnb-/-*. Indicated genes were measured by RT-PCR. Each symbol represents one animal.

2.6 Materials and Methods

2.6.1 L. pneumophila Bacteria and Infection

All *L. pneumophila* strains used in the present study are deficient for flagellin (*ΔflaA*) so as to mimic growth in amoeba and human macrophages and bypass the NLRP4/Naip5/Caspase-1 cell death pathway that occurs on the C57BL/6J genetic background. *L. pneumophila* derivatives used in this study were Lp02*ΔflaA* (*thyA rpsL ΔflaA;* referred to as WT), Lp02*ΔflaAΔsdhA* (*thyA rpsL ΔflaA ΔsdhA*; referred to as *ΔsdhA*), and Lp03*ΔflaA* (*dotA3 thyA rpsL ΔflaA*; referred to as *dotA*$^{-}$). All strains were derived originally from *Legionella pneumophila* Philadelphia-1(Berger & Isberg 1993). *L. pneumophila* was propagated on charcoal–N-(2-acetamido)-2-aminoethanesulfonic acid (ACES)–yeast extract plates with 0.1mg/mL thymidine (CYE/T) and in ACES-yeast extract broth (AYE/T) with 0.2mg/mL thymidine as previously described (Asrat, Dugan, et al. 2014; Creasey & Isberg 2012).

To generate *L. pneumophila*-GFP, PCR-amplified *gfp* gene was fused to P_{ahpC} (Coers et al. 2007) and inserted downstream of P_{tac} in the plasmid pMMB207*Δmob267* {Morales, 1991 #1; O'Connor, 2012 #2; kind gift of Dr. Kimberly Davis}. Strains harboring the plasmid were maintained on CYE plates containing 0.1mg/mL thymidine and 5μg/mL chloramphenicol. Prior to challenge of cultured cells, AYE broth cultures containing 0.2mg/mL thymidine and 2mM IPTG were grown to post-exponential phase, as described {Asrat, 2014 #3}. Inoculation into macrophage monolayer cultures was carried out at MOI = 10 in the presence of 2mM IPTG.

The plasmid pJB908 was described previously (pMMB66EH $ori_{RSF1010}$ *ΔoriT tdΔi* bla^{+}; Laguna et al. 2006). For selection, pJB908-containing strains were grown on CYE plates or in AYE broth in the absence of added thymidine.

2.6.2 Macrophages and Mice

C57BL/6 and *Ifnar*$^{-/-}$ mice were obtained from Jackson Laboratory. *Ifnb*$^{-/-}$ mice and *Casp11*$^{-/-}$ mice were kind gifts from Dr. Stephanie Vogel and Dr. Vishva Dixit respectively. Animals were housed under protocol approved by the Tufts University Medical School Animal Care and Use Committees. Bone marrow macrophages are from Gbp$^{chr3-/-}$ mice published previously (Yamamoto et al. 2012; Pilla et al. 2014a). Bone marrow-derived macrophages were isolated from mice and propagated for 7 days in RPMI containing 20% FBS, 30% L cell supernatant, 2% Penn/Strep on non-tissue culture treated Petri dishes. Unless otherwise noted, cells were plated at a density of 1x 10^6 cells per cm^2 for experiments in RPMI containing 10% FBS, no antibiotics were used during infection.

Animal infection protocols are approved by the Tufts University Medical School Animal Care and Use Committees. Mice were oropharyngeally inoculated with 1x10^7 bacteria under anesthesia. Temperature was monitored via rectal thermometer. At time points indicated in the text and figures, mice were sacrificed via CO_2 and blood and tissue were harvested for downstream cytokine and bacterial load quantification.

2.6.3 Human peripheral blood monocytes derived macrophages (MDM)

De-identified human peripheral blood was obtained from New York Biologics. The use of de-identified human samples followed a protocol approved by the Tufts University

School of Medicine Institutional Review Board. Monocytes were obtained from peripheral blood using the EasySep Direct Monocyte Isolation Kit (STEMCELL technologies). $CD14^{+}CD16^{-}CD68^{-}$ monocytes were extracted and differentiated into $CD14^{+}CD16^{-}CD68^{+}$ macrophages over the course of 7 days in RPMI containing 20% FBS, 200U/ml Penicillin and 200µg/ml Streptomycin. and 100 µg/ml of human monocyte colony stimulating factor (M-CSF; PeproTech) (Jaguin et al. 2013; Davies & Gordon 2005). Unpolarized MDMs were cultured for 40 hours further in RPMI containing 10% FBS, 200U/ml Penicillin and 200µg/ml Streptomycin, in the absence of M-CSF prior to infection. Infection was carried out at MOI = 10.

2.6.4 Human bronchalveolar lavage cells (BAL)

Bronchoalveolar (BAL) lavage was performed at Tufts Medical Center. BAL was obtained with informed consent under a protocol approved by the Tufts University School of Medicine Institutional Review Board. Subjects underwent fiberoptic bronchoscopy and BAL with 180 ml of lavage solution. With the subject under local anesthesia, a 5.5-mm O.D. fiberoptic bronchoscope was advanced through the mouth and into the trachea, and was wedged into a segmental or subsegmental bronchus of the right upper lobe. The wedged lung segment was lavaged with three aliquots of 60 ml each of normal sterile saline prewarmed to 37° C; and the fluid was gently aspirated (Freeman et al. 2015; St-Laurent et al. 2009). Cells were strained from BAL fluid using 70µm cell strainers and allowed to adhere to experimental dishes in RPMI containing 10% FBS and 200U/ml Penicillin and 200µg/ml Streptomycin, at a density of $0.5x\ 10^{6}$ cells per cm^{2}. Cells were allowed to attach for 2 hours at 37°C, 5% CO_2, at which point non-adherent

cells and antibiotics were washed away with RPMI plus 10% FBS (Davies & Gordon 2005). Bacteria were inoculated at an MOI = 10.

2.6.5 Kinetic cytotoxicity assay with propidium iodide uptake

Cells were incubated in clear bottom 96 well microplates (Costar 3603) in media containing 10μg/mL propidium iodide (PI; Life Technologies, P3566). A TECAN Infinite® 200 Pro plate reader was used to maintain temperature at 37°C and 5% CO_2 during incubations. PI uptake was monitored every 10 min at 535 nm excitation and 617 nm emission, using bottom reading setting. As a 100% cytotoxicity control, cells were treated with 0.1% Triton X-100, similar to protocols for measuring Lactate Dehydrogenase (Promega). All propidium iodide incorporation assays were performed in triplicate wells. Similar protocol was used previously (Case et al. 2013).

2.6.6 Western blotting

Macrophages were challenged with *L. pneumophila* as described (Asrat, Dugan, et al. 2014). At the desired time points, cells were lysed directly in 1X Laemmli Buffer with 5% β-mercaptoethanol, boiled for 10 minutes, and incubated on ice for 10 min prior to loading on SDS PAGE gels and Western blotting (Asrat, Dugan, et al. 2014). Primary antibodies used were anti-Caspase-11 clone 17D9 (Cell Signaling Technology #14340, 1:500), anti-GBP2 (Proteintech 11854-1-AP, 1:1000). Anti-phospho-STAT1(Tyr701) (58D6), anti-total STAT1, and anti-GAPDH were obtained from Cell Signaling Technology. Western blots were imaged using the LI-COR Odyssey CLx or by

chemiluminescent detection on film followed by analysis using LI-COR analysis software.

2.6.7 Quantitative RT-PCR

Cells were lysed with TRIzol (Thermo Fisher Scientific) and mRNA extracted by chloroform/isopropanol in accordance with TRIzol manufacturer's protocol. Quantitative PCR was performed with SYBR Green (Thermo Fisher Scientific) following cDNA generation by M-MuLV Reverse Transcriptase (New England BioLabs). Primers for Gbp genes were previously published (Kim et al. 2011). Primer sequences for *Casp11* were same as previously published (Kayagaki et al. 2011). Primers for mouse *Irf7*: (F) 5'-CTTCAGCACTTTCTTCCGAGA-3', (R) 5'-TGTAGTGTGGTGACCCTTGC-3'; *Isg15*: (F) 5'-GAGCTAGAGCCTGCAGCAAT-3', (R) 5'-TTCTGGGCAATCTGCTTCTT-3', *Mx1*: (F) 5'- TCTGAGGAGAGCCAGACGAT-3', (R) 5'-ACTCTGGTCCCCAATGACAG-3'; human *IRF7* (F) 5'-CTTGGCTCCTGAGAGGGCAG-3', (R) 5'-CGAAGTGCTTCCAGGGCA-3'; human *ISG15* (F) 5'-TCCTGCTGGTGGTGGACAA-3', (R) 5'-TTGTTATTCCTCACCAGGATGCT-3'; human *Mx1* (F) 5'-GTGCATTGCAGAAGGTCAGA-3', (R) 5'-TCAGGAGCCAGCTTAGGTGT-3'; human *GAPDH* (F) 5'-GCTCCTCCTGTTCGACAGTCA-3', (R) 5'-ACCTTCCCCATGGTGTCTGA-3'.

2.6.8 Recombinant Proteins and Inhibitors

Recombinant mouse IFNβ was purchased from Pbl Interferon Source (12405-1). Blocking antibody to mouse IFNAR (MAR1-5A3) and control IgG were purchased from BD Pharmingen. JAK1/2 inhibitor Ruxolitinib was purchased from Caymen Chemical.

2.6.9 Immunofluorescence microscopy.

Both mouse and human cells were seeded at a density of 0.5x 10^6 cells per cm^2 on MatriPlate 0.17mm glass bottom plates (DOT Scientific) in RPMI containing 10% FBS. Cells were challenged with *L. pneumophila-GFP* at MOI=10, in the presence of 0.1mg/mL thymidine and 2mM IPTG. Cultures were centrifuged at 1000rpm for 5 minutes, and at 1 hour post inoculation, extracellular bacteria were washed off with warm medium. At the desired time points, cells were washed, fixed with 2% paraformaldehyde and stained with polyclonal rabbit serum against *L. pneumophila* (1:5000), and detected with goat α-rabbit IgG-Texas Red (1:500) (Life technologies). Bacteria that were antibody reactive were quantified from the GFP^+ pool and counted as having cytosolic-permeable vacuoles. For IFN-pretreated macrophages, a second round of probing with anti-*L. pneumophila* following 0.1% TritonX-100 permeabilization was performed to expose the total bacterial population, detected with goat α-rabbit IgG-Alexa Fluor 488 (1:500) (Life technologies). Here, the total cytosolic permeable vacuoles was determined as the ratio of bacteria staining prior to permeabilization relative to the number of bacteria visualized after detergent permeabilization (Creasey & Isberg 2012).

2.6.10 Cytosolic plasmid extraction and quantification

For pJB908 plasmid extraction, the experimental protocol followed previous protocol (Ge, et al. 2012). BMDM were seeded at $12x10^6$ cells in a 10cm non-tissue culture treated dish with RPMI medium containing 10% FBS and 10% L929 cell supernatant to promote adherence. Cells were rested for 16 hours, then challenged with *L. pneumophila* harboring nontranferrable pJB908 for the amount of time indicated in the text and figure legends. Cells were lifted passively after 10 min incubation with ice-cold PBS, washed twice with ice-cold PBS, and quantified by hemocytometer. Cells were lysed with $1.0x10^7$ cells per ml of hypotonic buffer (20 mM HEPES-KOH [pH 7.5], 10 mM KCl, 1.5 mM $MgCl_2$, 1 mM Na EDTA, 1 mM Na EGTA, and the Roche protease inhibitor cocktail) on ice for 15 minutes. The lysate was then passaged 15 times through a 20G needle attached to a 3ml syringe to complete the mechanical disruption. An unrelated plasmid pUC18 was spiked into the lysate after needle disruption to control for plasmid lost during the following extraction, at a concentration of 100ng/ml. Cellular debris, including the nuclear fraction and membrane vesicles, was removed by serial centrifugation at 5 min at 1500g and 15 min at 5000g. The cleared cytosolic lysate was then subjected to 2x phenol/chloroform extraction, 2x chloroform wash, followed by precipitation in 2.5x vol ethanol and chilled to -80^oC. DNA was pelleted by centrifugation at 6,000g for 30 minutes at 4^oC. The precipitated DNA pellet was resuspended in 50ul of H_2O then serially diluted for quantitative PCR with primer sets specific to pJB908. Standard curves with known amounts of plasmids were used to back-calculate the amount of plasmid contained in cytosolic fractions. Primer sets for pJB908 was published previously (Ge et al. 2012). Primers for pUC18 flanks the M13 cloning

site of the vector. (F) 5'-CAGGAAACAGCTATGAC -3', (R) 5'-GTAAAACGACGGCCAG-3'.

2.6.11 ASC speck quantification

Cells were seeded at a density of 0.5x 10^6 cells per cm^2 on MatriPlate 0.17mm glass bottom plates (DOT Scientific) in RPMI containing 10% FBS. At indicated time point post challenge with *L. pneumophila,* cells were fixed/permeabilized via ice cold methanol. Polyclonal rat serum against *L. pneumophila* (1:5000) and rabbit anti-ASC antibody were used to recognize *L. pneumophila* and endogenous ASC. Goat anti-rat AF488 and goat anti-rabbit AF594 were used to visualize *L. pneumophial* and ASC, respectively. 25 fields at 20x magnification was captured and stitched by the Cytation3 automated microscope, generating field of view with 3000 cells each for image quantification. Signal intensity of *L. pneumophila* and ASC were analyzed with the Gen5 software, using un-infected wells, and Asc-/- macrophages as negative controls to determine the appropriate signal intensity and puncta size. Puncta signal less than 3um in size are considered positive events.

2.6.12 RNA-sequencing

Total RNA was isolated from uninfected mouse tissues and cellular populations using TRIzol and used to make a directional cDNA library using TrueSeq kit. For whole lungs and resident peritoneal cells, each sample was pooled from two animals of the same genotype. For alveolar macrophages and kupffer cells, each sample was pooled from 5 animals of the same genotype. cDNA libraries were sequenced on HiSeq (Illumina) and

aligned using TopHat2 and Cufflinks software. Fragments per kilobases mapped was plotted in Prism7. Colors for data visualization is described in the text and figure legends.

2.6.13 Statistical Analysis

Statistical analyses were performed using the Student's t test (two-tailed) using GraphPad Prism7. Experiments involving human samples were analyzed using paired analysis, in which each pair consists of cells from the same donor.

Chapter 3: Caspase-8 induces cleavage of multiple Gasdermins to elicit pyroptosis during *Yersinia* infection[2]

[2] Beiyun C. Liu*, Joseph Sarhan*, Rachael Nilson, Amy Tang, Anthony Rongvaux, Stephen C. Bunnell, Alexander Poltorak. To be submitted to *Nature Communications*

* These authors contributed equally to the work; names are listed by alphabetical order.

3.1 Background

Cell death and inflammation are critical regulators of immune responses which must be carefully balanced to ensure host survival during infection. Upon initial pathogen contact with innate immune cells, such as a macrophage, the host cell signals through pattern recognition receptors such as Toll-like Receptors (TLRs) that simultaneously engage a cell intrinsic pro-survival program while pumping out inflammatory cytokines to propagate the alarm of infection (O'Neill et al. 2013; Takeuchi & Akira 2010). These cytokines are critical for the activation and recruitment of further waves of innate and adaptive immunity, as well as reinforcing the inflammation loop via autocrine signaling in the current population. Successful pathogens have therefore evolved ways to evade host cytokine-induction to survive and replicate silently amongst host immune cells. This is done either by modifying surface pathogen associated molecular patterns that cannot be recognized by macrophage TLRs, or via active blockade of macrophage signaling pathways downstream of TLR activation (Reddick & Alto 2014; Krachler et al. 2011).

To counteract the latter, these same pro-survival, pro-cytokine signaling pathways also have in-built switches to engage cell death when the cell perceives a block to its ability to produce cytokines (Mihaly et al. 2014; Park et al. 2005). One of the best examples of such a switch lies downstream of Tumor Necrosis Factor (TNF) receptor. TNF receptor signaling engages the TNF receptor associated adaptor TRADD (Hsu et al. 1995) to recruit RIP1 via death domain (DD) interactions (Hsu et al. 1996), forming complex I. Complex I formation results in the activation of the MAP kinases and NFκB, which drive the production of inflammatory cytokines and pro-survival factors (Kelliher et al. 1998). In cases in which MAP kinases and/or NFκB signaling is blocked, RIP1 can

dissociate from TNF receptor to facilitate the formation of complex IIa by interacting with FADD and pro-Caspase-8. Complex IIa leads to caspase 8 activation and cell death (Micheau & Tschopp 2002). If caspase activity is blocked, the signaling complex transitions to complex IIb, in which RIP1 engages RIP3 to activate an MLKL dependent necrotic cell death mechanism known as necroptosis (Feltham et al. 2017; Li et al. 2012; Murphy et al. 2013; Cai et al. 2013). Necroptosis has similarly been shown to occur downstream of TLR signaling in recent years (Kaiser et al. 2013; He et al. 2011).

The success of MAP kinase and NFκB signaling thus are critical determinants of life and death of a cell. MAP kinase and NFκB pathways diverge from a single protein complex consisted of TGFβ-associated kinase (TAK1), TAB1, and TAB2, where TAK1 experiences constitutive phosphorylation and baseline activity (Omori et al. 2012; Mihaly et al. 2014). During embryogenesis, whole body TAK1 deficiency results in embryonic lethality between days 9.5-10.5, in part due to death of MEFs from TNF receptor ligation (Sato et al. 2005). Loss of TAK1 during macrophage development similarly lend the cell susceptibility to tonic TNF signaling-induced death (Wang et al. 2015). This was followed up by the discovery that TNF stimulation in the context of TAK1 deficiency leads to cell death via caspases - complex IIa, or death by necroptosis in the case of caspase inhibition - complex IIb (Lamothe et al. 2013; Morioka et al. 2014). Similarly, whole body RIP1 deficiency results in perinatal lethality, where *Rip1*$^{-/-}$ and conditionally null animals show exquisite sensitivity to tonic TNF induced death (Kelliher et al. 1998; Rajput et al. 2011).

Given such intertwining relationship between cytokine production and cell death during infection, the central question thus becomes, what is achieved upon cell death if

cytokines, the universal alarms, cannot be adequately made in the first place? The well-studied bacteria of the *Yersinia* species may lend an answer. *Yersinia* species express a number of *Yersinia outer proteins (YOPs)* that manipulate various macrophage cytosolic processes (Viboud & Bliska 2005). One such protein YopJ, has been well studied in its inhibition of TAK1via acetylation (Paquette et al. 2012) and consequent induction of macrophage cell death (Monack et al. 1997). Yersinia induced cell death was recently shown to be a caspase 8 dependent, RIP3 independent process. Paradoxically, while *Rip3*$^{-/-}$*Casp8*$^{-/-}$ macrophage are protected from cell death, the animals are exquisitely sensitive to the infection, characterized by uncontrolled bacterial outgrowth (Philip et al. 2014; Weng et al. 2014). Similarly, *Yersinia* induced macrophage cell death is strongly RIP1 kinase activity dependent, where RIP1 kinase inactive animals also show increased sensitivity to infection (Peterson et al. 2017). These studies suggest that macrophage death in the context of *Yersinia* infection is protective for the animal host.

Interestingly, despite the ability of YopJ to dampen cytokine production, *Yersinia* infections in mice elicit a robust IL-1 response, with IL-1 receptor signaling playing a crucial role in the survival of the animal (Ratner et al. 2016). IL-1 maturation requires the formation of a caspase nucleation event termed the inflammasome. The basic composition of the inflammasome involves a cytosolic "danger" sensor such as NLRP3 that nucleates upon activation, recruiting an adaptor protein containing a CARD domain to oligomerize multiple units of pro-caspase-1 (Sutterwala et al. 2014; Lawlor & Vince 2014). Caspase-1 is activated via induced proximity to cleave pro-IL-1 and pro-IL-18. The release of mature IL-1 during inflammasome-driven cell death was termed pyroptosis (Bergsbaken et al. 2009). With the discovery that Caspase-11 drives

pyroptosis via activation of pore forming protein Gasdermin D (GsdmD) (Shi et al. 2015; Aglietti et al. 2016), NLRP3 inflammasome was found to activate as a consequence of plasma membrane rupture and the efflux of potassium ions (He et al. 2015). More recently, activation of the NLRP3 inflammasome has also been observed during necroptosis (Conos et al. 2017), suggesting that inflammasome formation may be a commonality shared amongst many necrotic forms of cell death.

In this work, we set out to investigate the morphological features of the caspase-8 driven cell death elicited by *Yersinia* YopJ, using *Yersinia pseudotuberculosis* as our infection model. To simplify a complex infection system to minimal manipulate-able units, we additionally use LPS and 5Z-7-Oxozeaenol (5z7), a potent small molecule inhibitor of TAK1 (Jiaquan Wu et al. 2013), to mimic the basic cell death phenotype induced by *Yersinia.* We found that *Yersinia* induced cell death bears a striking resemblance to pyroptosis in morphology, the involvement of multiple Gasdermins, and the potency of IL-1 production. This led us to conclude that caspase 8 can drive pyroptosis in cases of TAK1 inhibition during inflammatory signaling, a phenomenon exemplified by *Yersinia* infection, and possessing far reaching possibilities.

3.2 Results

3.2.1 During TAK inhibition, TLR stimulation drives caspase-8 dependent cell death, with necroptosis as a backup mechanism.

Yersinia species, including *Yersinia pestis* and *pseudotuberculosis*, induce macrophage cell death via effector YopJ inhibition of level three MAP kinase TAK1 (Monack et al. 1997; Paquette et al. 2012). We use nuclear incorporation of propidium iodide to kinetically monitor the rapidity of cell death, and see that in B6 macrophages, cell death marked by loss of membrane integrity is complete by 4-6 hours post bacterial challenge (Fig 3.1). This rapid cell death can be partially rescued by inhibition of caspases or RIP kinases using small molecules inhibitors zVAD and Nec1, respectively. However, complete ablation of *Yersinia* driven cell death requires the addition of both zVAD and Nec1 (Fig 3.1A, right). We can effectively mimic this response by co-stimulation of macrophages with the small molecule inhibitor of TAK1 - 5z7 in combination with a TLR agonist, in this case LPS (Fig 3.1A, left).

Necrostatin-1 (Nec1), the small molecule inhibitor of RIP1 kinase activity, is used to block necroptosis as driven by RIP1/RIP3 and the effector of necroptotic cell death MLKL (Xie et al. 2013; Degterev et al. 2008). Given the partial protection with Nec1, we investigated the contribution of necroptotic players during *Yersinia*-driven, as well as LPS/5z7 driven cell death. Using genetic knock-outs of RIP3 and MLKL macrophages, we found that *Rip3*$^{-/-}$ and *Mlkl*$^{-/-}$ macrophages are fully susceptible to Yersinia and LPS/5z7 driven cell death (Fig 3.1B, C). With the addition of zVAD, *Rip3*$^{-/-}$ and *Mlkl*$^{-/-}$ macrophages become protected from death, indicating that in the context of TAK inhibition, necroptosis is engaged only when caspase activity is blocked. However, the

full susceptibility of RIP3 and MLKL deficient cells to *Yersinia*-driven death argues that necroptosis is not the primary pathway of cell death during *Yersinia* infection. Addition of Nec1 during *Yersinia* challenge or LPS/5z7 stimulation show partial protection regardless of the presence of RIP3 or MLKL.

Working upstream in the pathway, RIP1 kinase activity plays critical roles for the initiation of necroptosis during caspase inhibition (Cho et al. 2009; Tenev et al. 2011). However, RIP1 also has a role in TNF driven apoptosis via the formation of complex II (Micheau & Tschopp 2003; Hsu et al. 1996). We found that RIP1 kinase inactive (RIP1K45A) macrophages are partially protected from Yersinia and LPS/5z7 driven cell death, recapitulating the effect of Necrostatin-1 addition (Fig 3.1D) (Peterson et al. 2017). RIP3 kinase inactive macrophages behave as *Rip3*$^{-/-}$ macrophages (Fig 3.1E), and RIP1/3 double kinase inactive macrophages show similar susceptibility as RIP1 single kinase activity (Fig 3.1F). RIP1 thus plays an enhancement role in driving cell death during *Yersinia* infection, but is not the critical factor. Lastly, cells deficient for RIP3 and Caspase 8 are fully protected from Yersinia and LPS/5z7 driven cell death (Fig 3.1G) (Weng et al. 2014; Philip et al. 2014). Given that *Rip3*$^{-/-}$ macrophages are fully sensitive to cell death, the additional loss of Caspase 8 lending full protection indicates that caspase-8 is the primary driver of cell death, consistent with prior reports (Philip et al. 2014; Weng et al. 2014). Yersinia-induced, as well as TLR stimulation under TAK1 inhibition thus drives a mode of rapid cell death that is caspase-8 driven, with partial contribution from RIP kinase 1.

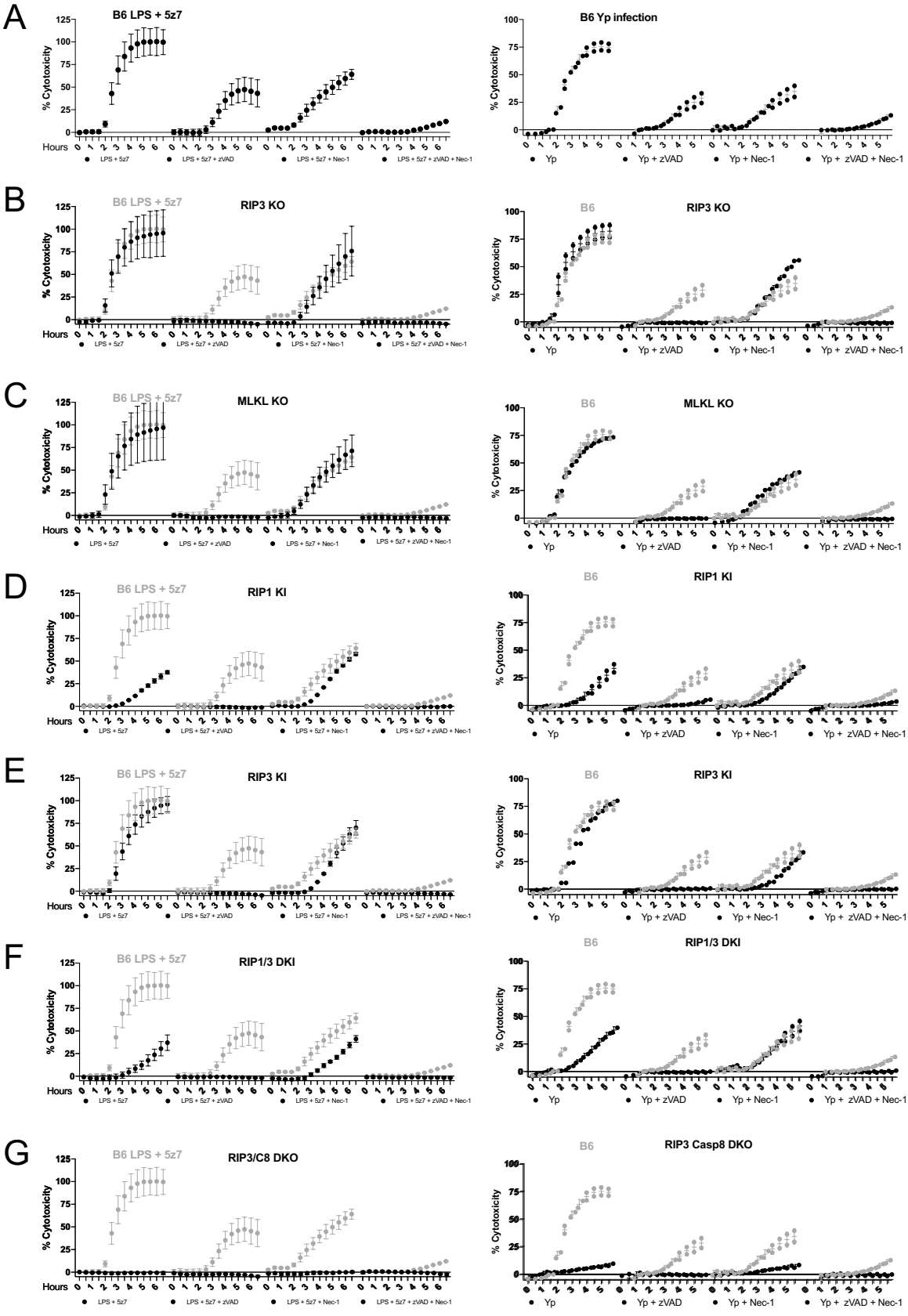
A
B6 LPS + 5z7
B6 Yp infection
% Cytotoxicity
Hours
LPS + 5z7
LPS + 5z7 + zVAD
LPS + 5z7 + Nec-1
LPS + 5z7 + zVAD + Nec-1
Yp
Yp + zVAD
Yp + Nec-1
Yp + zVAD + Nec-1
B
RIP3 KO
B6
C
MLKL KO
D
RIP1 KI
E
RIP3 KI
F
RIP1/3 DKI
G
RIP3/C8 DKO
RIP3 Casp8 DKO

Figure 3.1. During TAK inhibition, TLR stimulation drives caspase-8 dependent cell death, with necroptosis as a backup mechanism.
(A - G) Bone marrow derived macrophages from C57BL/6 (B6) and various genetically modified animals were stimulated with LPS/5z7 on the left and *Yersinia pseudotuberculosis* IP2999 on the right. Percentage cytotoxicity was calculated by microscopy via counts of propidium iodide positive nuclei per field of view, normalized to 100% lysis by 0.1% Triton-X. Caspases were inhibited with zVAD treatment, and RIP kinase activity was inhibited with Necrostatin-1 (Nec1).
Data for all panels generated by J.S.

3.2.2 TAK-inhibition results in necrotic cell death, exhibiting pan-caspase activation and the externalization of cytosolic content

Traditionally, caspase-8 activation has been associated with apoptosis, characterized morphologically by the shedding of apoptotic bodies and retainment of membrane integrity during death in order to promote efferocytosis over secondary necrosis and the release of cytosolic contents (Taylor et al. 2008). However, the rapidity of propidium iodide uptake during Yersinia and LPS/5z7 driven cell death is suggestive of a lytic cell death. Indeed, LPS/5z7 induces rapid and indiscriminate release of cytosolic contents into the surrounding culture media as compared to the canonical apoptosis stimulant etoposide, and the recently synthesized small molecule raptinal, which drives cell death via caspase-9 activation of caspases 3 and 7 (Fig 3.2A) (Palchaudhuri et al. 2015; Hande 1998).

Probing for caspase activation and their appearance in the supernatant. We found that the majority of fragments corresponding to active caspase 8, caspase 9, caspase 3, and caspase 7 have accumulated in the supernatant by 5 hours of LPS/5z7 stimulation (Fig 3.2B). In contrast, these cleaved caspase fragments can be seen at 5 hours in cell lysates of etoposide treated cells, but the appearance of cleaved caspase 3 and caspase 7 is not seen in the supernatant until over 16 hours.

Amongst the other cytosolic contents released upon LPS/5z7 stimulation include cleaved PARP, cyclophilinA, and Gapdh. Congruent with the cell death kinetics, the apoptosis machinery is blocked with addition of zVAD, which switches the cell fate to necroptosis, as indicated by the appearance of phosphorylated-MLKL in conditions with zVAD addition (Fig 3.2C). We confirmed with macrophages deficient for both RIP3 and

Caspase 8 that the release of cytosolic content during LPS/5z7 stimulation is as a consequence of cell death. With Caspase 8 absent, the cleavage of Caspase 3 and PARP are no longer present beyond baseline levels, and cytosolic proteins such as cyclophilinA, Gapdh, and Actin remains intracellular during LPS/5z7 stimulation (Fig3. 2D).

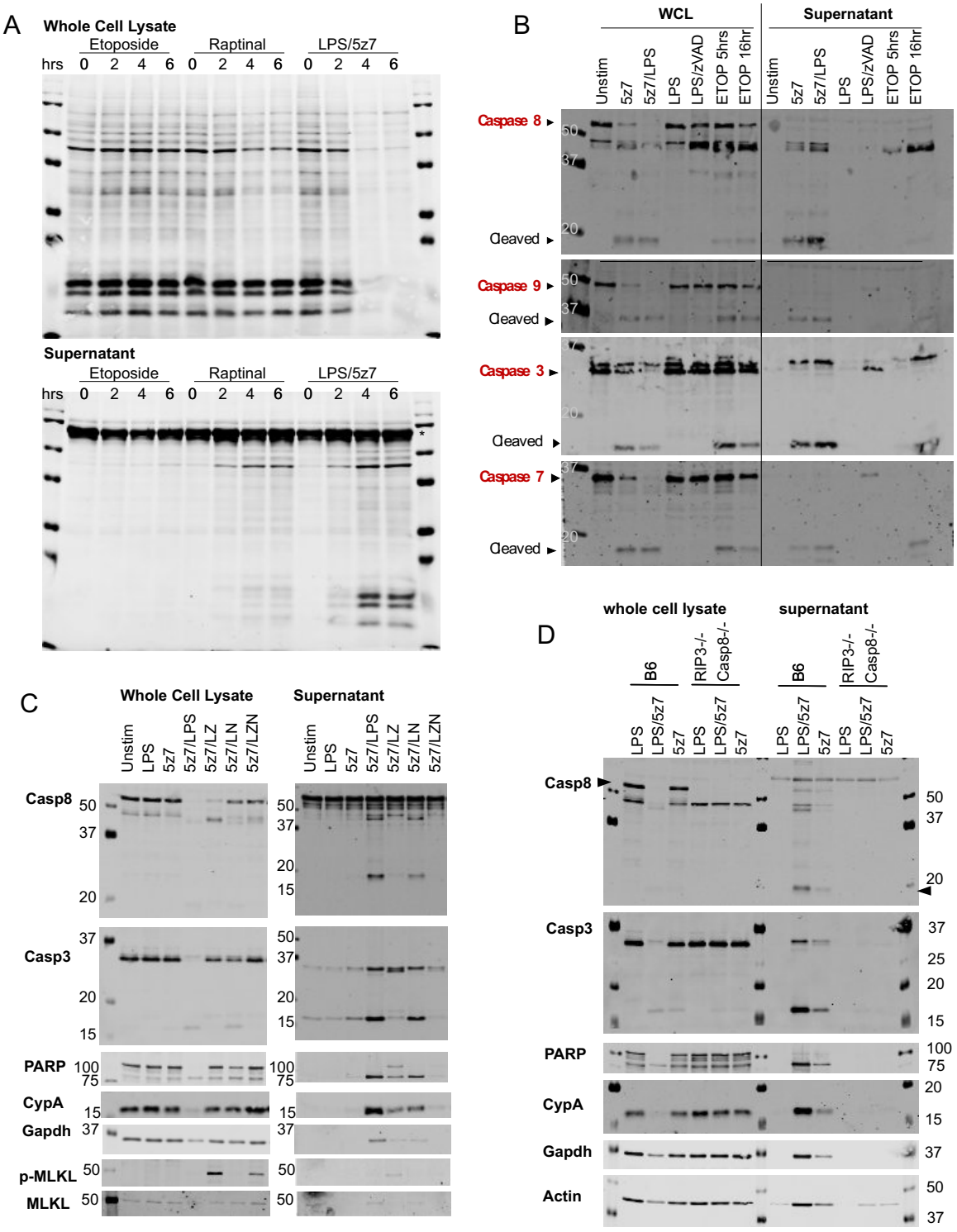

Figure 3.2. TAK-inhibition results in necrotic cell death, exhibiting pan-caspase activation and the externalization of cytosolic content

(A) Bone marrow derived macrophages were stimulated with etoposide, raptinal, or LPS/5z7 for 0-6 hours. Cellular lysate and precipitated supernatant were run on SDS-PAGE gels and total protein was stained by LiCOR total protein stain. * indicates serum proteins from residual FBS in the culture media.
(B) Bone marrow derived macrophages were stimulated as indicated for 5 hours, expect for etoposide, which had an additional 16hr stimulation timepoint. Cellular lysate and precipitated supernatant were run on SDS-PAGE gels and probed for pro- and cleaved forms of various apoptotic caspases.
(C) Bone marrow derived macrophages were stimulated with LPS/5z7 for 5 hours, in the presence of zVAD or Nec1 to block caspase or RIP kinase activity, respectively. Cellular lysate and precipitated supernatant were run on SDS-PAGE gels and probed for caspases, caspase substrate PARP, cytosolic proteins CyclophilinA (CypA) and Gapdh, and phosphorylated/total MLKL.
(D) Bone marrow derived macrophages from B6 and *Rip3*$^{-/-}$ *Casp8*$^{-/-}$ animals were stimulated with LPS, LPS/5z7, or 5z7 for 5 hours. Cellular lysate and precipitated supernatant were run on SDS-PAGE gels and probed for caspases, caspase substrate PARP, cytosolic proteins CyclophilinA (CypA), Gapdh, and actin.
Panel A, C, D generated by B.C.L.; Panel B generated by R.N.

3.2.3 Yersinia and LPS/5z7 driven cell death resembles pyroptosis by morphology

Apoptosis, necroptosis, and pyroptosis are morphologically distinct from each other. Using time lapse microscopy, we followed the progression of macrophages undergoing each of these three well defined modes of cell death to determine the form taken by cells dying by LPS/5z7 or *Yersinia* (Fig 3.3A-E).

For a rapid form of apoptosis, we use the recently characterized small molecule raptinal, which engages caspase 9 activation (Palchaudhuri et al. 2015). Raptinal treated cells progress to membrane rupture by 2-3 hours post stimulation, therefore placing it on a similar timescale to LPS/5z7 induced cell death (Fig 3.3A). Cells undergoing raptinal treatment display classic signs of cell shrinkage and blebbing as early as 30 minutes post stimulation. AnnexinV positivity as an indication of phosphatidylserine externalization is rampant by 40 minutes, and this phase is extended for at least one hour. Perturbations to the plasma membrane in the form of multiple small necrotic bubbles per cell finally sets in at 2 hours post stimulation, with nuclear propidium iodide signal appearing 10-20 minutes later.

Recently, Gong *et. al.* showed that necroptosis, although a necrotic form of cell death, can display phosphatidylserine externalization prior to membrane rupture (Gong et al. 2017). We confirm that with LPS/zVAD induced necroptosis, AnnexinV binding is evident by 50-60 minutes post stimulation in the absence of cell shrinkage as seen in apoptosis. Membrane ruffling is seen during the AnnexinV positive phase, and plasma membrane rupture takes the form of 1-2 large necrotic bubbles per cell that coincides with nuclear propidium iodide positivity. Necroptotic cells takes 50 minutes to 1 hour

from the onset of phosphatidylserine externalization to plasma membrane rupture (Fig 3.3B).

To trigger pyroptosis, LPS was transfected into the cytosol to activate caspase-11 (Kayagaki et al. 2013; Hagar et al. 2013). Unlike necroptosis and apoptosis, cells undergoing pyroptosis do not show overt signs of impending membrane rupture in the hours leading up to cell death. 10 minutes prior to membrane rupture, the pyroptoting cell show a weak attempt at cell shrinkage before bursting into one spherical AnnexinV positive necrotic bubble simultaneous with nuclear propidium iodide positivity (Fig 3.3C).

With LPS/5z7 co-stimulation, dying cells retain extensive lammelipodia up to 10-20 minutes before membrane rupture. At 10 minutes prior to loss of membrane integrity, the cell rapidly shrinks, followed by simultaneous onset of weak AnnexinV positivity, blebbing, and a weak propidium iodide signal seeping into the nucleus. Within 10 minutes of AnnexinV binding, the cell then bursts with one large, spherical necrotic bubble along with full nuclear propidium iodide signal (Fig 3.3D). The identical progression of cell death is seen during *Yersinia*-induced cell death (Fig 3.3E).

To quantify this phenotype on a population level, images were taken at 4x magnification with 3000-4000 cells captured per frame. AnnexinV and propidium iodide signal intensity per cell were plotted on the Y and X axis, respectively. Representative frames at 1.5hr and 3hr are shown for LPS/zVAD and LPS/5z7 (Fig 3.3F, G). On a population level, necroptotic cells show a distinct population of AnnexinV+PI- cells that transition into PI positivity (Fig 3.3F). In contrast, LPS/5z7 stimulated cells progress from dual negative to PI+AnnexinV^{weak} state, and gains AnnexinV positivity over time

(Fig 3.3G). Our data show that rapidity of membrane rupture curtails the process of phosphatidylserine externalization, leading to a pyroptotic-like cell death morphology.

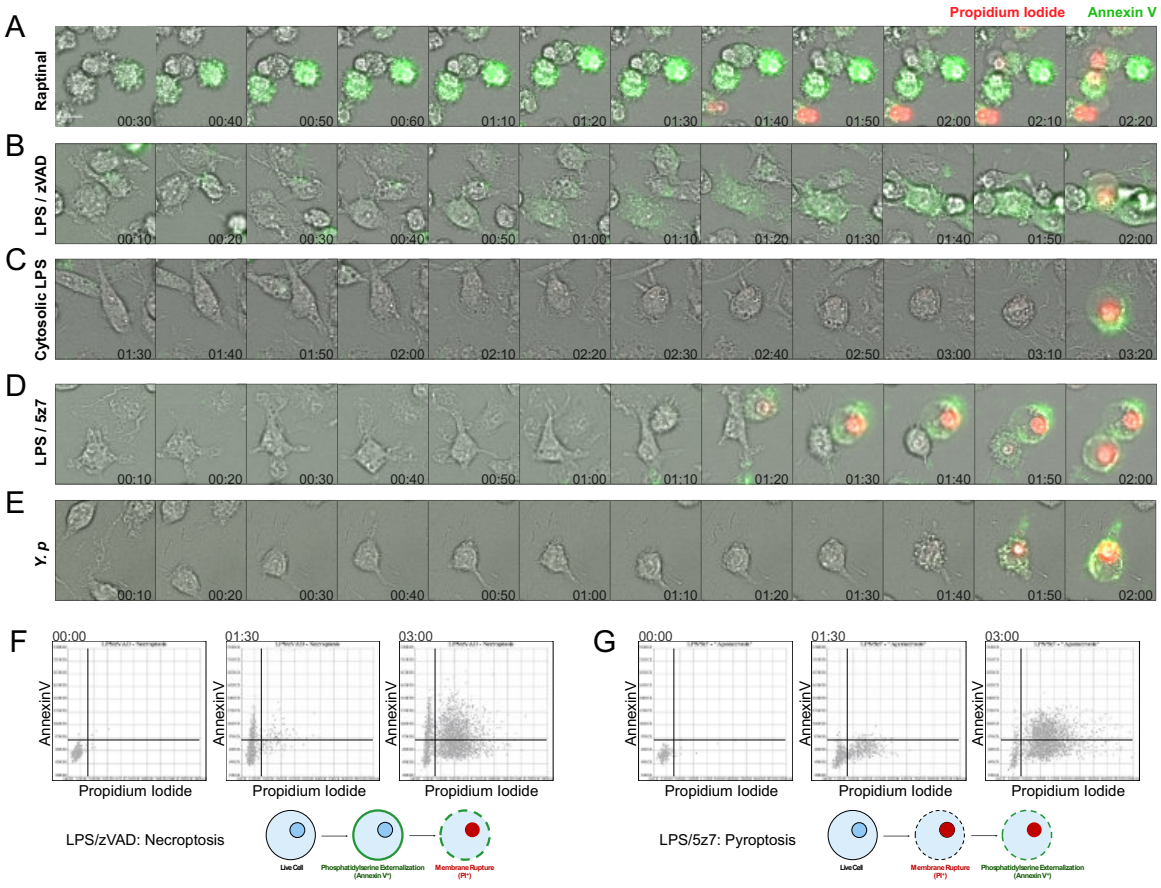

Figure 3.3. Yersinia and LPS/5z7 driven cell death resembles pyroptosis by morphology
(A - E) B6 bone marrow derived macrophages were stimulated as indicated. *Y.p.* stands for *Y. pseudotuberculosis.* Shown are 10 minute frames from time lapse microscopy performed at 40x magnification of AnnexinV and propidium iodide dual staining during the progression of cell death. 12 frames preceding membrane rupture are shown to depict the two hours of cell death progression leading to loss of membrane integrity. Scale bar = 10um
(F, G) Cells are stained with wheat germ agglutinin, AnnexinV, and PI are imaged at 4x magnification, 2 minute intervals, with 4000 cells per field of view. AnnexinV and PI signals were extracted from wheat germ agglutinin labeled cells, converted into numerical values, and plotted on the Y axis for AnnexinV, and X axis for PI. Representative time points of 0, 1.5hr, and 3hr are shown. Bottom cartoons depict our simplified model of the progression of phosphatidylserine externalization and membrane rupture during necroptosis or LPS/5z7 driven cell death.
Method for all panels generated by B.C.L. Experiments for panels A-E conducted by J.S. Experiments for panels F-G conducted by B.C.L. Image analysis for all panels by B.C.L. Scripting help for panels F-G by S.C.B. and A.T.

3.2.4 Caspase-8 induces GsdmD cleavage to drive pyroptosis, curtailing apoptosis

GasderminD and GasderminE are two effectors of pyroptosis downstream of caspase activation (Shi et al. 2015; Kayagaki et al. 2015; Wang et al. 2017; Rogers et al. 2017). To determine whether GsdmD and GsdmE are involved for LPS/5z7 and Yersinia induced cell death, macrophages were stimulated with various cell death stimulants, and cell lysates were probed for active cleavage products of GsdmD and GsdmE. We observed that GsdmD and GsdmE are both cleaved to generate the active p30 fragment within 3 hours of LPS/5z7 stimulation as well as *Yersinia* challenge (Fig 3.4A). In addition to the active p30 fragment generated by caspase-1 and caspase-11 as previously described (Shi et al. 2015; Kayagaki et al. 2015; Aglietti et al. 2016; Sborgi et al. 2016), we also observe a higher 40kDa fragment, likely the inactive p43 recently reported downstream of caspase-3 activity (Taabazuing et al. 2017). Macrophages lacking GsdmD show a significant delay in propidium iodide incorporation during challenge with either LPS/5z7 or *Yersinia* (Fig 3.4B, C). Morphologically, the curtailed AnnexinV staining in GsdmD sufficient cells became robust and prolonged with the loss of GsdmD, recapitulating an apoptotic morphology (Fig 3.4D, E). This can be seen on a population view with LPS/5z7 that drives a synchronized cell death response (Fig 3.4D), as well as on individual cellular basis during *Yersinia* infection (Fig 3.4E).

To determine which caspases are responsible for the cleavage of GsdmD and GsdmE, we stimulated macrophages from various combinations of caspase knock-out animals with LPS/5z7 to observe for gasdermin cleavage as well as cell death. We found that all three cleavage products of GsdmD were abolished in *Rip3*$^{-/-}$ *Casp8*$^{-/-}$ macrophages (Fig 3.4F). The p43 subunit is no longer present in *Casp3*$^{-/-}$ and *Casp3*$^{-/-}$*7*$^{-/-}$ macrophages, with

heightened presence of the p30 fragment. All three fragments are present in the *Casp9*$^{-/-}$ macrophages. *Casp1*$^{-/-}$*11*$^{-/-}$ and *Asc*$^{-/-}$ macrophages show minor to no decrease in the appearance of p30. The complete loss of all three fragments in the RIP3/Casp8 double knockout in conjunction with the minor loss of the p30 fragment in the absence of Casp1 and Casp11 indicate a possibility that Caspase 8 is directly able to cleave and generate active GsdmD during TAK1 inhibition.

For GsdmE cleavage, just as with GsdmD, the p30 fragment is absent in *Rip3*$^{-/-}$ *Casp8*$^{-/-}$ macrophages. The p30 fragment is mostly abolished in *Casp3*$^{-/-}$ macrophages and completely abolished in *Casp3*$^{-/-}$*7*$^{-/-}$ macrophages. Caspase-8 hence drive GsdmE cleavage primarily via Caspase 3 with minor contribution from Caspase 7, consistent with previous report (Taabazuing et al. 2017).

Testing the Caspase knockout macrophages for cell death, we observed mild kinetic delays in from *Casp3*$^{-/-}$*7*$^{-/-}$, *Casp9*$^{-/-}$, *Casp1*$^{-/-}$*11*$^{-/-}$ and *Asc*$^{-/-}$ macrophages (Fig 3.4G). These mild delays in cell death are consistent with the model that with Caspase 8 driving both arms of Gasdermin activation, the p30 fragments of GsdmD and GsdmE may be compensating for the loss of the other to drive necrotic cell death. *Casp9*$^{-/-}$ show no defect in the cleavage of either Gasdermins, yet do display a mild delay in cell death kinetics. Given that TAK inhibition has been shown to be associated ROS accumulation with possible damage to the mitochondria (Omori et al. 2012; Wang et al. 2015), it is likely that Caspase 9 acts in a separate and parallel arm to Caspase 8 to drive a third arm of cell death (Chen et al. 2007).

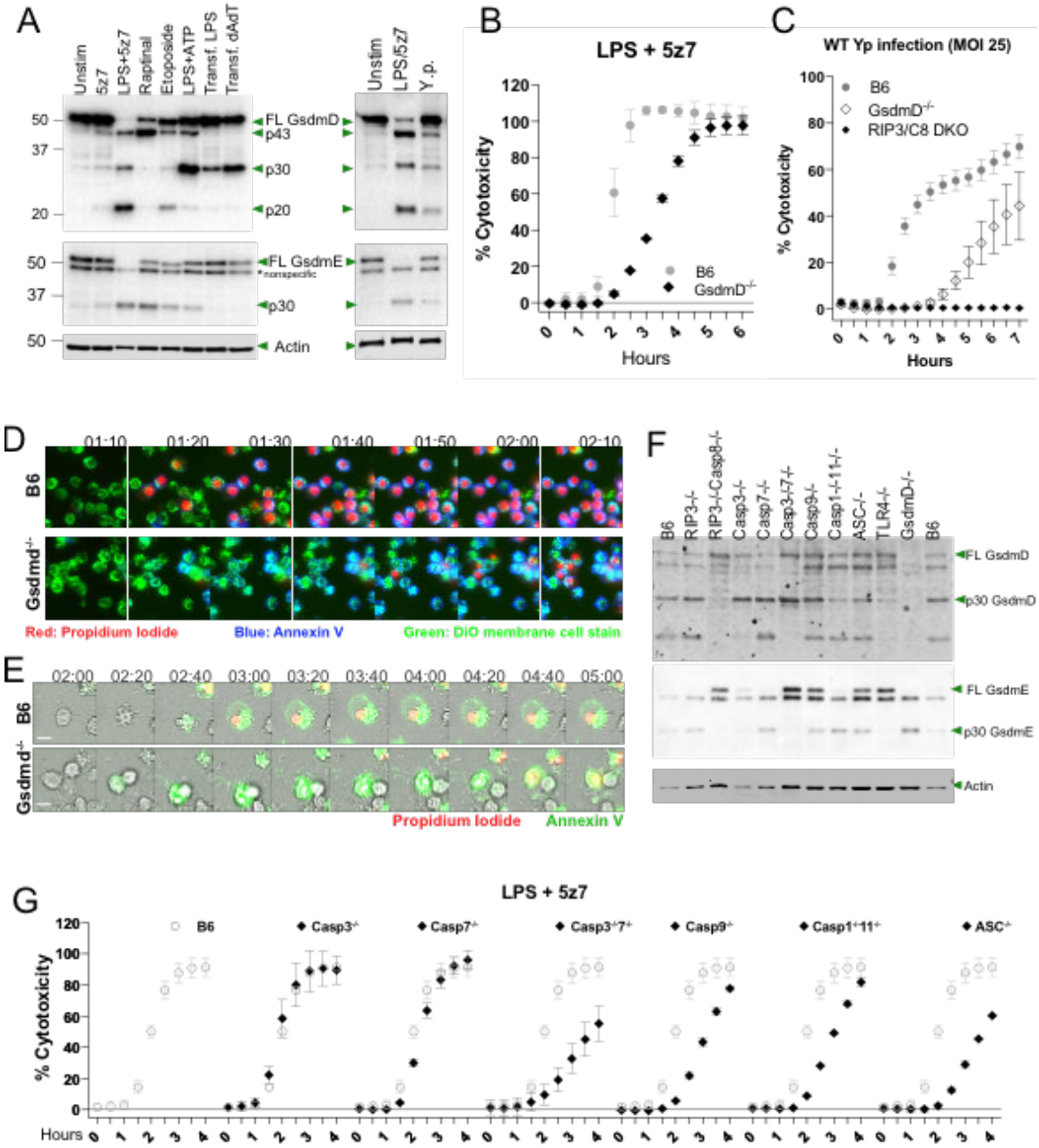

Figure 3.4. Caspase-8 induces GsdmD cleavage to drive pyroptosis, curtailing apoptosis
(A) Cleavage products of GsdmD and GsdmE in cell lysate when BMDMs are stimulated with various cell death triggers and *Yersinia* infection. Time point shown is 3 hours post stimulation or infection.

(B) Cell death kinetics by PI incorporation in B6 and *Gsdmd*$^{-/-}$ BMDMs stimulated with LPS/5z7.

(C) Cell death kinetics by PI incorporation in B6, *Gsdmd*$^{-/-}$, *Rip3*$^{-/-}$*Casp8*$^{-/-}$ BMDMs infected with *Yersinia*.

(D) Time lapse microscopy of B6 and *GsdmD*$^{-/-}$ BMDMs triple stained with Neuro-DiO, AnnexinV, and PI imaged at 20x magnification. Cells were stimulated with LPS/5z7. Image series depict the hour leading up to membrane rupture in *GsdmD*$^{-/-}$ BMDMs. Scale bar = 10um.

(E) Time lapse microscopy of B6 and *GsdmD*$^{-/-}$ BMDMs triple stained with AnnexinV and PI imaged at 40x magnification. Cells were infected with Yersinia and imaged series depict the 3 hours leading to membrane rupture in *GsdmD*$^{-/-}$ BMDMs. Scale bar = 10um.
(F) Cleavage products of GsdmD and GsdmE in cell lysate of BMDMs deficient for various caspases when stimulated with LPS/5z7 for 2 hours.
(G) LPS/5z7 driven cell death kinetics by PI incorporation in BMDMs deficient for various caspases.
Panel A by B.C.L. Panels B-C by J.S. Panel D by B.C.L. Panel E experiment performed by J.S., analyzed by B.C.L. Panel F by B.C.L. Panel G by J.S.

3.2.5 IL-1 maturation requires two distinct cell populations to generate signal 1 and signal 2

NLRP3 activation via potassium efflux as a consequence of membrane pores have recently been shown to occur during both pyroptosis and necroptosis (Conos et al. 2017; He et al. 2015; Kayagaki et al. 2015), suggesting that potassium efflux induced inflammasome activation may be commonality shared amongst various necrotic modes of cell death (Wallach et al. 2016). We therefore wanted to know if TAK inhibition induced death, with its semblance to pyroptosis in morphology, has the ability to induce inflammasome activation and the maturation of functional IL-1 family cytokines.

BMDMs stimulated simultaneously with LPS/5z7 or LPS alone did not lead to release of IL-1β in the supernatant, perhaps unsurprising due to the requirement of MAPK and NFκB signaling for pro-IL-1 synthesis, which would be inhibited with 5z7, as is the case for TNF (Fig 3.5A). Yet during *Yersinia* infection, IL-1α and IL-1β are secreted in a RIP3/Casp8 dependent manner. Curiously, we observed an inverse correlation between IL-1 abundance and infection MOI, with lower MOI of infection correlating with higher mature cytokines (Fig 3.5B). Peterson *et. al.* has recently shown with TNF that during *Yersinia* infection, since the bacterial population do not uniformly express adequate levels of YopJ to fully block TAK1 activity, non-intoxicated cells retain the ability to synthesize cytokines (Peterson et al. 2016). This phenomenon was most apparent with single signal cytokines such as TNF, where loss of cell death with *Rip3*$^{-/-}$ *Casp8*$^{-/-}$ provides for more cells competent for making cytokines (Fig 3.5B, third panel). In the case of IL-1α and IL-1β, an additional inflammasome signal is required for non-TAK1 inhibited cells to generate mature cytokines. Of note, at doses where abundant IL-1

secretion is observed, cell death as measured by PI+ nuclei is diminished (Fig 3.5C). These lower MOI infections also result in more rapid outgrowth of bacteria in *Rip3*$^{-/-}$ *Casp8*$^{-/-}$ macrophages as compared to B6, suggesting a functional role of IL-1 signaling in bacterial control perhaps via upregulation of MyD88-dependent responses (Fig 3.5D). With IL-1 maturation being inverse to cell death, yet still requiring cell death, we hypothesized that two cellular populations are needed to generate the two signals required for IL-1 maturation. We modeled that pro-IL-1 is synthesized in the non-TAK inhibited cells, which can be experiencing TLR activity via contact with lesser virulent bacteria in the population or outer membrane vesicles (Eddy et al. 2014), which has been shown to be immunogenic in other bacterial infections (Cecil et al. 2017; Jung et al. 2017). The inflammasome signal is provided by the TAK-inhibited cells that are unable to synthesize cytokines, but are driven to necrotic cell death via Caspase 8 induced GsdmD and GsdmE activation. Upon the death of TAK-inhibited cells, the release of active inflammasome results in the cleavage and maturation of IL-1 in pro-IL-1 sufficient cells. Our line of thinking is supported by findings that oligomerized ASC and functional NLRP3 inflammasome can be transferred from cell to cell (Franklin et al. 2014; Baroja-Mazo et al. 2014).

We tested this model by artificially generating two populations during LPS/5z7 treatment (Fig 3.5E, F, G). To generate pro-IL-1 synthesis, we stimulated B6 macrophages with LPS in the absence of 5z7. 6 hours later, we added 5z7 to the original population, or a second population of B6 macrophages in the presence of 5z7. We found that unlike cells treated simultaneously with LPS and 5z7, cultures where cells experienced sequential LPS treatment followed by TAK inhibition were able to produce

mature IL-1. This effect is even more pronounced when the culture contained a mixture of cells, some of which received the LPS signal alone, while others received the 5z7 simultaneous with the LPS signal (Fig 3.5F).

Taking this one step further, we used *Rip3*$^{-/-}$ *Casp8*$^{-/-}$ macrophages as the LPS-stimulated population. 6 hours after LPS stimulation, a second layer of B6 cells were added in the presence or absence of 5z7. Robust IL-1 secretion was detected in mixed cultures that contained LPS-activated *Rip3*$^{-/-}$ *Casp8*$^{-/-}$ cells and B6 cells in the presence of 5z7. Mixed cultures containing LPS-activated *Rip3*$^{-/-}$ *Casp8*$^{-/-}$ cells and B6 cells in the absence of 5z7 did not produce more IL-1 than homogeneous *Rip3*$^{-/-}$ *Casp8*$^{-/-}$ cell cultures stimulated with LPS alone (Fig 3.5G). Our findings indicate that a population of actively pyroptotic cells as well as a population of non-TAK inhibited cells are both needed for IL-1 secretion.

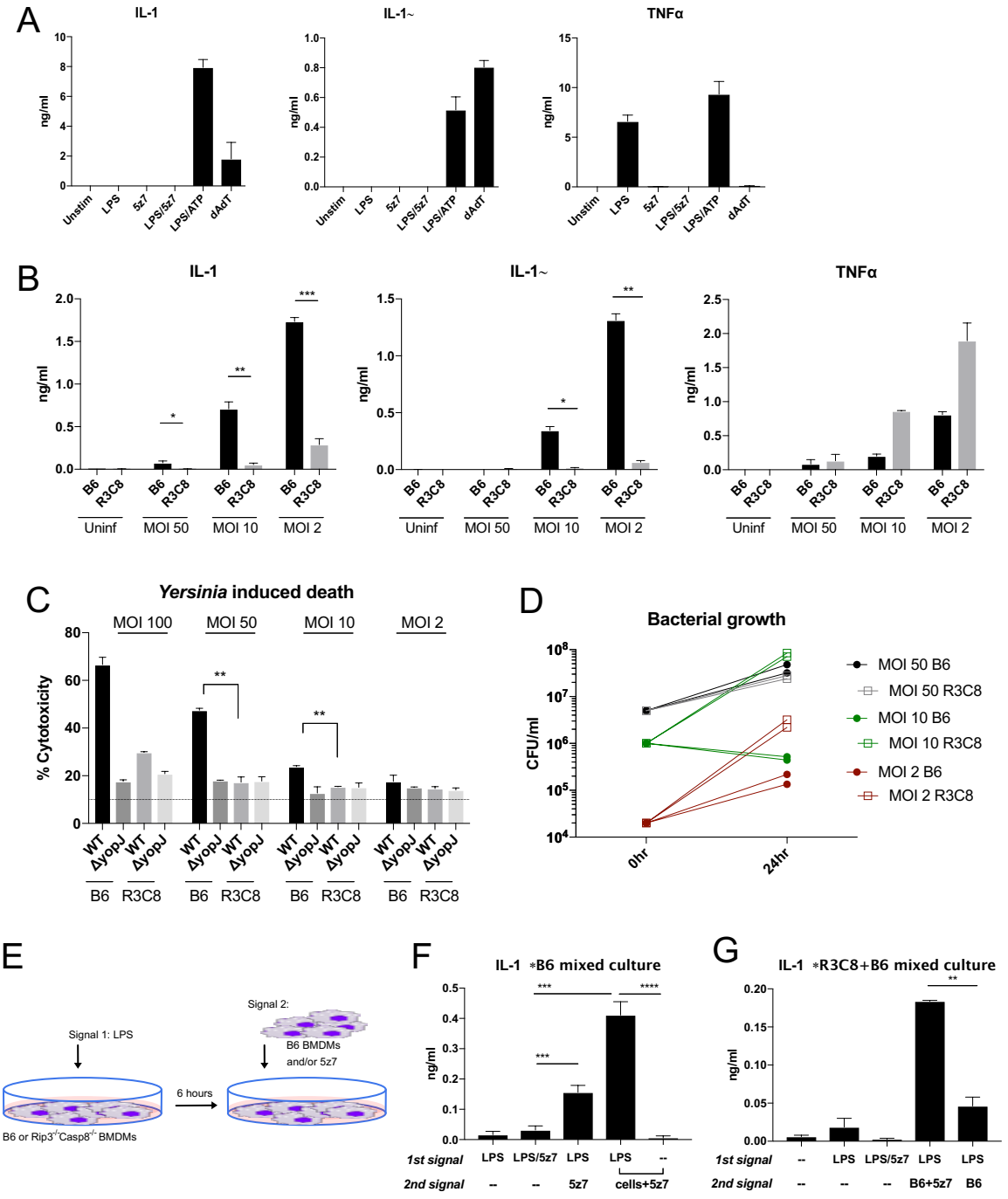

Figure 3.5. IL-1 maturation requires two distinct cell populations to generate signal 1 and signal 2
(A) IL-1β, IL-1α, and TNF secretion measured by ELISA during stimulation by LPS/5z7 as compared to canonical inflammasome stimuli.

(B) IL-1β, IL-1α, and TNF secretion measured by ELISA during *Yersinia* infection of B6 and *Rip3*$^{-/-}$ *Casp8*$^{-/-}$ BMDMs as a function of decreasing bacterial MOI.

(C) *Yersinia* yopJ induced cytotoxicity in B6 and *Rip3*$^{-/-}$*Casp8*$^{-/-}$ BMDMs as a function of decreasing bacterial MOI.

(D) *Yersinia* colony forming units (CFU) in B6 and *Rip3*$^{-/-}$*Casp8*$^{-/-}$ BMDM cultures at various bacterial MOI.
(E) Experimental schematics for (F, G)
(F) IL-1β from mixed B6 cultures where cells are asynchronously stimulated with LPS and 5z7, as described in (E).
(G) IL-1β from mixed cultures of B6 and *Rip3*$^{-/-}$*Casp8*$^{-/-}$ BMDMs where cells are asynchronously stimulated with LPS and 5z7, as described in (E).
All panels by B.C.L.

3.2.6 Human macrophages are resistant to TAK-inhibition induced cell death with no consequent secretion of IL-1

In mouse macrophage cultures, YopJ-induced cell death is most readily seen around the MOIs of 60 and 30, with higher doses eliciting bacterial outgrowth-driven cell death, and lower doses approaching background levels (Fig 3.6A). Human cells, in contrast, do not display a YopJ dependent cell death process at any MOI tested. We tested three human macrophage populations from various sources including the monocyte-like cell line U937 (Fig 3.6B), peripheral blood mononuclear cell derived macrophages (Fig 3.6C), and peripheral blood monocyte derived macrophages (Fig 3.6D). All three cell types uniformly show MOI-dependent killing, with no difference correlating to the presence or absence of YopJ. Similarly, human cells are resistant to killing by LPS/5z7 (Fig 3.6E, F). With the additional treatment of zVAD, human cells undergo rapid necroptosis with dual Annexin and PI positivity, showing that the backup cell death mechanism is fully intact (Fig 3.6E, F). In terms of cytokines, IL-1β secretion from human PBMC-derived macrophages and monocyte derived macrophages toward *Yersinia* infection are at the level of LPS-induced IL-1 secretion (Fig 3.6G). The 5z7 dose used for human cell stimulation was sufficient to fully abolish LPS-induced TNF production (Fig 3.6H).

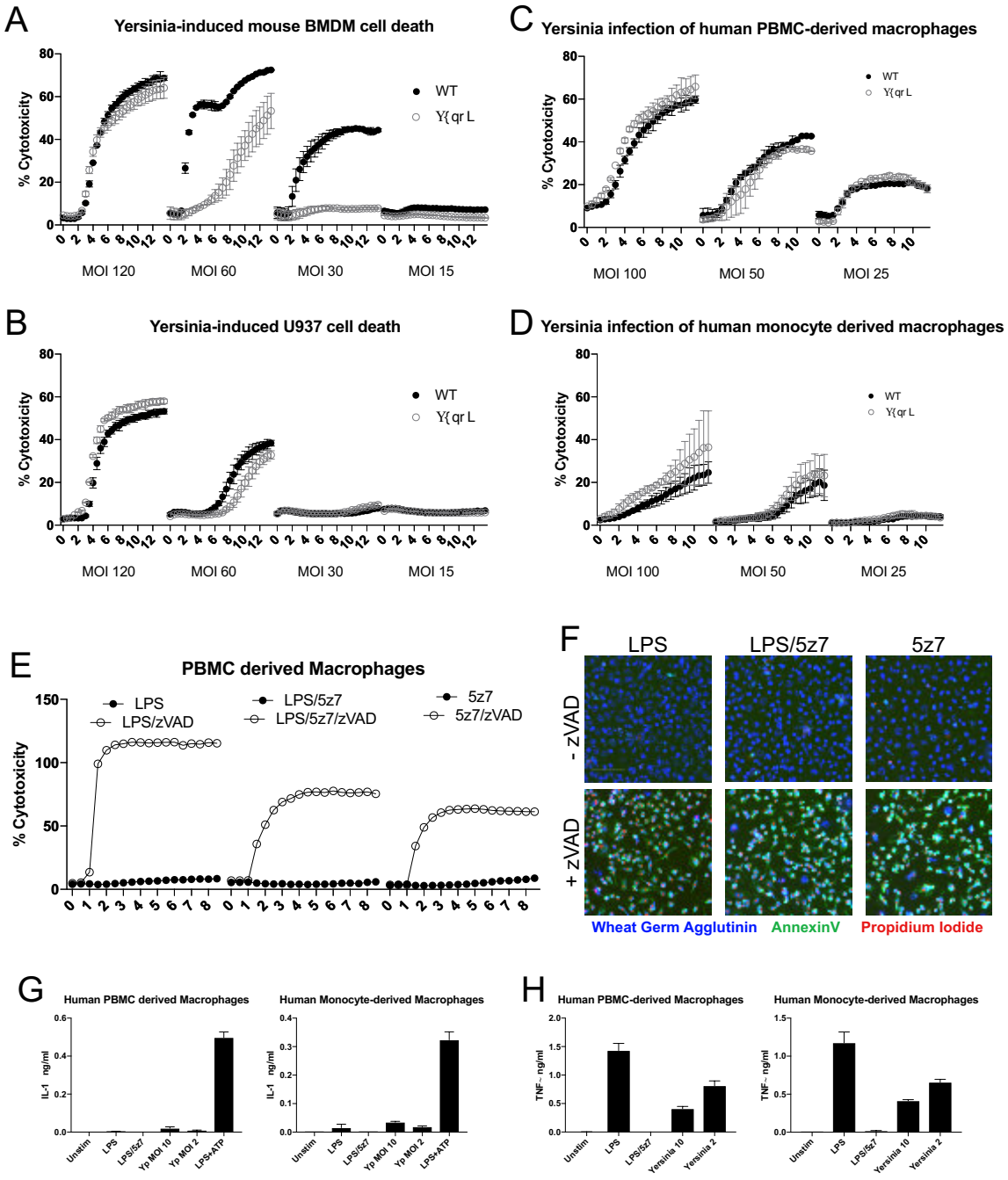

Figure 3.6. human macrophages are resistant to TAK-inhibition induced cell death with no consequent secretion of IL-1

(A) *Yersinia* induced murine macrophage cell death at various bacterial MOI, where MOI of 60-30 show YopJ specific cell death.

(B) *Yersinia* induced death of PMA activated U937 cells. No YopJ dependent killing is observed.

(C, D) Yersinia induced death of human peripheral blood mononuclear cell (PBMC) derived macrophages (C) or peripheral blood monocyte derived macrophages (D). Bacteria were infected at multiple MOI, with no YopJ dependent killing observed. PBMCs and monocytes were from different donors.

(E) Human PBMC-derived macrophages were treated with LPS, LPS/5z7, or 5z7, in the presence of absence of zVAD. Kinetics of cell death was measured by PI+ nuclei.

(F) Representative images of triple stained human PBMC-derived macrophages taken at 4x magnification. PBMC-derived macrophages were stimulated as in (E), image shown is at 7.5 hours post stimulation. Scale bar = 100um.
(G) IL-1β secretion from human PBMC derived macrophages or monocyte derived macrophages stimulated with LPS/5z7 or Yersinia at doses that elicit robust IL-1α/β secretion from murine macrophages.
(H) TNF secretion from human PBMC derived macrophages or monocyte derived macrophages stimulated with LPS/5z7 or *Yersinia* at doses that elicit robust IL-1α/β secretion from murine macrophages.
Panels A-F by J.S. Panels G-H by B.C.L.

3.3 Discussion

In the present study, we demonstrate that *Yersinia* YopJ-induced murine macrophage death involved caspase-8 induced cleavage of both GsdmD and GsdmE. The ensuing cell death is rapid, morphologically pyroptosis, and induces IL-1 maturation. Our simplified model of co-stimulation with LPS and 5z7 in generating near 100% cytotoxicity of the macrophage population harkens to the age-long difficulty of TAK1 ablation *in vivo*. The use of polyI:C, a TRIF-engaging TLR agonist, to induce the deletion of TAK1 resulted in rampant necrosis of the treated area along with heightened IL-1 response (Tang et al. 2008). Similarly, the *in vivo* reduction of TAK1 using an inducible shRNA also proved difficult, since cells losing sufficient TAK1 levels inevitably experience tonic TNF-mediated activation of complex IIa (Vink et al. 2013).

Recent work by the Shao group has re-defined pyroptosis as cell death mediated by gasdermin activation (Wang et al. 2017). Gasdermin D is a critical effector of pyroptosis which upon cleavage by caspase 1/11 disrupts cell membranes (Sborgi et al. 2016; Aglietti et al. 2016; Gaidt & Hornung 2016; Shi et al. 2015; Kayagaki et al. 2015). Similarly, Gasdermin E is an effector driving necrosis downstream of caspase-3 (Wang et al. 2017; Rogers et al. 2017). Our work extends these studies and shows that caspase 8 activation in the context of TAK1 inhibition can result in cleavage of both GsdmD and GsdmE, leading to a pyroptotic-like cell death. Further study is needed to determine whether caspase 8 can cleave GsdmD directly or if there are other intermediary substrates independent of Casp1/11 to generate the pore forming p30 subunit. Additionally, the cell death response is only kinetically delayed in *Gsdmd-/-* macrophages, suggesting that GsdmE, and likely mitochondrial damage amplified via Caspase 9 activation (Wang et al.

2015; Chen et al. 2007), may act to ensure the eventual demise of the cell under conditions of infection-driven TAK inhibition.

The cleavage of Gasdermins may have farther reaching implications than celluar obliteration. Work by both the Shao and Lieberman labs elegantly demonstrated that cleaved GsdmD can attack bacteria and reduce their viability (Ding et al. 2016; Liu et al. 2016). Other work by the Miao lab has also shown that pyroptosis can result in pore induced intracellular traps (PITs), leading to retainment of intracellular bacteria within the carcass of dying cells to facilitate phagocytic clearance (Jorgensen et al. 2016). Jorgensen's work places the importance of macrophage pyroptosis into an *in vivo* context, in which IL-1 production during pyroptosis recruits secondary phagocytic cells to the site of infection to engulf dead cell carcasses along with its damaged bacterial load. These results are in line with our findings that *Yersinia* replication is limited by macrophages competent for cell death, suggesting that pyroptosis can be protective even in the setting of macrophage cultures.

During traditionally pyroptotic infections such as *Legionella, Salmonella, Francisella*, and *Burkholdia,* IL-1 maturation is intrinsic to the infected, dying cell (Case et al. 2009; Shenoy et al. 2012; Man et al. 2016; Meunier et al. 2015; Miao et al. 2010). The case of *Yersinia* infection is particularly interesting since MAPK signaling is inhibited by YopJ, effectively blocking pro-IL-1 synthesis in doomed, infected macrophages. Since bacterial populations are not a homogenous in their virulence, some percentage of macrophages at the site of infection will not be sufficiently intoxicated by YopJ, thus retaining the ability to synthesize MAPK dependent cytokines (Peterson et al. 2016). We postulate that these MAPK competent cells are also the producers of pro-IL-1,

with neighboring pyroptosing cells serving as platforms for potassium efflux induced inflammasome formation. We predict that the MAPK competent cells then complete the processing of IL-1 by efferocytosing dead cells (Martin et al. 2014; Kolb et al. 2017) or by acquiring extracellular ASC/NLRP3 inflammasomes released by dying cells (Franklin et al. 2014; Baroja-Mazo et al. 2014). Macrophages that are defective for the death response, such as *Rip3*$^{-/-}$*Casp8*$^{-/-}$ and RIP1 kinase dead (RIP1K45A), would therefore be defective for IL-1 maturation as well, lending the animals more susceptible to uncontrolled *Yersinia* replication (Peterson et al. 2017; Weng et al. 2014; Philip et al. 2014).

Along the same vain, our finding that human macrophages do not undergo YopJ dependent cell death and fail to produce mature IL-1β during Yersinia infection, may provide an insight to the devastation of the Plague. In the present study, we used IP2666 *Y. pseudotuberculosis*, which expresses hexa-acylated LPS capable of triggering TLR4. The more dangerous *Yersinia pestis* evolved from *Yersinia pseudotberculosis* and in the process acquired a hypoacylated TLR4-evasive LPS (Chain et al. 2004; Knirel & Anisimov 2012). If the backup mechanism of inflammation via cell death is absent in human macrophages in response to TAK1 inhibition downstream of an immunogenic LPS, an immune evasive bacterium would effectively create a silent infection. This point is neatly demonstrated by the Kim4 strain of *Y. pestis* by expression of the E.coli LPS as an attenuation strategy (Montminy et al. 2006).

Other examples of necrotic forms of cell death lending protection to the infected host can be found with necroptosis studies. RIP3 has been shown to be protective in the case of vaccinia virus infection (Cho et al. 2009), CMV infection (Upton et al. 2012) as well

as during HSV replication by induction of cell death in infected mouse cells (Huang et al. 2015; Guo et al. 2015). In the case of HSV, necroptosis in mouse cells serves to limit viral replication, while the absence of necroptosis in human cells leads to uncontrolled viral replication. These findings with HSV bear striking similarity to the differential species-based cell death responses and pathogen replication highlighted in our study.

Human macrophages therefore may have an inborn tolerance to highly pathogenic bacterial neighbors, to the detriment of the organism. On the macrophage level, the resistance to death may lie in higher expression or longer half-life of key pro-survival proteins. In mouse macrophages, complex IIa forms when there is inadequate pro-survival factors including Cellular FLICE-inhibitory protein (c-FLIP) (Micheau & Tschopp 2002; Vanlangenakker et al. 2011) and inhibitors of apoptosis (IAPs) (Tenev et al. 2011). More recent work has also implicated the loss of IAP and cFLIP during TAK1 inhibition as a reason for cell death (Guo et al. 2016). The regulation of IAPs and FLIP are top candidates to investigate the defect in cell death in human macrophages.

Very recent investigations in the field of cell death also show that MAPK-activated protein kinase 2 (MK2), a downstream target of P38 and TAK1, is required for RIP1 phosphorylation at Ser321 (Jaco et al. 2017; Geng et al. 2017; Menon et al. 2017; Dondelinger et al. 2017). This MAPK driven RIP1 phosphorylation inhibits complex II formation and thus limits cell death. The state of RIP1 regulation in human macrophages may also be an area of interest.

The differential response of human and murine macrophages demonstrated by our study and others (Huang et al. 2015; Guo et al. 2015) thus call to attention the need to study both mouse and human cells to understand course of illness in humans, especially

when rodents are vectors for the human disease of interest. Beyond *Yersinia*, the anthrax toxin and lethal factor effectors of *Bacillus anthracis* inhibit MAPK activation and has been observed to elicit cell death and IL-1 production (Park et al. 2002; Ali et al. 2011). Investigating the role of gasdermins and the presence of pyroptotic features in this and other infectious systems known to inhibit MAPK or NFκB signaling may provide deeper understanding of the mechanism and scope of necrotic cell death in host defense.

3.4 Author Contribution

B.C.L., J.S., R.N., and A.T. conducted experiments. B.C.L. and J.S. initiated the study, designed experiments, interpreted results, and wrote the paper. A.R. generated and provided various caspase single and double deletion animals. S.C.B. aided in image analysis and critical discussion. A.P. sponsored the research.

B.C.L. and J.S. agree to share first authorship for this manuscript, and both consider the work to be of equal contribution intellectually and technically. Specificities of each author's experimental contributions are noted within the figure legends. Experiments conducted by R.N. and A.T. were under the direct supervision of B.C.L., discussed with J.S. Their specific experimental contributions are denoted in the figure legends.

3.5 Materials and Methods

3.5.1 Macrophages and Mice

C57BL/6, *Casp1*$^{-/-}$*Casp11*$^{-/-}$ mice were obtained from Jackson Laboratory. *Casp11*$^{-/-}$ mice were kind gifts from Dr. Vishva Dixit (Genentech) (Kayagaki et al. 2011). Animals were housed under protocol approved by the Tufts University Medical School Animal Care and Use Committees. Bones from *Casp3*$^{-/-}$, *Casp3*$^{-/-}$*Casp7*$^{-/-}$, *Casp9*$^{-/-}$ were provided and generated by Dr. Anthony Rongvaux (Rongvaux et al. 2014). Bones from *Gsdmd*$^{-/-}$ mice and *Rip3*$^{-/-}$ mice were gifts from Dr. Kate Fitzgerald, generated by Dr. Vishva Dixit (Kayagaki et al. 2015; Newton et al. 2004). Bones from *Rip3*$^{-/-}$*Casp8*$^{-/-}$ mice were given by Dr. Kate Fitzgerald, generated by Dr. Doug Green (Oberst et al. 2011). Bones from *Ripk1K45A/K45A*, *Ripk3K51A/K51A* mice were gifts from Dr. Alexi Degterev and generated by Dr. John Bertin and Dr. Peter J Gough from GlaxoSmithKline (PA, USA) (Berger et al. 2014; Mandal et al. 2014). Bone marrow-derived macrophages were isolated from mice and propagated for 7 days in RPMI containing 20% FBS, 30% L cell supernatant, 2% Penn/Strep on non-tissue culture treated Petri dishes. Unless otherwise noted, cells were plated at a density of 1x 10^6 cells per cm^2 for experiments in RPMI containing 10% FBS, no antibiotics were used during infection.

3.5.2 Inhibitors and TLR agonists

Lipopolysaccharide (LPS) *S. minnesota* R5 used with 5z7 and *E. coli* 0111:B4 used for transfection were purchased from Sigma. zVAD.fmk was purchased from Millipore. Necrostatin-1 and (5Z)-7-Oxozeaenol were purchased from Sigma.

3.5.3 Yersinia pseudotuberculosis Infection

Y. pseudotuberculosis strains of IP2666 wild type and *ΔyopJ* were used as previously described (Auerbuch et al. 2009). *Yersinia* bacteria were grown on LB plates containing Irgasan. Single colonies were picked for 16hr overnight cultures grown in 2xYT media at 26°C, followed by back-dilution to an OD_{600} of 0.2 with supplemented 20mM $MgCl_2$ and 20mM NaC_2O_4. Back-diluted cultures were grown at 26°C for 2 hours followed by 37°C for 2 hours. Macrophage cultures were infected at MOI ranges indicated in figures and figure legends.

3.5.4 Human macrophages

De-identified human peripheral blood was obtained from New York Biologics. The use of de-identified human samples followed a protocol approved by the Tufts University School of Medicine Institutional Review Board. Peripheral blood mononuclear cells were isolated via Ficoll gradient. Monocytes were obtained from peripheral blood using the EasySep Direct Monocyte Isolation Kit (STEMCELL technologies). $CD14^+CD16^-CD68^-$ monocytes were extracted and differentiated into $CD14^+CD16^-CD68^+$ macrophages over the course of 7 days in RPMI containing 20% FBS, 200U/ml Penicillin and 200μg/ml Streptomycin. and 100 μg/ml of human monocyte colony stimulating factor (M-CSF; PeproTech) (Jaguin et al. 2013; Davies & Gordon 2005). Differentiated macrophages were cultured for 40 hours further in RPMI containing 10% FBS, 200U/ml Penicillin and

200μg/ml Streptomycin, in the absence of M-CSF prior to infection or agonist stimulation.

3.5.5 Time lapse microscopy and kinetic cytotoxicity assay

The Cytation3 automated microscope was used to maintain temperature at 37°C and 5% CO_2 for kinetic imaging of live cell cultures. Cells were seeded in 0.17mm thickness glass bottom imaging plates, in RPMI (Hyclone) media. For kinetic cytotoxicity assays, cells were imaged at 30 minute interviews with 4x magnification to capture 3000-4000 cells per field of view. Propidium iodide (10μg/mL, Life Technologies, P3566) was detected via 535 nm excitation and 617 nm emission, with individual puncta of 4um-10um in size counted as nuclei. For 100% cytotoxicity control, cells were treated with 0.1% Triton X-100, similar to protocols for measuring Lactate Dehydrogenase (Promega). AnnexinV binding requires media controlled at pH 7.2-7.5 and supplemented up to 2uM calcium (Logue et al. 2009; Brumatti et al. 2008). For kinetic image cytometry in detection of dual AnnexinV and PI positivity, cells were labeled with a total cell stain via Neuro-DiO (ex. 488) or Wheat Germ Agglutinin (ex. 350). AnnexinV was imaged on ex.350 or ex.488, depending on the total cell stain used. Images were taken at 4x magnification, every 2 minutes, and image stacks were analyzed on iVision, where cellular masks were generated via the total cell stain. Signal intensities of AnnexinV and PI were extracted from masked area, and signal intensity was plotted as numerical values to generate kinetic cytometry plots. 20x and 40x magnification images were taken under the same conditions.

3.5.6 Western blotting

At the desired time points post stimulation or infection, media supernatant was collected, and cells were lysed directly in 1X Laemmli Buffer with 5% β-mercaptoethanol, boiled for 10 minutes, and incubated on ice for 10 min prior to loading on SDS PAGE gels. Supernatant proteins were precipitated via methanol/chloroform extraction, and precipitated proteins were resuspended and denatured in 1X Laemmli Buffer with 5% β-mercaptoethanol. Primary antibodies against caspase-3, caspase-7, caspase-8, caspase-9, CypA, Gapdh, and PARP were purchased from Cell Signaling Technologies. Antibodies to GsdmD and GsdmE were purchased from Abcam (ab209845/ab215191). Total MLKL antibody was purchased from Millipore (#MABC604). Phospho-MLKL- S345 (#ab196436) antibody purchased from Abcam.

3.5.7 ELISA for cytokine secretion

Murine IL-1α, IL-β, TNFα ELISAs, and human IL-1α, IL-1β, TNFα ELISAs were DuoSet ELISA kits purchased from R&D, used according to manufacturer's instructions.

3.5.8 Statistical Analysis

Statistical analyses were performed using the Student's t test (two-tailed) using GraphPad Prism. Where *$p < 0.05$; **$p<0.01$; ***$p < 0.001$.

Chapter 4: Discussion

An evolutionary theme of cell death is starting to emerge. Apoptosis, with its propensity for silence and favoring of efferocytosis by neighboring cells over plasma membrane rupture, is the cell death of physiology. Necroptosis, which is engaged with caspase inhibition, is the cell death of viral infections, many of which encode endogenous caspase inhibitors. Pyroptosis, as I am starting to understand from my studies, may be the cell death against bacteria. Despite this simplistic equation, a number of interconnections exist that can result in a switch to a secondary cell death mode when the primary route is blocked. The switch is more obvious with necroptosis as a backup for apoptosis, since a critical trigger for necroptosis is the presence of an inhibitor of apoptotic caspase activation. The novelty is that apoptosis, and indeed necroptosis, can both act as secondary modes of cell death in cases where pyroptosis is blocked. The concept that apoptosis can act as a backup for pyroptosis was best shown with the genetic ablation of GsdmD, the pyroptotic effector. By getting rid of GsdmD and ablating pyroptosis, we were able to observe that blockade of cell death resulted in upstream machinery engaging a mechanism that it normally would not need to. One particular case is that during activation of the caspase-1 inflammasome, if GsdmD is not cleaved to execute pyroptosis, ASC will engage caspase-8 to induce apoptosis (Mascarenhas et al. 2017). In this particular concept, ASC act as a node for caspase-8 activation to engage apoptosis in the absence of pyroptosis (Pierini et al. 2012; Sagulenko et al. 2013). In the second story, we describe an event in which what has long been considered complex II mediated apoptosis, is in fact caspase-8 mediated pyroptosis. The particular checkpoint for pyroptotic engagement over apoptosis is yet to be defined. Interestingly, in this particular case, necroptosis can be engaged with the inhibition of caspases. In our experiments, we

used zVAD to artificially block all caspases. Whether a mixture of necroptosis and pyroptosis can occur during a bacterial/viral co-infection would be an interesting avenue to investigate. Since whole organisms are colonized by a mass of microbiome that consists of both bacteria and viruses, the switches and mixes of cell death modes upon a pathogenic encounter become even more relevant.

In fact, the underlying condition of the organismal state at the time of infection can be more deterministic of the infection outcome than the immune response driven by the infection directly. This concept resounds in the first story, in which constitutive Interferon signaling was needed to maintain the expression of specific anti-microbial factors. The transcriptome governed by constitutive Interferon status was found to vary from tissue to tissue. Although the field has not started to focus on Interferon transcriptome in particular, recent studies have started to pay attention to the alteration of cytokine states during aging (Van Bussel et al. 2016). In a parallel study in the lab in which I was heavily involved in (Sarhan *et al.* manuscript in review at Cell Death and Differentiation), we found that constitutive Interferon also regulated the cell's propensity for undergoing necroptosis. Sarhan's work showed that MLKL, an Interferon Stimulated Genes, exhibit a threshold of expression in which stimulation-dependent MLKL oligomers can only form with sufficient expression of the protein. That expression level is in turn, governed by the baseline Interferon status of the cell. Extending the concept further, he tested the cellular potential for necroptosis with macrophages from a mouse model of lupus, a disease well known for its chronically heightened Interferon state (Hooks et al. 1982; Baechler et al. 2003; Bauer et al. 2006). We found that necroptosis

was enhanced in both resident peritoneal macrophages as well as bone marrow derived macrophages, suggesting the heightened circulating cytokines may even promote epigenetic level changes and influencing gene expression of cells undergoing differentiation. Lastly, we found that dependency on constitutive Interferon for both pyroptosis and necroptosis exist in human monocyte derived macrophages as well, where chronic inhibition of JAK/STAT signaling reduces baseline ISG expression of the cells, making them less responsive to both pyroptotic and necroptotic stimuli.

In the second project, the phenotype of human macrophages and murine macrophages to *Yersinia* induced cell death are strikingly opposite. Whereas murine macrophages undergo rampant cell death that is associated with control of bacterial loads, human macrophages are able to co-exist in a culture dish with a blossoming bacterial population. This is particularly interesting given the historical account of the Plague, where rodents were the reservoir of disease (Raoult et al. 2013) and may possess better control of bacterial replication *in vivo*. The laboratory strain of *Y. pestis* and the wild type *Y. pseudotuberculosis* are attenuated by the expression of hexa-acylated LPS for TLR4 sensing (Knirel & Anisimov 2012). This attenuation strategy not only makes it safer for experimentation, but also allow for easier manipulation of the bacteria using the C57BL/6 laboratory mouse strain, which is considerably more susceptible to virulent *Yersinia* as compared to the wild-derive mouse strain SEG/Pas (Chevallier et al. 2013). The SEG/Pas inbred line evolved from the *Mus spretus* subspecies, which resides on the European continent and may be a more relevant model as a natural reservoir of *Y. pestis* (Liu et al. 2015). In fact, Blanchet *et al.* reported the subcutaneous lethal infection dose of fully

virulent *Y. pestis* to be 10^6 times higher for SEG/Pas than for C57BL/6 (Blanchet et al. 2011). In subcutaneously infected SEG/Pas mice, the bacteria become systemic within 2 days of inoculation, followed by rapid clearance from the bloodstream. Continual and steady bacterial presence was observed in solid organs, with low levels of organ damage (Demeure et al. 2012). The length of time in which bacteria persist in the tissues of SEG/Pas mice is unclear. The controlled, low-dose infection of virulent *Y. pestis* in SEG/Pas mice suggest that *Mus spretus* may be an optimal natural reservoir. Interestingly, Quantitative Trait Loci analysis between SEG/Pas and C57BL/6 revealed three genetic loci located on chromosomes 3, 4, and 6 that contributed to the differential infection outcome (Blanchet et al. 2011; Chevallier et al. 2013). *Tnfrsf1a*, the gene encoding TNF receptor 1, and *Gsdme* both reside within the boundaries of the locus on chromosome 6. Additionally, *Map3k7*, the gene encoding TAK1, resides on chromosome 4, also within the region mapped. Is it possible that we have stumbled upon one of the pathways critical for the control of this infection?

Chapter 5: Bibliography

Aachoui, Y., Leaf, I.A., Hagar, J.A., Fontana, M.F., Campos, C.G., Zak, D.E., Tan, M.H., Cotter, P.A., Vance, R.E., Aderem, A., et al., 2013. Caspase-11 Protects Against Bacteria That Escape the Vacuole. *Science*, 339(6122), pp.975–978. Available at: http://www.sciencemag.org/content/339/6122/975.abstract [Accessed August 7, 2013].

Abt, M.C., Osborne, L.C., Monticelli, L.A., Doering, T.A., Alenghat, T., Sonnenberg, G.F., Paley, M.A., Antenus, M., Williams, K.L., Erikson, J., et al., 2012. Commensal bacteria calibrate the activation threshold of innate antiviral immunity. *Immunity*, 37(1), pp.158–70. Available at: http://www.ncbi.nlm.nih.gov/pubmed/22705104.

Aglietti, R.A., Estevez, A., Gupta, A., Ramirez, M.G., Liu, P.S., Kayagaki, N., Ciferri, C., Dixit, V.M. & Dueber, E.C., 2016. GsdmD p30 elicited by caspase-11 during pyroptosis forms pores in membranes. *Proceedings of the National Academy of Sciences of the United States of America*, 113(28), pp.7858–63. Available at: http://www.ncbi.nlm.nih.gov/pubmed/27339137.

Ahn, J., Gutman, D., Saijo, S. & Barber, G.N., 2012. STING manifests self DNA-dependent inflammatory disease. *Proceedings of the National Academy of Sciences of the United States of America*, 109(47), pp.19386–91. Available at: http://eutils.ncbi.nlm.nih.gov/entrez/eutils/elink.fcgi?dbfrom=pubmed&id=23132945&retmode=ref&cmd=prlinks%5Cnpapers2://publication/doi/10.1073/pnas.1215006109.

Albert-Weissenberger, C., Cazalet, C. & Buchrieser, C., 2007. Legionella pneumophila - A human pathogen that co-evolved with fresh water protozoa. *Cellular and Molecular Life Sciences*, 64(4), pp.432–448. Available at: http://www.ncbi.nlm.nih.gov/pubmed/17192810 [Accessed November 20, 2014].

Ali, S.R., Timmer, A.M., Bilgrami, S., Park, E.J., Eckmann, L., Nizet, V. & Karin, M., 2011. Anthrax toxin induces macrophage death by p38 MAPK inhibition but leads to inflammasome activation via ATP leakage. *Immunity*, 35(1), pp.34–44. Available at: http://linkinghub.elsevier.com/retrieve/pii/S1074761311001786.

Archer, K. a, Alexopoulou, L., Flavell, R. a & Roy, C.R., 2009. Multiple MyD88-dependent responses contribute to pulmonary clearance of Legionella pneumophila. *Cellular microbiology*, 11(1), pp.21–36. Available at: http://www.pubmedcentral.nih.gov/articlerender.fcgi?artid=2752851&tool=pmcentrez&rendertype=abstract [Accessed December 26, 2013].

Asrat, S., Dugan, A.S. & Isberg, R.R., 2014. The frustrated host response to Legionella pneumophila is bypassed by MyD88-dependent translation of pro-inflammatory cytokines. *PLoS pathogens*, 10(7), p.e1004229. Available at: http://www.pubmedcentral.nih.gov/articlerender.fcgi?artid=4110041&tool=pmcentrez&rendertype=abstract [Accessed November 6, 2014].

Asrat, S., de Jesús, D. a, Hempstead, A.D., Ramabhadran, V. & Isberg, R.R., 2014. Bacterial pathogen manipulation of host membrane trafficking. *Annual review of cell and developmental biology*, 30, pp.79–109. Available at: http://www.ncbi.nlm.nih.gov/pubmed/25103867 [Accessed October 20, 2014].

Auerbuch, V., Golenbock, D.T. & Isberg, R.R., 2009. Innate immune recognition of Yersinia pseudotuberculosis type III secretion. *PLoS Pathogens*, 5(12).

Baechler, E.C., Batliwalla, F.M., Karypis, G., Gaffney, P.M., Ortmann, W.A., Espe, K.J., Shark, K.B., Grande, W.J., Hughes, K.M., Kapur, V., et al., 2003. Interferon-inducible gene expression signature in peripheral blood cells of patients with severe lupus. *Proceedings of the National Academy of Sciences*, 100(5), pp.2610–2615. Available at: http://www.pnas.org/cgi/doi/10.1073/pnas.0337679100.

Barber, G.N., 2011. Cytoplasmic DNA innate immune pathways. *Immunological reviews*, 243(1), pp.99–108. Available at: http://www.ncbi.nlm.nih.gov/pubmed/21884170.

Baroja-Mazo, A., Martín-Sánchez, F., Gomez, A.I., Martínez, C.M., Amores-Iniesta, J., Compan, V., Barberà-Cremades, M., Yagüe, J., Ruiz-Ortiz, E., Antón, J., et al., 2014. The NLRP3 inflammasome is released as a particulate danger signal that amplifies the inflammatory response. *Nature immunology*, 15(8), pp.738–48. Available at: http://www.ncbi.nlm.nih.gov/pubmed/24952504.

Barry, K.C., Fontana, M.F., Portman, J.L., Dugan, A.S. & Vance, R.E., 2013. IL-1α signaling initiates the inflammatory response to virulent Legionella pneumophila in vivo. *Journal of immunology (Baltimore, Md. : 1950)*, 190(12), pp.6329–39. Available at: http://www.ncbi.nlm.nih.gov/pubmed/23686480 [Accessed December 26, 2013].

Bauer, J.W., Baechler, E.C., Petri, M., Batliwalla, F.M., Crawford, D., Ortmann, W.A., Espe, K.J., Li, W., Patel, D.D., Gregersen, P.K., et al., 2006. Elevated serum levels of interferon-regulated chemokines are biomarkers for active human systemic lupus erythematosus. *PLoS Medicine*, 3(12), pp.2274–2284.

Berger, K.H. & Isberg, R.R., 1993. Two distinct defects in intracellular growth complemented by a single genetic locus in Legionella pneumophila. *Molecular Microbiology*, 7(1), pp.7–19. Available at: http://www.ncbi.nlm.nih.gov/pubmed/8382332.

Berger, S.B., Kasparcova, V., Hoffman, S., Swift, B., Dare, L., Schaeffer, M., Capriotti, C., Cook, M., Finger, J., Hughes-Earle, A., et al., 2014. Cutting Edge: RIP1 Kinase Activity Is Dispensable for Normal Development but Is a Key Regulator of Inflammation in SHARPIN-Deficient Mice. *The Journal of Immunology*, 192(12), pp.5476–5480. Available at: http://www.jimmunol.org/cgi/doi/10.4049/jimmunol.1400499.

Vanden Berghe, T., Vanlangenakker, N., Parthoens, E., Deckers, W., Devos, M., Festjens, N., Guerin, C.J., Brunk, U.T., Declercq, W., Vandenabeele, P., et al., 2010. Necroptosis, necrosis and secondary necrosis converge on similar cellular disintegration features. *Cell death and differentiation*, 17(6), pp.922–930. Available at: http://dx.doi.org/10.1038/cdd.2009.184%5Cnhttp://www.ncbi.nlm.nih.gov/pubmed/20010783%5Cnhttp://www.nature.com/cdd/journal/v17/n6/pdf/cdd2009184a.pdf.

Bergsbaken, T., Fink, S.L. & Cookson, B.T., 2009. Pyroptosis: host cell death and inflammation. *Nature Reviews Microbiology*, 7(2), pp.99–109. Available at: http://www.nature.com/doifinder/10.1038/nrmicro2070.

Black, R.A., Kronheim, S.R. & Sleath, P.R., 1989. Activation of interleukin-1 beta by a co-induced protease. *FEBS letters*, 247(2), pp.386–90. Available at: http://www.ncbi.nlm.nih.gov/pubmed/2653864.

Blanchet, C., Jaubert, J., Carniel, E., Fayolle, C., Milon, G., Szatanik, M., Panthier, J.-J. & Montagutelli, X., 2011. Mus spretus SEG/Pas mice resist virulent Yersinia pestis, under multigenic control. *Genes and Immunity*, 12(1), pp.23–30. Available at: http://www.nature.com/doifinder/10.1038/gene.2010.45.

Bocci, V., 1985. The physiological interferon response. *Immunology today*, 6(1), pp.7–9. Available at: http://www.ncbi.nlm.nih.gov/pubmed/25291198.

Brennan, M.A. & Cookson, B.T., 2000. Salmonella induces macrophage death by caspase-1-dependent necrosis. *Molecular Microbiology*, 38(1), pp.31–40.

Brieland, J., Freeman, P., Kunkel, R., Chrisp, C., Hurley, M., Fantone, J. & Engleberg, C., 1994. Replicative Legionella pneumophila lung infection in intratracheally inoculated A/J mice. A murine model of human Legionnaires' disease. *The American journal of pathology*, 145(6), pp.1537–46. Available at: http://www.pubmedcentral.nih.gov/articlerender.fcgi?artid=1887509&tool=pmcentrez&rendertype=abstract.

Broz, P. & Monack, D.M., 2013. Noncanonical inflammasomes: caspase-11 activation and effector mechanisms. *PLoS pathogens*, 9(2), p.e1003144. Available at: http://www.pubmedcentral.nih.gov/articlerender.fcgi?artid=3585133&tool=pmcentrez&rendertype=abstract [Accessed February 3, 2014].

Broz, P., Ruby, T., Belhocine, K., Bouley, D.M., Kayagaki, N., Dixit, V.M. & Monack, D.M., 2012. Caspase-11 increases susceptibility to Salmonella infection in the absence of caspase-1. *Nature*, 490(7419), pp.288–91. Available at: http://www.pubmedcentral.nih.gov/articlerender.fcgi?artid=3470772&tool=pmcentrez&rendertype=abstract [Accessed January 27, 2014].

Brumatti, G., Sheridan, C. & Martin, S.J., 2008. Expression and purification of recombinant annexin V for the detection of membrane alterations on apoptotic cells. *Methods*, 44(3), pp.235–240.

Van Bussel, I.P.G., Jolink-Stoppelenburg, A., De Groot, C.P.G.M., Müller, M.R. & Afman, L.A., 2016. Differences in genome-wide gene expression response in peripheral blood mononuclear cells between young and old men upon caloric restriction. *Genes & Nutrition*, 11(1), p.13. Available at: http://genesandnutrition.biomedcentral.com/articles/10.1186/s12263-016-0528-0.

Cai, Z., Jitkaew, S., Zhao, J., Chiang, H.-C., Choksi, S., Liu, J., Ward, Y., Wu, L. & Liu, Z.-G., 2013. Plasma membrane translocation of trimerized MLKL protein is required for TNF-induced necroptosis. *Nature Cell Biology*, 16(1), pp.55–65. Available at: http://www.nature.com/doifinder/10.1038/ncb2883.

Case, C.L., Kohler, L.J., Lima, J.B., Strowig, T., de Zoete, M.R., Flavell, R.A., Zamboni, D.S. & Roy, C.R., 2013. Caspase-11 stimulates rapid flagellin-independent pyroptosis in response to Legionella pneumophila. *Proceedings of the National Academy of Sciences of the United States of America*, 110(5), pp.1851–1856.

Available at: http://www.ncbi.nlm.nih.gov/pubmed/23307811%5Cnhttp://www.pnas.org/content/110/5/1851%5Cnhttp://www.pnas.org/content/110/5/1851.full.pdf [Accessed October 6, 2013].

Case, C.L., Shin, S. & Roy, C.R., 2009. Asc and Ipaf Inflammasomes direct distinct pathways for caspase-1 activation in response to Legionella pneumophila. *Infection and immunity*, 77(5), pp.1981–91. Available at: http://www.pubmedcentral.nih.gov/articlerender.fcgi?artid=2681768&tool=pmcentrez&rendertype=abstract [Accessed December 19, 2013].

Casson, C.N., Yu, J., Reyes, V.M., Taschuk, F.O., Yadav, A., Copenhaver, A.M., Nguyen, H.T., Collman, R.G. & Shin, S., 2015. Human caspase-4 mediates noncanonical inflammasome activation against gram-negative bacterial pathogens. *Proceedings of the National Academy of Sciences*, 112(21), pp.6688–93. Available at: http://www.pnas.org/lookup/doi/10.1073/pnas.1421699112.

Cecil, J.D., O'Brien-Simpson, N.M., Lenzo, J.C., Holden, J.A., Singleton, W., Perez-Gonzalez, A., Mansell, A. & Reynolds, E.C., 2017. Outer membrane vesicles prime and activate macrophage inflammasomes and cytokine secretion in vitro and in vivo. *Frontiers in Immunology*, 8(AUG), pp.1–22.

Chai, Y., Chen, D., Wang, X., Wu, H. & Yang, T., 2017. A novel splice site mutation in DFNA5 causes late-onset progressive non-syndromic hearing loss in a Chinese family. *International Journal of Pediatric Otorhinolaryngology*, 78(8), pp.1265–1268. Available at: http://dx.doi.org/10.1016/j.ijporl.2014.05.007.

Chain, P.S.G., Carniel, E., Larimer, F.W., Lamerdin, J., Stoutland, P.O., Regala, W.M., Georgescu, A.M., Vergez, L.M., Land, M.L., Motin, V.L., et al., 2004. Insights into the evolution of Yersinia pestis through whole-genome comparison with Yersinia pseudotuberculosis. *Proceedings of the National Academy of Sciences*, 101(38), pp.13826–13831. Available at: http://www.pnas.org/cgi/doi/10.1073/pnas.0404012101.

Chen, M., Guerrero, A.D., Huang, L., Shabier, Z., Pan, M., Tan, T.H. & Wang, J., 2007. Caspase-9-induced mitochondrial disruption through cleavage of anti-apoptotic BCL-2 family members. *Journal of Biological Chemistry*, 282(46), pp.33888–33895.

Chen, X., He, W., Hu, L., Li, J., Fang, Y., Wang, X., Xu, X., Wang, Z., Huang, K. & Han, J., 2016. Pyroptosis is driven by non-selective gasdermin-D pore and its morphology is different from MLKL channel-mediated necroptosis. *Cell Research*, 26(9), pp.1–14. Available at: http://dx.doi.org/10.1038/cr.2016.100.

Chevallier, L., Blanchet, C., Jaubert, J., Pachulec, E., Demeure, C., Carniel, E., Panthier, J.-J. & Montagutelli, X., 2013. Resistance to plague of Mus spretus SEG/Pas mice requires the combined action of at least four genetic factors. *Genes and immunity*, 14(1), pp.35–41. Available at: http://www.ncbi.nlm.nih.gov/pubmed/23151488.

Cho, Y.S., Challa, S., Moquin, D., Genga, R., Ray, T.D., Guildford, M. & Chan, F.K.M., 2009. Phosphorylation-Driven Assembly of the RIP1-RIP3 Complex Regulates Programmed Necrosis and Virus-Induced Inflammation. *Cell*, 137(6), pp.1112–

1123.

Chow, S.S.W., Craig, M.E., Jones, C.A., Hall, B., Catteau, J., Lloyd, A.R. & Rawlinson, W.D., 2008. Differences in amniotic fluid and maternal serum cytokine levels in early midtrimester women without evidence of infection. *Cytokine*, 44(1), pp.78–84.

Coers, J., Vance, R.E., Fontana, M.F. & Dietrich, W.F., 2007. Restriction of Legionella pneumophila growth in macrophages requires the concerted action of cytokine and Naip5/Ipaf signalling pathways. *Cellular microbiology*, 9(10), pp.2344–57. Available at: http://www.ncbi.nlm.nih.gov/pubmed/17506816 [Accessed February 17, 2014].

Cogswell, J.P., Codlevski, M.M., Wisely, C.B., Leesnitzer, L.M., Ways, J.P., Gray, J.G. & Clay, C., 1994. NF-KB Regulates IL-1beta Transcription Through a Consensus NF-KB Binding Site and a Nonconsensus CRE-Like Site. *Journal of immunology*, 153, pp.712–723.

Conos, S.A., Chen, K.W., De Nardo, D., Hara, H., Whitehead, L., Núñez, G., Masters, S.L., Murphy, J.M., Schroder, K., Vaux, D.L., et al., 2017. Active MLKL triggers the NLRP3 inflammasome in a cell-intrinsic manner. *Proceedings of the National Academy of Sciences*, p.201613305. Available at: http://www.pnas.org/lookup/doi/10.1073/pnas.1613305114.

Cookson, B.T. & Brennan, M.A., 2001. Pro-inflammatory programmed cell death. *Trends in microbiology*, 9(3), pp.113–4. Available at: http://www.ncbi.nlm.nih.gov/pubmed/11303500.

Cordoba-Rodriguez, R., Fang, H., Lankford, C.S.R. & Frucht, D.M., 2004. Anthrax lethal toxin rapidly activates Caspase-1/ICE and induces extracellular release of interleukin (IL)-1?? and IL-18. *Journal of Biological Chemistry*, 279(20), pp.20563–20566.

Corrales, L., Woo, S.-R., Williams, J.B., McWhirter, S.M., Dubensky, T.W. & Gajewski, T.F., 2016. Antagonism of the STING Pathway via Activation of the AIM2 Inflammasome by Intracellular DNA. *The Journal of Immunology*, 196(7), pp.3191–3198. Available at: http://www.jimmunol.org/cgi/doi/10.4049/jimmunol.1502538%5Cnhttp://www.ncbi.nlm.nih.gov/pubmed/26927800%5Cnhttp://www.pubmedcentral.nih.gov/articlerender.fcgi?artid=PMC4800192.

Creasey, E.A. & Isberg, R.R., 2012. The protein SdhA maintains the integrity of the Legionella-containing vacuole. *Proceedings of the National Academy of Sciences of the United States of America*, 109(9), pp.3481–6. Available at: http://www.pubmedcentral.nih.gov/articlerender.fcgi?artid=3295292&tool=pmcentrez&rendertype=abstract [Accessed August 7, 2013].

Davies, J.Q. & Gordon, S., 2005. Isolation and Culture of Human Macrophages. In C. D. Helgason & C. L. Miller, eds. *Basic Cell Culture Protocols*. New Jersey: Humana Press, pp. 105–116. Available at: http://dx.doi.org/10.1385/1-59259-838-2:105.

Degterev, A., Hitomi, J., Germscheid, M., Ch'en, I.L., Korkina, O., Teng, X., Abbott, D., Cuny, G.D., Yuan, C., Wagner, G., et al., 2008. Identification of RIP1 kinase as a

specific cellular target of necrostatins. *Nature chemical biology*, 4(5), pp.313–21. Available at: http://www.ncbi.nlm.nih.gov/pubmed/18408713 [Accessed October 29, 2014].

Demeure, C.E., Blanchet, C., Fitting, C., Fayolle, C., Khun, H., Szatanik, M., Milon, G., Panthier, J.J., Jaubert, J., Montagutelli, X., et al., 2012. Early systemic bacterial dissemination and a rapid innate immune response characterize genetic resistance to plague of SEG mice. *Journal of Infectious Diseases*, 205(1), pp.134–143.

Ding, J., Wang, K., Liu, W., She, Y., Sun, Q., Shi, J., Sun, H., Wang, D. & Shao, F., 2016. Pore-forming activity and structural autoinhibition of the gasdermin family. *Nature*, 535(7610), pp.111–116. Available at: http://dx.doi.org/10.1038/nature18590.

Dondelinger, Y., Delanghe, T., Rojas-Rivera, D., Priem, D., Delvaeye, T., Bruggeman, I., Van Herreweghe, F., Vandenabeele, P. & Bertrand, M.J.M., 2017. MK2 phosphorylation of RIPK1 regulates TNF-mediated cell death. *Nature Cell Biology*, 19(10), pp.1237–1247. Available at: http://www.nature.com/doifinder/10.1038/ncb3608.

Eddy, J.L., Gielda, L.M., Caulfield, A.J., Rangel, S.M. & Lathem, W.W., 2014. Production of outer membrane vesicles by the plague pathogen Yersinia pestis. *PLoS ONE*, 9(9), pp.1–11.

Erridge, C., Pridmore, A., Eley, A., Stewart, J. & Poxton, I.R., 2004. Lipopolysaccharides of Bacteroides fragilis, Chlamydia trachomatis and Pseudomonas aeruginosa signal via Toll-like receptor 2. *Journal of Medical Microbiology*, 53(8), pp.735–740. Available at: http://jmm.sgmjournals.org/cgi/doi/10.1099/jmm.0.45598-0 [Accessed December 26, 2013].

Feeley, E.M., Pilla-Moffett, D.M., Zwack, E.E., Piro, A.S., Finethy, R., Kolb, J.P., Martinez, J., Brodsky, I.E. & Coers, J., 2017. Galectin-3 directs antimicrobial guanylate binding proteins to vacuoles furnished with bacterial secretion systems. *Proceedings of the National Academy of Sciences of the United States of America*, 114(9), pp.E1698–E1706. Available at: http://www.pnas.org/lookup/doi/10.1073/pnas.1615771114.

Feltham, R., Vince, J.E. & Lawlor, K.E., 2017. Caspase-8: not so silently deadly. *Clinical & Translational Immunology*, 6(1), p.e124. Available at: http://www.nature.com/doifinder/10.1038/cti.2016.83.

Finethy, R., Jorgensen, I., Haldar, A.K., De Zoete, M.R., Strowig, T., Flavell, R.A., Yamamoto, M., Nagarajan, U.M., Miao, E.A. & Coers, J., 2015. Guanylate binding proteins enable rapid activation of canonical and noncanonical inflammasomes in Chlamydia-infected macrophages. *Infection and Immunity*, 83(12), pp.4740–4749. Available at: http://www.ncbi.nlm.nih.gov/pubmed/26416908.

Fontana, M.F., Banga, S., Barry, K.C., Shen, X., Tan, Y., Luo, Z.Q. & Vance, R.E., 2011. Secreted bacterial effectors that inhibit host protein synthesis are critical for induction of the innate immune response to virulent Legionella pneumophila. *PLoS Pathogens*, 7(2).

Fontana, M.F. & Vance, R.E., 2011. Two signal models in innate immunity. *Immunological reviews*, 243(1), pp.26–39. Available at: http://www.ncbi.nlm.nih.gov/pubmed/21884165.

Fortier, A., Doiron, K., Saleh, M., Grinstein, S. & Gros, P., 2009. Restriction of Legionella pneumophila replication in macrophages requires concerted action of the transcriptional regulators Irf1 and Irf8 and nod-like receptors Naip5 and Nlrc4. *Infection and immunity*, 77(11), pp.4794–805. Available at: http://www.pubmedcentral.nih.gov/articlerender.fcgi?artid=2772531&tool=pmcentrez&rendertype=abstract [Accessed September 9, 2013].

Franchi, L., Eigenbrod, T., Muñoz-Planillo, R. & Nuñez, G., 2009. The Inflammasome: A Caspase-1 Activation Platform Regulating Immune Responses and Disease Pathogenesis. *Nat. Immun.*, 10(3), p.241.

Franklin, B.S., Bossaller, L., De Nardo, D., Ratter, J.M., Stutz, A., Engels, G., Brenker, C., Nordhoff, M., Mirandola, S.R., Al-Amoudi, A., et al., 2014. The adaptor ASC has extracellular and "prionoid" activities that propagate inflammation. *Nature immunology*, 15(8), pp.727–37. Available at: http://www.ncbi.nlm.nih.gov/pubmed/24952505.

Freeman, C.M., Crudgington, S., Stolberg, V.R., Brown, J.P., Sonstein, J., Alexis, N.E., Doerschuk, C.M., Basta, P. V, Carretta, E.E., Couper, D.J., et al., 2015. Design of a multi-center immunophenotyping analysis of peripheral blood, sputum and bronchoalveolar lavage fluid in the Subpopulations and Intermediate Outcome Measures in COPD Study (SPIROMICS). *Journal of translational medicine*, 13(1), p.19. Available at: http://dx.doi.org/10.1186/s12967-014-0374-z.

Friedlander, A.M., 1986. Macrophages are sensitive to anthrax lethal toxin through an acid-dependent process. *The Journal of biological chemistry*, 261(16), pp.7123–6. Available at: http://www.jbc.org/content/261/16/7123.short.

Fuse, E.T., Tateda, K., Kikuchi, Y., Matsumoto, T., Gondaira, F., Azuma, A., Kudoh, S., Standiford, T.J. & Yamaguchi, K., 2007. Role of Toll-like receptor 2 in recognition of Legionella pneumophila in a murine pneumonia model. *Journal of Medical Microbiology*, 56(3), pp.305–312. Available at: http://www.ncbi.nlm.nih.gov/pubmed/17314358 [Accessed November 11, 2013].

Gaidt, M.M. & Hornung, V., 2016. Pore formation by GSDMD is the effector mechanism of pyroptosis. *Embo*, pp.1–3.

Galluzzi, L., Bravo-San Pedro, J.M., Vitale, I., Aaronson, S.A., Abrams, J.M., Adam, D., Alnemri, E.S., Altucci, L., Andrews, D., Annicchiarico-Petruzzelli, M., et al., 2015. Essential versus accessory aspects of cell death: recommendations of the NCCD 2015. *Cell Death and Differentiation*, 22(1), pp.58–73. Available at: http://www.nature.com/doifinder/10.1038/cdd.2014.137.

Ge, J., Gong, Y.-N., Xu, Y. & Shao, F., 2012. Preventing bacterial DNA release and absent in melanoma 2 inflammasome activation by a Legionella effector functioning in membrane trafficking. *Proceedings of the National Academy of Sciences of the United States of America*, 109(16), pp.6193–8. Available at: http://www.ncbi.nlm.nih.gov/pubmed/22474394 [Accessed November 11, 2013].

Geng, J., Ito, Y., Shi, L., Amin, P., Chu, J., Ouchida, A.T., Mookhtiar, A.K., Zhao, H., Xu, D., Shan, B., et al., 2017. Regulation of RIPK1 activation by TAK1-mediated phosphorylation dictates apoptosis and necroptosis. *Nature Communications*, 8(1), p.359. Available at: http://dx.doi.org/10.1038/s41467-017-00406-w.

Girard, R., Pedron, T., Uematsu, S., Balloy, V., Chignard, M., Akira, S. & Chaby, R., 2003. Lipopolysaccharides from Legionella and Rhizobium stimulate mouse bone marrow granulocytes via Toll-like receptor 2. *J.Cell Sci*, 116(Pt 2), pp.293–302. Available at: http://jcs.biologists.org/cgi/doi/10.1242/jcs.00212 [Accessed December 26, 2013].

Golenbock, D.T., Hampton, R.Y., Qureshi, N., Takayama, K. & Raetz, C.R.H., 1991. Lipid A-like Molecules That Antagonize the Effects of Endotoxins on Human Monocytes. *Journal of Biological Chemistry*, 266(29), pp.19490–19496.

Gong, Y.-N., Guy, C., Olauson, H., Becker, J.U., Yang, M., Fitzgerald, P., Linkermann, A. & Green, D.R., 2017. ESCRT-III Acts Downstream of MLKL to Regulate Necroptotic Cell Death and Its Consequences. *Cell*, 169(2), p.286–300.e16. Available at: http://dx.doi.org/10.1016/j.cell.2017.03.020.

Gough, D.J., Messina, N.L., Clarke, C.J.P., Johnstone, R.W. & Levy, D.E., 2012. Constitutive type I interferon modulates homeostatic balance through tonic signaling. *Immunity*, 36(2), pp.166–74. Available at: http://dx.doi.org/10.1016/j.immuni.2012.01.011.

Gough, D.J., Messina, N.L., Hii, L., Gould, J. a., Sabapathy, K., Robertson, A.P.S., Trapani, J. a., Levy, D.E., Hertzog, P.J., Clarke, C.J.P., et al., 2010. Functional crosstalk between type I and II interferon through the regulated expression of STAT1. *PLoS biology*, 8(4), p.e1000361. Available at: http://www.ncbi.nlm.nih.gov/pubmed/20436908.

Gray, E.E., Treuting, P.M., Woodward, J.J. & Stetson, D.B., 2015. Cutting Edge: cGAS Is Required for Lethal Autoimmune Disease in the Trex1-Deficient Mouse Model of Aicardi-Goutières Syndrome. *Journal of immunology (Baltimore, Md. : 1950)*, 195(5), pp.1939–43. Available at: http://www.ncbi.nlm.nih.gov/pubmed/26223655.

Green, D.R., 2016. The cell's dilemma, or the story of cell death: an entertainment in three acts. *The FEBS journal*, 283(14), pp.2568–2576.

Gresser, I., Belardelli, F., Maury, C., Maunoury, M.T. & Tovey, M.G., 1983. Injection of mice with antibody to interferon enhances the growth of transplantable murine tumors. *The Journal of experimental medicine*, 158(6), pp.2095–107. Available at: http://www.pubmedcentral.nih.gov/articlerender.fcgi?artid=2187158&tool=pmcentrez&rendertype=abstract.

Gresser, I., Vignaux, F., Belardelli, F., Tovey, M.G. & Maunoury, M.T., 1985. Injection of mice with antibody to mouse interferon alpha/beta decreases the level of 2'-5' oligoadenylate synthetase in peritoneal macrophages. *Journal of virology*, 53(1), pp.221–7. Available at: http://www.pubmedcentral.nih.gov/articlerender.fcgi?artid=255016&tool=pmcentrez&rendertype=abstract.

Günther, C., Martini, E., Wittkopf, N., Amann, K., Weigmann, B., Neumann, H., Waldner, M.J., Hedrick, S.M., Tenzer, S., Neurath, M.F., et al., 2011. Caspase-8 regulates TNF-α-induced epithelial necroptosis and terminal ileitis. *Nature*, 477(7364), pp.335–339. Available at: http://www.nature.com/doifinder/10.1038/nature10400.

Guo, H., Omoto, S., Harris, P. a., Finger, J.N., Bertin, J., Gough, P.J., Kaiser, W.J. & Mocarski, E.S., 2015. Herpes simplex virus suppresses necroptosis in human cells. *Cell Host and Microbe*, 17(2), pp.243–251.

Guo, X., Yin, H., Chen, Y., Li, L., Li, J. & Liu, Q., 2016. TAK1 regulates caspase 8 activation and necroptotic signaling via multiple cell death checkpoints. *Cell Death and Disease*, 7(9), p.e2381. Available at: http://www.nature.com/doifinder/10.1038/cddis.2016.294.

Gutierrez, K.D., Davis, M.A., Daniels, B.P., Olsen, T.M., Ralli-Jain, P., Tait, S.W.G., Gale, M. & Oberst, A., 2017. MLKL Activation Triggers NLRP3-Mediated Processing and Release of IL-1β Independently of Gasdermin-D. *Journal of immunology (Baltimore, Md. : 1950)*, 198(5), pp.2156–2164. Available at: http://www.ncbi.nlm.nih.gov/pubmed/28130493.

Hagar, J.A., Powell, D. a, Aachoui, Y., Ernst, R.K. & Miao, E.A., 2013. Cytoplasmic LPS activates caspase-11: implications in TLR4-independent endotoxic shock. *Science (New York, N.Y.)*, 341(6151), pp.1250–3. Available at: http://www.ncbi.nlm.nih.gov/pubmed/24031018 [Accessed January 21, 2014].

Haldar, A.K., Foltz, C., Finethy, R., Piro, A.S., Feeley, E.M., Pilla-Moffett, D.M., Komatsu, M., Frickel, E.-M. & Coers, J., 2015. Ubiquitin systems mark pathogen-containing vacuoles as targets for host defense by guanylate binding proteins. *Proceedings of the National Academy of Sciences*, p.201515966. Available at: http://www.pnas.org/lookup/doi/10.1073/pnas.1515966112.

Haldar, A.K., Saka, H. a, Piro, A.S., Dunn, J.D., Henry, S.C., Taylor, G. a, Frickel, E.M., Valdivia, R.H. & Coers, J., 2013. IRG and GBP host resistance factors target aberrant, "non-self" vacuoles characterized by the missing of "self" IRGM proteins. *PLoS pathogens*, 9(6), p.e1003414. Available at: http://www.pubmedcentral.nih.gov/articlerender.fcgi?artid=3681737&tool=pmcentrez&rendertype=abstract [Accessed May 27, 2014].

Halff, E.F., Diebolder, C. a, Versteeg, M., Schouten, A., Brondijk, T.H.C. & Huizinga, E.G., 2012. Formation and structure of a NAIP5-NLRC4 inflammasome induced by direct interactions with conserved N- and C-terminal regions of flagellin. *The Journal of biological chemistry*, 287(46), pp.38460–72. Available at: http://www.pubmedcentral.nih.gov/articlerender.fcgi?artid=3493891&tool=pmcentrez&rendertype=abstract [Accessed December 26, 2013].

Hande, K.R., 1998. Etoposide: Four decades of development of a topoisomerase II inhibitor. *European Journal of Cancer*, 34(10), pp.1514–1521.

Härtlova, A., Erttmann, S.F.F., Raffi, F.A.A., Schmalz, A.M.M., Resch, U., Anugula, S., Lienenklaus, S., Nilsson, L.M.M., Kröger, A., Nilsson, J.A.A., et al., 2015. DNA damage primes the type I interferon system via the cytosolic DNA sensor STING to

promote anti-microbial innate immunity. *Immunity*, 42(2), pp.332–43. Available at: http://linkinghub.elsevier.com/retrieve/pii/S1074761315000382.

He, S., Liang, Y., Shao, F. & Wang, X., 2011. Toll-like receptors activate programmed necrosis in macrophages through a receptor-interacting kinase-3-mediated pathway. *Proceedings of the National Academy of Sciences*, 108(50), pp.20054–20059. Available at: http://www.pnas.org/cgi/doi/10.1073/pnas.1116302108.

He, W., Wan, H., Hu, L., Chen, P., Wang, X., Huang, Z., Yang, Z.-H., Zhong, C.-Q. & Han, J., 2015. Gasdermin D is an executor of pyroptosis and required for interleukin-1β secretion. *Cell Research*, 25(12), pp.1285–1298. Available at: http://www.nature.com/doifinder/10.1038/cr.2015.139.

Hilbi, H., Moss, J.E., Hersh, D., Chen, Y., Arondel, J., Banerjee, S., Flavell, R.A., Yuan, J., Sansonetti, P.J. & Zychlinsky, A., 1998. Shigella-induced apoptosis is dependent on caspase-1 which binds to IpaB. *Journal of Biological Chemistry*, 273(49), pp.32895–32900.

Hiscott, J., Ryals, J., Dierks, P., Hofmann, V. & Weissmann, C., 1984. The expression of human interferon alpha genes.

Hooks, J.J., Jordan, G.W. & Cupps, T., 1982. Multiple interferons with the circulation of patients with systemic lupus erythematosus and vasculitis. *Arthritis and Rheumatism*, 25(4), pp.396–400. Available at: http://www.embase.com/search/results?subaction=viewrecord&from=export&id=L12158947%5Cnhttp://sfx.library.uu.nl/utrecht?sid=EMBASE&issn=00043591&id=doi:&atitle=Multiple+interferons+with+the+circulation+of+patients+with+systemic+lupus+erythematosus+and+vasc.

Hornung, V., Ablasser, A., Charrel-Dennis, M., Bauernfeind, F., Horvath, G., Caffrey, D.R., Latz, E. & Fitzgerald, K.A., 2009. AIM2 recognizes cytosolic dsDNA and forms a caspase-1-activating inflammasome with ASC. *Nature*, 458(7237), pp.514–518. Available at: http://dx.doi.org/10.1038/nature07725.

Horwitz, M.A., 1983. Formation of a novel phagosome by the Legionnaires' disease bacterium (Legionella pneumophila) in human monocytes. *The Journal of experimental medicine*, 158(4), pp.1319–31. Available at: http://www.pubmedcentral.nih.gov/articlerender.fcgi?artid=2187375&tool=pmcentrez&rendertype=abstract.

Hsu, H., Huang, J., Shu, H.B., Baichwal, V. & Goeddel, D. V., 1996. TNF-dependent recruitment of the protein kinase RIP to the TNF receptor-1 signaling complex. *Immunity*, 4(4), pp.387–396.

Hsu, H., Xiong, J. & Goeddel, D. V., 1995. The TNF receptor 1-associated protein TRADD signals cell death and NF-κB activation. *Cell*, 81(4), pp.495–504.

Huang, Z., Wu, S.Q., Liang, Y., Zhou, X., Chen, W., Li, L., Wu, J., Zhuang, Q., Chen, C., Li, J., et al., 2015. RIP1/RIP3 binding to HSV-1 ICP6 initiates necroptosis to restrict virus propagation in mice. *Cell Host and Microbe*, 17(2), pp.229–242.

Isberg, R.R., O'Connor, T.J. & Heidtman, M., 2009. The Legionella pneumophila replication vacuole: making a cosy niche inside host cells. *Nature reviews.*

Microbiology, 7(1), pp.13–24. Available at: http://www.pubmedcentral.nih.gov/articlerender.fcgi?artid=2631402&tool=pmcentrez&rendertype=abstract [Accessed January 24, 2014].

Ivanov, S.S. & Roy, C.R., 2013. Pathogen signatures activate a ubiquitination pathway that modulates the function of the metabolic checkpoint kinase mTOR. *Nature immunology*, 14(12), pp.1219–28. Available at: http://dx.doi.org/10.1038/ni.2740 [Accessed January 14, 2014].

Jackson, J.D., Markert, J.M., Li, L., Carroll, S.L. & Cassady, K.A., 2016. STAT1 and NF-κB Inhibitors Diminish Basal Interferon-Stimulated Gene Expression and Improve the Productive Infection of Oncolytic HSV in MPNST Cells. *Molecular cancer research : MCR*, 14(5), pp.482–492. Available at: http://mcr.aacrjournals.org/content/14/5/482.abstract?etoc.

Jaco, I., Annibaldi, A., Lalaoui, N., Wilson, R., Tenev, T., Laurien, L., Kim, C., Jamal, K., Wicky John, S., Liccardi, G., et al., 2017. MK2 Phosphorylates RIPK1 to Prevent TNF-Induced Cell Death. *Molecular Cell*, 66(5), p.698–710.e5.

Jaguin, M., Houlbert, N., Fardel, O. & Lecureur, V., 2013. Polarization profiles of human M-CSF-generated macrophages and comparison of M1-markers in classically activated macrophages from GM-CSF and M-CSF origin. *Cellular immunology*, 281(1), pp.51–61. Available at: http://dx.doi.org/10.1016/j.cellimm.2013.01.010.

Jorgensen, I., Zhang, Y., Krantz, B.A. & Miao, E.A., 2016. Pyroptosis triggers pore-induced intracellular traps (PITs) that capture bacteria and lead to their clearance by efferocytosis. *The Journal of Experimental Medicine*, 213(10), pp.2113–2128. Available at: http://www.jem.org/lookup/doi/10.1084/jem.20151613.

Jung, A.L., Herkt, C.E., Schulz, C., Bolte, K., Seidel, K., Scheller, N., Sittka-Stark, A., Bertrams, W. & Schmeck, B., 2017. Legionella pneumophila infection activates bystander cells differentially by bacterial and host cell vesicles. *Scientific Reports*, 7(1), p.6301. Available at: http://www.nature.com/articles/s41598-017-06443-1.

Kaiser, W.J., Sridharan, H., Huang, C., Mandal, P., Upton, J.W., Gough, P.J., Sehon, C. a., Marquis, R.W., Bertin, J. & Mocarski, E.S., 2013. Toll-like receptor 3-mediated necrosis via TRIF, RIP3, and MLKL. *Journal of Biological Chemistry*, 288(43), pp.31268–31279.

Kaiser, W.J., Upton, J.W., Long, A.B., Livingston-Rosanoff, D., Daley-Bauer, L.P., Hakem, R., Caspary, T. & Mocarski, E.S., 2011. RIP3 mediates the embryonic lethality of caspase-8-deficient mice. *Nature*, 471(7338), pp.368–72. Available at: http://www.ncbi.nlm.nih.gov/pubmed/21368762.

Kaiser, W.J., Upton, J.W. & Mocarski, E.S., 2008. Receptor-Interacting Protein Homotypic Interaction Motif-Dependent Control of NF- B Activation via the DNA-Dependent Activator of IFN Regulatory Factors. *The Journal of Immunology*, 181(9), pp.6427–6434. Available at: http://www.jimmunol.org/cgi/doi/10.4049/jimmunol.181.9.6427.

Kang, S.J., Wang, S., Hara, H., Peterson, E.P., Namura, S., Amin-Hanjani, S., Huang, Z., Srinivasan, A., Tomaselli, K.J., Thornberry, N.A., et al., 2000. Dual role of caspase-

11 in mediating activation of caspase-1 and caspase-3 under pathological conditions. *The Journal of cell biology*, 149(3), pp.613–22. Available at: http://www.pubmedcentral.nih.gov/articlerender.fcgi?artid=2174843&tool=pmcentrez&rendertype=abstract.

Kayagaki, N., Stowe, I.B., Lee, B.L., O'Rourke, K., Anderson, K., Warming, S., Cuellar, T., Haley, B., Roose-Girma, M., Phung, Q.T., et al., 2015. Caspase-11 cleaves gasdermin D for non-canonical inflammasome signalling. *Nature*, 526(7575), pp.666–671. Available at: http://www.ncbi.nlm.nih.gov/pubmed/26375259.

Kayagaki, N., Warming, S., Lamkanfi, M., Walle, L. Vande, Louie, S., Dong, J., Newton, K., Qu, Y., Liu, J., Heldens, S., et al., 2011. Non-canonical inflammasome activation targets caspase-11. *Nature*, 479(7371), pp.117–121. Available at: http://www.ncbi.nlm.nih.gov/pubmed/22002608 [Accessed February 20, 2014].

Kayagaki, N., Wong, M.T., Stowe, I.B., Ramani, S.R., Gonzalez, L.C., Akashi-Takamura, S., Miyake, K., Zhang, J., Lee, W.P., Muszyński, A., et al., 2013. Noncanonical inflammasome activation by intracellular LPS independent of TLR4. *Science (New York, N.Y.)*, 341(6151), pp.1246–9. Available at: http://www.ncbi.nlm.nih.gov/pubmed/23887873 [Accessed February 20, 2014].

Kelliher, M.A., Grimm, S., Ishida, Y., Kuo, F., Stanger, B.Z. & Leder, P., 1998. The death domain kinase RIP mediates the TNF-induced NF-κB signal. *Immunity*, 8(3), pp.297–303.

Kim, B.-H., Shenoy, A.R., Kumar, P., Das, R., Tiwari, S. & MacMicking, J.D., 2011. A family of IFN-γ-inducible 65-kD GTPases protects against bacterial infection. *Science (New York, N.Y.)*, 332(6030), pp.717–21. Available at: http://www.ncbi.nlm.nih.gov/pubmed/21551061 [Accessed January 22, 2014].

Knirel, Y.A. & Anisimov, A.P., 2012. Lipopolysaccharide of Yersinia pestis, the Cause of Plague: Structure, Genetics, Biological Properties. *Acta naturae*, 4(3), pp.46–58. Available at: http://www.ncbi.nlm.nih.gov/pubmed/23150803%5Cnhttp://www.pubmedcentral.nih.gov/articlerender.fcgi?artid=PMC3492934%5Cnhttp://www.pubmedcentral.nih.gov/articlerender.fcgi?artid=3492934&tool=pmcentrez&rendertype=abstract.

Kofoed, E.M. & Vance, R.E., 2011. Innate immune recognition of bacterial ligands by NAIPs determines inflammasome specificity. *Nature*, 477(7366), pp.592–5. Available at: http://www.pubmedcentral.nih.gov/articlerender.fcgi?artid=3184209&tool=pmcentrez&rendertype=abstract [Accessed August 20, 2013].

Kolb, J.P., Oguin, T.H., Oberst, A. & Martinez, J., 2017. Programmed Cell Death and Inflammation: Winter Is Coming. *Trends in Immunology*, 38(10), pp.705–718. Available at: http://dx.doi.org/10.1016/j.it.2017.06.009.

Kostura, M.J., Tocci, M.J., Limjuco, G., Chin, J., Cameron, P., Hillman, a G., Chartrain, N. a & Schmidt, J. a, 1989. Identification of a monocyte specific pre-interleukin 1 beta convertase activity. *Proceedings of the National Academy of Sciences of the United States of America*, 86(14), pp.5227–31. Available at: http://www.ncbi.nlm.nih.gov/pubmed/2787508.

Kovacs, S.B. & Miao, E.A., 2017. Gasdermins: Effectors of Pyroptosis. *Trends in Cell Biology*, 27(9), pp.673–684. Available at: http://dx.doi.org/10.1016/j.tcb.2017.05.005.

Krachler, A.M., Woolery, A.R. & Orth, K., 2011. Manipulation of kinase signaling by bacterial pathogens. *Journal of Cell Biology*, 195(7), pp.1083–1092.

Kroemer, G., Galluzzi, L., Vandenabeele, P., Abrams, J., Alnemri, E.S., Baehrecke, E.H., Blagosklonny, M. V., El-Deiry, W.S., Golstein, P., Green, D.R., et al., 2009. Classification of cell death: Recommendations of the Nomenclature Committee on Cell Death 2009. *Cell Death and Differentiation*, 16(1), pp.3–11.

Kuida, K., Lippke, J. a, Ku, G., Harding, M.W., Livingston, D.J., Su, M.S. & Flavell, R. a, 1995. Altered cytokine export and apoptosis in mice deficient in interleukin-1 beta converting enzyme. *Science (New York, N.Y.)*, 267(5206), pp.2000–3. Available at: http://www.ncbi.nlm.nih.gov/pubmed/7535475.

Laguna, R.K., Creasey, E.A., Li, Z., Valtz, N. & Isberg, R.R., 2006. A Legionella pneumophila-translocated substrate that is required for growth within macrophages and protection from host cell death. *Proceedings of the National Academy of Sciences of the United States of America*, 103(49), pp.18745–50. Available at: http://www.pubmedcentral.nih.gov/articlerender.fcgi?artid=1656969&tool=pmcentrez&rendertype=abstract.

Lamothe, B., Lai, Y., Xie, M., Schneider, M.D. & Darnay, B.G., 2013. TAK1 Is Essential for Osteoclast Differentiation and Is an Important Modulator of Cell Death by Apoptosis and Necroptosis. *Molecular and Cellular Biology*, 33(3), pp.582–595. Available at: http://mcb.asm.org/cgi/doi/10.1128/MCB.01225-12.

LaRock, D.L., Chaudhary, A. & Miller, S.I., 2015. Salmonellae interactions with host processes. *Nature Reviews Microbiology*, 13(4), pp.191–205. Available at: http://dx.doi.org/10.1038/nrmicro3420.

Lau, A., Wang, S., Jiang, J., Haig, A., Pavlosky, A., Linkermann, A., Zhang, Z.X. & Jevnikar, A.M., 2013. RIPK3-mediated necroptosis promotes donor kidney inflammatory injury and reduces allograft survival. *American Journal of Transplantation*, 13(11), pp.2805–2818.

Lawlor, K.E. & Vince, J.E., 2014. Ambiguities in NLRP3 inflammasome regulation: Is there a role for mitochondria? *Biochimica et Biophysica Acta (BBA) - General Subjects*, 1840(4), pp.1433–1440. Available at: http://dx.doi.org/10.1016/j.bbagen.2013.08.014.

Lebon, P., Girard, S., Thépot, F. & Chany, C., 1982. The presence of alpha-interferon in human amniotic fluid. *The Journal of general virology*, 59(Pt 2), pp.393–6. Available at: http://www.ncbi.nlm.nih.gov/pubmed/6176680.

Lemaître, N., Sebbane, F., Long, D. & Hinnebusch, B.J., 2006. Yersinia pestis YopJ suppresses tumor necrosis factor alpha induction and contributes to apoptosis of immune cells in the lymph node but is not required for virulence in a rat model of bubonic plague. *Infection and immunity*, 74(9), pp.5126–31. Available at: http://www.ncbi.nlm.nih.gov/pubmed/16926404.

Li, J., McQuade, T., Siemer, A.B., Napetschnig, J., Moriwaki, K., Hsiao, Y.S., Damko, E., Moquin, D., Walz, T., McDermott, A., et al., 2012. The RIP1/RIP3 necrosome forms a functional amyloid signaling complex required for programmed necrosis. *Cell*, 150(2), pp.339–350.

Li, P., Allen, H., Banerjee, S., Franklin, S., Herzog, L., Johnston, C., McDowell, J., Paskind, M., Rodman, L. & Salfeld, J., 1995. Mice deficient in IL-1 beta-converting enzyme are defective in production of mature IL-1 beta and resistant to endotoxic shock. *Cell*, 80(3), pp.401–11. Available at: http://www.ncbi.nlm.nih.gov/pubmed/7859282.

Li, P., Jiang, W., Yu, Q., Liu, W., Zhou, P., Li, J., Xu, J., Xu, B., Wang, F. & Shao, F., 2017. Ubiquitination and degradation of GBPs by a Shigella effector to suppress host defence. *Nature*. Available at: http://www.nature.com/doifinder/10.1038/nature24467.

Lienenklaus, S., Cornitescu, M., Zietara, N., Łyszkiewicz, M., Gekara, N., Jabłónska, J., Edenhofer, F., Rajewsky, K., Bruder, D., Hafner, M., et al., 2009. Novel reporter mouse reveals constitutive and inflammatory expression of IFN-beta in vivo. *Journal of immunology (Baltimore, Md. : 1950)*, 183(5), pp.3229–36. Available at: http://www.jimmunol.org/content/183/5/3229.full.pdf.

Lightfield, K.L., Persson, J., Trinidad, N.J., Brubaker, W., Kofoed, E.M., Sauer, J., Eric, A., Warren, S.E., Miao, E.A., Russell, E., et al., 2011. Differential Requirements for NAIP5 in Activation of the NLRC4 Inflammasome Differential Requirements for NAIP5 in Activation of. *Infection and Immunity*, 79(4), p.1606.

Lin, J., Kumari, S., Kim, C., Van, T.-M., Wachsmuth, L., Polykratis, A. & Pasparakis, M., 2016. RIPK1 counteracts ZBP1-mediated necroptosis to inhibit inflammation. *Nature*, 540(7631), pp.124–128. Available at: http://dx.doi.org/10.1038/nature20558.

Linkermann, A., Brasen, J.H., Darding, M., Jin, M.K., Sanz, A.B., Heller, J.-O., De Zen, F., Weinlich, R., Ortiz, A., Walczak, H., et al., 2013. Two independent pathways of regulated necrosis mediate ischemia-reperfusion injury. *Proceedings of the National Academy of Sciences*, 110(29), pp.12024–12029. Available at: http://www.pnas.org/cgi/doi/10.1073/pnas.1305538110.

Lippmann, J., Müller, H.C., Naujoks, J., Tabeling, C., Shin, S., Witzenrath, M., Hellwig, K., Kirschning, C.J., Taylor, G. a, Barchet, W., et al., 2011. Dissection of a type I interferon pathway in controlling bacterial intracellular infection in mice. *Cellular microbiology*, 13(11), pp.1668–82. Available at: http://www.pubmedcentral.nih.gov/articlerender.fcgi?artid=3196383&tool=pmcentrez&rendertype=abstract [Accessed September 9, 2013].

Liu, K.J., Steinberg, E., Yozzo, A., Song, Y., Kohn, M.H. & Nakhleh, L., 2015. Interspecific introgressive origin of genomic diversity in the house mouse. *Proceedings of the National Academy of Sciences*, 112(1), pp.196–201. Available at: http://www.pnas.org/lookup/doi/10.1073/pnas.1406298111.

Liu, X., Zhang, Z., Ruan, J., Pan, Y., Magupalli, V.G., Wu, H. & Lieberman, J., 2016. Inflammasome-activated gasdermin D causes pyroptosis by forming membrane

pores. *Nature*, 535(7610), pp.153–8. Available at: http://www.nature.com/doifinder/10.1038/nature18629.

Logue, S.E., Elgendy, M. & Martin, S.J., 2009. Expression, purification and use of recombinant annexin V for the detection of apoptotic cells. *Nature Protocols*, 4(9), pp.1383–1395. Available at: http://www.nature.com/doifinder/10.1038/nprot.2009.143.

Losick, V.P., Stephan, K., Smirnova, I.I., Isberg, R.R. & Poltorak, A., 2009. A hemidominant Naip5 allele in mouse strain MOLF/Ei-derived macrophages restricts Legionella pneumophila intracellular growth. *Infection and Immunity*, 77(1), pp.196–204. Available at: http://www.pubmedcentral.nih.gov/articlerender.fcgi?artid=2612277&tool=pmcentrez&rendertype=abstract [Accessed August 6, 2013].

MacMicking, J.D., 2012. Interferon-inducible effector mechanisms in cell-autonomous immunity. *Nature reviews. Immunology*, 12(5), pp.367–82. Available at: http://www.pubmedcentral.nih.gov/articlerender.fcgi?artid=4150610&tool=pmcentrez&rendertype=abstract [Accessed December 9, 2014].

Man, S.M., Karki, R., Malireddi, R.K.S., Neale, G., Vogel, P., Yamamoto, M., Lamkanfi, M. & Kanneganti, T., 2015. The transcription factor IRF1 and guanylate-binding proteins target activation of the AIM2 inflammasome by Francisella infection. *Nature immunology*, 16(5), pp.467–75. Available at: http://dx.doi.org/10.1038/ni.3118.

Man, S.M., Karki, R., Sasai, M., Place, D.E., Kesavardhana, S., Temirov, J., Frase, S., Zhu, Q., Malireddi, R.K.S., Kuriakose, T., et al., 2016. IRGB10 Liberates Bacterial Ligands for Sensing by the AIM2 and Caspase-11-NLRP3 Inflammasomes. *Cell*, 167(2), p.382–396.e17. Available at: http://linkinghub.elsevier.com/retrieve/pii/S0092867416312454.

Mandal, P., Berger, S.B., Pillay, S., Moriwaki, K., Huang, C., Guo, H., Lich, J.D., Finger, J., Kasparcova, V., Votta, B., et al., 2014. RIP3 Induces Apoptosis Independent of Pronecrotic Kinase Activity. *Molecular Cell*, 56(4), pp.481–495. Available at: http://dx.doi.org/10.1016/j.molcel.2014.10.021.

Martin, C.J., Peters, K.N. & Behar, S.M., 2014. Macrophages clean up: Efferocytosis and microbial control. *Current Opinion in Microbiology*, 17(1), pp.17–23. Available at: http://dx.doi.org/10.1016/j.mib.2013.10.007.

Mascarenhas, D.P.A., Cerqueira, D.M., Pereira, M.S.F., Castanheira, F.V.S., Fernandes, T.D., Manin, G.Z., Cunha, L.D. & Zamboni, D.S., 2017. Inhibition of caspase-1 or gasdermin-D enable caspase-8 activation in the Naip5/NLRC4/ASC inflammasome. *PLoS Pathogens*, 13(8), pp.1–28.

Menon, M.B., Gropengießer, J., Fischer, J., Novikova, L., Deuretzbacher, A., Lafera, J., Schimmeck, H., Czymmeck, N., Ronkina, N., Kotlyarov, A., et al., 2017. p38MAPK/MK2-dependent phosphorylation controls cytotoxic RIPK1 signalling in inflammation and infection. *Nature Cell Biology*, 19(10), pp.1248–1259. Available at: http://www.nature.com/doifinder/10.1038/ncb3614.

Meunier, E. & Broz, P., 2014. Interferon-Induced Guanylate-Binding Proteins Promote Cytosolic Lipopolysaccharide Detection by Caspase-11. *DNA and Cell Biology*, 34(1), pp.1–5. Available at: http://www.ncbi.nlm.nih.gov/pubmed/25347553 [Accessed January 18, 2015].

Meunier, E., Dick, M.S., Dreier, R.F., Schürmann, N., Kenzelmann Broz, D., Warming, S., Roose-Girma, M., Bumann, D., Kayagaki, N., Takeda, K., et al., 2014. Caspase-11 activation requires lysis of pathogen-containing vacuoles by IFN-induced GTPases. *Nature*, 509(7500), pp.366–70. Available at: http://www.nature.com/doifinder/10.1038/nature13157%5Cnhttp://www.ncbi.nlm.nih.gov/pubmed/24739961 [Accessed April 16, 2014].

Meunier, E., Wallet, P., Dreier, R.F., Costanzo, S., Anton, L., Rühl, S., Dussurgey, S., Dick, M.S., Kistner, A., Rigard, M., et al., 2015. Guanylate-binding proteins promote activation of the AIM2 inflammasome during infection with Francisella novicida. *Nature immunology*, 16(5), pp.476–84. Available at: http://www.pubmedcentral.nih.gov/articlerender.fcgi?artid=4568307&tool=pmcentrez&rendertype=abstract.

Meylan, E., Burns, K., Hofmann, K., Blancheteau, V., Martinon, F., Kelliher, M. & Tschopp, J., 2004. RIP1 is an essential mediator of Toll-like receptor 3-induced NF κB activation. *Nature Immunology*, 5(5), pp.503–507.

Miao, E. a, Leaf, I. a, Treuting, P.M., Mao, D.P., Dors, M., Sarkar, A., Warren, S.E., Wewers, M.D. & Aderem, A., 2010. Caspase-1-induced pyroptosis is an innate immune effector mechanism against intracellular bacteria. *Nature immunology*, 11(12), pp.1136–42. Available at: http://www.pubmedcentral.nih.gov/articlerender.fcgi?artid=3058225&tool=pmcentrez&rendertype=abstract [Accessed September 19, 2013].

Micheau, O. & Tschopp, J., 2002. Induction of TNF Receptor I- Mediated Apoptosis via Two Sequential Signaling Complexes. , 114, pp.181–190.

Micheau, O. & Tschopp, J., 2003. Induction of TNF receptor I-mediated apoptosis via two sequential signaling complexes. *Cell*, 114(2), pp.181–190.

Mihaly, S.R., Ninomiya-Tsuji, J. & Morioka, S., 2014. TAK1 control of cell death. *Cell death and differentiation*, 21(11), pp.1667–76. Available at: http://dx.doi.org/10.1038/cdd.2014.123.

Monack, D.M., Mecsas, J., Ghori, N. & Falkow, S., 1997. Yersinia signals macrophages to undergo apoptosis and YopJ is necessary for this cell death. *Proceedings of the National Academy of Sciences of the United States of America*, 94(19), pp.10385–90. Available at: http://www.ncbi.nlm.nih.gov/pubmed/9294220.

Monroe, K.M., McWhirter, S.M. & Vance, R.E., 2009. Identification of host cytosolic sensors and bacterial factors regulating the type I interferon response to Legionella pneumophila. *PLoS pathogens*, 5(11), p.e1000665. Available at: http://www.pubmedcentral.nih.gov/articlerender.fcgi?artid=2773930&tool=pmcentrez&rendertype=abstract [Accessed August 7, 2013].

Montminy, S.W., Khan, N., McGrath, S., Walkowicz, M.J., Sharp, F., Conlon, J.E.,

Fukase, K., Kusumoto, S., Sweet, C., Miyake, K., et al., 2006. Virulence factors of Yersinia pestis are overcome by a strong lipopolysaccharide response. *Nature Immunology*, 7(10), pp.1066–1073. Available at: http://www.nature.com/doifinder/10.1038/ni1386.

Morioka, S., Broglie, P., Omori, E., Ikeda, Y., Takaesu, G., Matsumoto, K. & Ninomiya-Tsuji, J., 2014. TAK1 kinase switches cell fate from apoptosis to necrosis following TNF stimulation. *Journal of Cell Biology*, 204(4), pp.607–623.

Mostafavi, S., Yoshida, H., Moodley, D., LeBoité, H., Rothamel, K., Raj, T., Ye, C.J., Chevrier, N., Zhang, S.-Y., Feng, T., et al., 2016. Parsing the Interferon Transcriptional Network and Its Disease Associations. *Cell*, 164(3), pp.564–578. Available at: http://ac.els-cdn.com/S0092867415016967/1-s2.0-S0092867415016967-main.pdf?_tid=3ee24cc6-21f9-11e6-a264-00000aab0f02&acdnat=1464126686_c131a791efdf0ac87d496f84bc88c091.

Mostafavi, S., Yoshida, H., Moodley, D., Leboité, H., Rothamel, K., Raj, T., Ye, C.J., Chevrier, N., Zhang, S.-Y.Y., Feng, T., et al., 2016. Parsing the Interferon Transcriptional Network and Its Disease Associations. *Cell*, 164(3), pp.564–578. Available at: http://ac.els-cdn.com/S0092867415016967/1-s2.0-S0092867415016967-main.pdf?_tid=3ee24cc6-21f9-11e6-a264-00000aab0f02&acdnat=1464126686_c131a791efdf0ac87d496f84bc88c091.

Murphy, J.M., Czabotar, P.E., Hildebrand, J.M., Lucet, I.S., Zhang, J.G., Alvarez-Diaz, S., Lewis, R., Lalaoui, N., Metcalf, D., Webb, A.I., et al., 2013. The pseudokinase MLKL mediates necroptosis via a molecular switch mechanism. *Immunity*, 39(3), pp.443–453.

Nash, T.W., Ubby, D.M. & Horwitz, M. a, 1984. Interaction between the Legionnaires ' Disease Bacterium (Legionella pneumophila) and Human Alveolar Macrophages. *Journal of clinical investigations*, 74, pp.771–782. Available at: http://dx.doi.org/10.1172/JCI111493.

Newton, K., Dugger, D.L., Maltzman, A., Greve, J.M., Hedehus, M., Martin-McNulty, B., Carano, R.A.D., Cao, T.C., van Bruggen, N., Bernstein, L., et al., 2016. RIPK3 deficiency or catalytically inactive RIPK1 provides greater benefit than MLKL deficiency in mouse models of inflammation and tissue injury. *Cell death and differentiation*, 23(9), pp.1565–76. Available at: http://www.ncbi.nlm.nih.gov/pubmed/27177019.

Newton, K., Sun, X. & Dixit, V.M., 2004. Kinase RIP3 is dispensable for normal NF-kappa Bs, signaling by the B-cell and T-cell receptors, tumor necrosis factor receptor 1, and Toll-like receptors 2 and 4. *Molecular and cellular biology*, 24(4), pp.1464–1469. Available at: http://mcb.asm.org/content/24/4/1464.full.pdf.

Newton, K., Wickliffe, K.E., Maltzman, A., Dugger, D.L., Strasser, A., Pham, V.C., Lill, J.R., Roose-Girma, M., Warming, S., Solon, M., et al., 2016. RIPK1 inhibits ZBP1-driven necroptosis during development. *Nature*, 540(7631), pp.129–133. Available at: http://dx.doi.org/10.1038/nature20559.

Nishio, A., Noguchi, Y., Sato, T., Naruse, T.K., Kimura, A., Takagi, A. & Kitamura, K., 2014. A DFNA5 mutation identified in japanese families with autosomal dominant

hereditary hearing loss. *Annals of Human Genetics*, 78(2), pp.83–91.

O'Neill, L.A.J., Golenbock, D. & Bowie, A.G., 2013. The history of Toll-like receptors - redefining innate immunity. *Nature reviews. Immunology*, 13(6), pp.453–60. Available at: http://dx.doi.org/10.1038/nri3446.

Oberst, A., Dillon, C.P., Weinlich, R., McCormick, L.L., Fitzgerald, P., Pop, C., Hakem, R., Salvesen, G.S. & Green, D.R., 2011. Catalytic activity of the caspase-8–FLIPL complex inhibits RIPK3-dependent necrosis. *Nature*, 471(7338), pp.363–367. Available at: http://dx.doi.org/10.1038/nature09852.

Oblak, A. & Jerala, R., 2015. The molecular mechanism of species-specific recognition of lipopolysaccharides by the MD-2/TLR4 receptor complex. *Molecular Immunology*, 63(2), pp.134–142.

Omori, E., Inagaki, M., Mishina, Y., Matsumoto, K. & Ninomiya-Tsuji, J., 2012. Epithelial transforming growth factor -activated kinase 1 (TAK1) is activated through two independent mechanisms and regulates reactive oxygen species. *Proceedings of the National Academy of Sciences*, 109(9), pp.3365–3370.

Ouyang, S., Song, X., Wang, Y., Ru, H., Shaw, N., Jiang, Y., Niu, F., Zhu, Y., Qiu, W., Parvatiyar, K., et al., 2012. Structural Analysis of the STING Adaptor Protein Reveals a Hydrophobic Dimer Interface and Mode of Cyclic di-GMP Binding. *Immunity*, 36(6), pp.1073–1086. Available at: http://dx.doi.org/10.1016/j.immuni.2012.03.019 [Accessed May 24, 2014].

Palchaudhuri, R., Lambrecht, M.J., Botham, R.C., Partlow, K.C., van Ham, T.J., Putt, K.S., Nguyen, L.T., Kim, S.H., Peterson, R.T., Fan, T.M., et al., 2015. A Small Molecule that Induces Intrinsic Pathway Apoptosis with Unparalleled Speed. *Cell Reports*, 13(9), pp.2027–2036.

Paquette, N., Conlon, J., Sweet, C., Rus, F., Wilson, L., Pereira, A., Rosadini, C. V, Goutagny, N., Weber, A.N.R., Lane, W.S., et al., 2012. Serine/threonine acetylation of TGFβ-activated kinase (TAK1) by Yersinia pestis YopJ inhibits innate immune signaling. *Proceedings of the National Academy of Sciences of the United States of America*, 109(31), pp.12710–5. Available at: http://www.ncbi.nlm.nih.gov/pubmed/22802624.

Park, B.S., Song, D.H., Kim, H.M., Choi, B., Lee, H. & Lee, J., 2009. The structural basis of lipopolysaccharide recognition by the TLR4 – MD-2 complex. *Nature*, 458(7242), pp.1191–1195. Available at: http://dx.doi.org/10.1038/nature07830.

Park, J.M., Greten, F.R., Li, Z.-W. & Karin, M., 2002. Macrophage Apoptosis by Anthrax Lethal Factor Through p38 MAP Kinase Inhibition. *Science*, 297(5589), pp.2048–2051. Available at: http://www.sciencemag.org/cgi/doi/10.1126/science.1073163.

Park, J.M., Greten, F.R., Wong, A., Westrick, R.J., Arthur, J.S.C., Otsu, K., Hoffmann, A., Montminy, M. & Karin, M., 2005. Signaling pathways and genes that inhibit pathogen-induced macrophage apoptosis - CREB and NF-κB as key regulators. *Immunity*, 23(3), pp.319–329.

Peterson, L.W., Philip, N.H., DeLaney, A., Wynosky-Dolfi, M.A., Asklof, K., Gray, F.,

Choa, R., Bjanes, E., Buza, E.L., Hu, B., et al., 2017. RIPK1-dependent apoptosis bypasses pathogen blockade of innate signaling to promote immune defense. *The Journal of Experimental Medicine*, p.jem.20170347. Available at: http://www.jem.org/lookup/doi/10.1084/jem.20170347.

Peterson, L.W., Philip, N.H., Dillon, C.P., Bertin, J., Gough, P.J., Green, D.R. & Brodsky, I.E., 2016a. Cell-Extrinsic TNF Collaborates with TRIF Signaling To Promote Yersinia-Induced Apoptosis. *Journal of immunology (Baltimore, Md. : 1950)*, 197(10), pp.4110–4117. Available at: http://www.jimmunol.org/lookup/doi/10.4049/jimmunol.1601294.

Peterson, L.W., Philip, N.H., Dillon, C.P., Bertin, J., Gough, P.J., Green, D.R. & Brodsky, I.E., 2016b. Cell-Extrinsic TNF Collaborates with TRIF Signaling To Promote Yersinia -Induced Apoptosis. *The Journal of Immunology*, 197(10), pp.4110–4117. Available at: http://www.jimmunol.org/lookup/doi/10.4049/jimmunol.1601294.

Philip, N.H., Dillon, C.P., Snyder, A.G., Fitzgerald, P., Wynosky-Dolfi, M.A., Zwack, E.E., Hu, B., Fitzgerald, L., Mauldin, E.A., Copenhaver, A.M., et al., 2014. Caspase-8 mediates caspase-1 processing and innate immune defense in response to bacterial blockade of NF- B and MAPK signaling. *Proceedings of the National Academy of Sciences*, 111(20), pp.7385–90. Available at: http://www.pnas.org/cgi/doi/10.1073/pnas.1403252111.

Pierini, R., Juruj, C., Perret, M., Jones, C.L., Mangeot, P., Weiss, D.S. & Henry, T., 2012. AIM2/ASC triggers caspase-8-dependent apoptosis in Francisella-infected caspase-1-deficient macrophages. *Cell death and differentiation*, 19(10), pp.1709–21. Available at: http://www.pubmedcentral.nih.gov/articlerender.fcgi?artid=3438500&tool=pmcentrez&rendertype=abstract [Accessed January 26, 2014].

Pilla-Moffett, D., Barber, M.F., Taylor, G.A. & Coers, J., 2016. Interferon-Inducible GTPases in Host Resistance, Inflammation and Disease. *Journal of Molecular Biology*, 428(17), pp.3495–3513. Available at: http://dx.doi.org/10.1016/j.jmb.2016.04.032.

Pilla, D.M., Hagar, J.A., Haldar, A.K., Mason, A.K., Degrandi, D., Pfeffer, K., Ernst, R.K., Yamamoto, M., Miao, E.A. & Coers, J., 2014a. Guanylate binding proteins promote caspase-11-dependent pyroptosis in response to cytoplasmic LPS. *Proceedings of the National Academy of Sciences of the United States of America*, 111(16), pp.6046–51. Available at: http://www.ncbi.nlm.nih.gov/pubmed/24715728 [Accessed April 11, 2014].

Pilla, D.M., Hagar, J.A., Haldar, A.K., Mason, A.K., Degrandi, D., Pfeffer, K., Ernst, R.K., Yamamoto, M., Miao, E.A. & Coers, J., 2014b. Guanylate binding proteins promote caspase-11 – dependent pyroptosis in response to cytoplasmic LPS. *Proceedings of the National Academy of Sciences of the United States of America*.

Plumlee, C.R., Lee, C., Beg, A. a., Decker, T., Shuman, H. a. & Schindler, C., 2009. Interferons direct an effective innate response to Legionella pneumophila infection. *The Journal of biological chemistry*, 284(44), pp.30058–66. Available at:

http://www.ncbi.nlm.nih.gov/pubmed/19720834.

Rajput, A., Kovalenko, A., Bogdanov, K., Yang, S.-H., Kang, T.-B., Kim, J.-C., Du, J. & Wallach, D., 2011. RIG-I RNA helicase activation of IRF3 transcription factor is negatively regulated by caspase-8-mediated cleavage of the RIP1 protein. *Immunity*, 34(3), pp.340–51. Available at: http://www.ncbi.nlm.nih.gov/pubmed/21419663 [Accessed May 24, 2014].

Randow, F., MacMicking, J.D. & James, L.C., 2013. Cellular Self-Defense : How Cell-Autonomous Immunity Protects Against Pathogens. , 701(May), pp.701–707.

Raoult, D., Mouffok, N., Bitam, I., Piarroux, R. & Drancourt, M., 2013. Plague: History and contemporary analysis. *Journal of Infection*, 66(1), pp.18–26. Available at: http://dx.doi.org/10.1016/j.jinf.2012.09.010.

Rathinam, V.A.K., Jiang, Z., Waggoner, S.N., Sharma, S., Cole, L.E., Waggoner, L., Vanaja, S.K., Monks, B.G., Ganesan, S., Latz, E., et al., 2010. The AIM2 inflammasome is essential for host defense against cytosolic bacteria and DNA viruses. *Nature immunology*, 11(5), pp.395–402. Available at: http://dx.doi.org/10.1038/ni.1864.

Ratner, D., Orning, M.P.A., Starheim, K.K., Marty-Roix, R., Proulx, M.K., Goguen, J.D. & Lien, E., 2016. Manipulation of Interleukin-1β and Interleukin-18 Production by Yersinia pestis Effectors YopJ and YopM and Redundant Impact on Virulence. *The Journal of biological chemistry*, 291(19), pp.9894–905. Available at: http://www.ncbi.nlm.nih.gov/pubmed/26884330.

Rebeil, R., Ernst, R.K., Gowen, B.B., Miller, S.I. & Hinnebusch, B.J., 2004. Variation in lipid A structure in the pathogenic yersiniae. *Molecular Microbiology*, 52(5), pp.1363–1373.

Rebsamen, M., Heinz, L.X., Meylan, E., Michallet, M.-C., Schroder, K., Hofmann, K., Vazquez, J., Benedict, C.A. & Tschopp, J., 2009. DAI/ZBP1 recruits RIP1 and RIP3 through RIP homotypic interaction motifs to activate NF-κB. *EMBO reports*, 10(8), pp.916–922. Available at: http://embor.embopress.org/cgi/doi/10.1038/embor.2009.109.

Reddick, L.E. & Alto, N.M., 2014. Bacteria fighting back: How pathogens target and subvert the host innate immune system. *Molecular Cell*, 54(2), pp.321–328.

Ren, T., Zamboni, D.S., Roy, C.R., Dietrich, W.F. & Vance, R.E., 2006. Flagellin-deficient Legionella mutants evade caspase-1- and Naip5-mediated macrophage immunity. *PLoS pathogens*, 2(3), p.e18. Available at: http://www.ncbi.nlm.nih.gov/pubmed/16552444.

Rogers, C., Fernandes-Alnemri, T., Mayes, L., Alnemri, D., Cingolani, G. & Alnemri, E.S., 2017. Cleavage of DFNA5 by caspase-3 during apoptosis mediates progression to secondary necrotic/pyroptotic cell death. *Nature communications*, 8, p.14128. Available at: http://www.nature.com/doifinder/10.1038/ncomms14128.

Rongvaux, A., Jackson, R., Harman, C.C.D., Li, T., West, A.P., De Zoete, M.R., Wu, Y., Yordy, B., Lakhani, S.A., Kuan, C.-Y.Y., et al., 2014. Apoptotic caspases prevent the induction of type i interferons by mitochondrial DNA. *Cell*, 159(7), pp.1563–

1577. Available at: http://www.ncbi.nlm.nih.gov/pubmed/25525875.

Roy, C.R. & Tilney, L.G., 2002. The road less traveled: Transport of Legionella to the endoplasmic reticulum. *Journal of Cell Biology*, 158(3), pp.415–419. Available at: http://www.pubmedcentral.nih.gov/articlerender.fcgi?artid=2173838&tool=pmcentrez&rendertype=abstract [Accessed December 21, 2013].

Saeki, N., Usui, T., Aoyagi, K., Kim, D.H., Sato, M., Mabuchi, T., Yanagihara, K., Ogawa, K., Sakamoto, H., Yoshida, T., et al., 2009. Distinctive expression and function of four GSDM family genes (GSDMA-D) in normal and malignant upper gastrointestinal epithelium. *Genes, Chromosomes and Cancer*, 48(3), pp.261–271. Available at: http://doi.wiley.com/10.1002/gcc.20636 [Accessed November 19, 2017].

Sagulenko, V., Thygesen, S.J., Sester, D.P., Idris, A., Cridland, J.A., Vajjhala, P.R., Roberts, T.L., Schroder, K., Vince, J.E., Hill, J.M., et al., 2013. AIM2 and NLRP3 inflammasomes activate both apoptotic and pyroptotic death pathways via ASC. *Cell Death Differ*, 20(9), pp.1149–1160. Available at: http://www.ncbi.nlm.nih.gov/pubmed/23645208 [Accessed February 8, 2014].

Sato, S., Sanjo, H., Takeda, K., Ninomiya-Tsuji, J., Yamamoto, M., Kawai, T., Matsumoto, K., Takeuchi, O. & Akira, S., 2005. Essential function for the kinase TAK1 in innate and adaptive immune responses. *Nature Immunology*, 6(11), pp.1087–1095. Available at: http://www.nature.com/doifinder/10.1038/ni1255.

Sborgi, L., Rühl, S., Mulvihill, E., Pipercevic, J., Heilig, R., Stahlberg, H., Farady, C.J., Müller, D.J., Broz, P. & Hiller, S., 2016. GSDMD membrane pore formation constitutes the mechanism of pyroptotic cell death. *The EMBO journal*, 35(16), pp.1766–78. Available at: http://emboj.embopress.org/lookup/doi/10.15252/embj.201694696%5Cnpapers3://publication/doi/10.15252/embj.201694696.

Schauvliege, R., Vanrobaeys, J., Schotte, P. & Beyaert, R., 2002. Caspase-11 gene expression in response to lipopolysaccharide and interferon-gamma requires nuclear factor-kappa B and signal transducer and activator of transcription (STAT) 1. *The Journal of biological chemistry*, 277(44), pp.41624–30. Available at: http://www.ncbi.nlm.nih.gov/pubmed/12198138 [Accessed November 11, 2013].

Schneider, W.M., Chevillotte, M.D. & Rice, C.M., 2014. Interferon-stimulated genes: a complex web of host defenses. *Annual review of immunology*, 32, pp.513–45. Available at: http://www.ncbi.nlm.nih.gov/pubmed/24555472.

Selleck, E.M., Fentress, S.J., Beatty, W.L., Degrandi, D., Pfeffer, K., Virgin, H.W., Macmicking, J.D. & Sibley, L.D., 2013. Guanylate-binding protein 1 (Gbp1) contributes to cell-autonomous immunity against Toxoplasma gondii. *PLoS pathogens*, 9(4), p.e1003320. Available at: http://www.pubmedcentral.nih.gov/articlerender.fcgi?artid=3635975&tool=pmcentrez&rendertype=abstract [Accessed January 19, 2014].

Shenoy, A.R., Wellington, D.A., Kumar, P., Kassa, H., Booth, C.J., Cresswell, P. & MacMicking, J.D., 2012. GBP5 promotes NLRP3 inflammasome assembly and immunity in mammals. *Science*, 336(6080), pp.481–485. Available at:

http://www.ncbi.nlm.nih.gov/pubmed/22461501%5Cnhttp://www.sciencemag.org/content/336/6080/481.full.pdf [Accessed January 27, 2014].

Shi, J., Gao, W. & Shao, F., 2017. Pyroptosis: Gasdermin-Mediated Programmed Necrotic Cell Death. *Trends in Biochemical Sciences*, 42(4), pp.245–254. Available at: http://dx.doi.org/10.1016/j.tibs.2016.10.004.

Shi, J., Zhao, Y., Wang, K., Shi, X., Wang, Y., Huang, H., Zhuang, Y., Cai, T., Wang, F. & Shao, F., 2015. Cleavage of GSDMD by inflammatory caspases determines pyroptotic cell death. *Nature*, 526(7575), pp.660–5. Available at: http://www.ncbi.nlm.nih.gov/pubmed/26375003.

Shi, J., Zhao, Y., Wang, Y., Gao, W., Ding, J., Li, P., Hu, L. & Shao, F., 2014. Inflammatory caspases are innate immune receptors for intracellular LPS. *Nature*, 514(7521), pp.187–92. Available at: http://www.nature.com/doifinder/10.1038/nature13683 [Accessed August 6, 2014].

Shim, H.K., Kim, J.Y., Kim, M.J., Sim, H.S., Park, D.W., Sohn, J.W. & Kim, M.J., 2009. Legionella lipoprotein activates toll-like receptor 2 and induces cytokine production and expression of costimulatory molecules in peritoneal macrophages. *Experimental & molecular medicine*, 41(10), pp.687–94. Available at: http://www.pubmedcentral.nih.gov/articlerender.fcgi?artid=2772971&tool=pmcentrez&rendertype=abstract [Accessed December 26, 2013].

Shin, S. & Roy, C.R., 2008. Host cell processes that influence the intracellular survival of Legionella pneumophila. *Cellular Microbiology*, 10(6), pp.1209–1220. Available at: http://www.ncbi.nlm.nih.gov/pubmed/18363881 [Accessed December 26, 2013].

St-Laurent, J., Turmel, V., Boulet, L.P. & Bissonnette, E., 2009. Alveolar macrophage subpopulations in bronchoalveolar lavage and induced sputum of asthmatic and control subjects. *Journal of Asthma*, 46(1), pp.1–8.

Stetson, D.B., Ko, J.S., Heidmann, T. & Medzhitov, R., 2008. Trex1 prevents cell-intrinsic initiation of autoimmunity. *Cell*, 134(4), pp.587–98. Available at: http://www.ncbi.nlm.nih.gov/pubmed/18724932.

Sun, L., Wu, J., Du, F., Chen, X. & Chen, Z.J., 2013. Cyclic GMP-AMP synthase is a cytosolic DNA sensor that activates the type I interferon pathway. *Science (New York, N.Y.)*, 339(6121), pp.786–91. Available at: http://www.ncbi.nlm.nih.gov/pubmed/23258413.

Sutterwala, F.S., Haasken, S. & Cassel, S.L., 2014. Mechanism of NLRP3 inflammasome activation. *Annals of the New York Academy of Sciences*, 1319(1), pp.82–95. Available at: http://www.ncbi.nlm.nih.gov/pubmed/24840700 [Accessed July 23, 2014].

Taabazuing, C.Y., Okondo, M.C. & Bachovchin, D.A., 2017. Pyroptosis and Apoptosis Pathways Engage in Bidirectional Crosstalk in Monocytes and Macrophages. *Cell Chemical Biology*, 24(4), p.507–514.e4. Available at: http://dx.doi.org/10.1016/j.chembiol.2017.03.009.

Takeuchi, O. & Akira, S., 2010. Pattern recognition receptors and inflammation. *Cell*, 140(6), pp.805–20. Available at: http://www.ncbi.nlm.nih.gov/pubmed/20303872

[Accessed August 9, 2013].

Talanian, R. V., Quinlan, C., Trautz, S., Hackett, M.C., Mankovich, J.A., Banach, D., Ghayur, T., Brady, K.D., Wong, W.W., Talanian, R. V., et al., 1997. Substrate specificities of caspase family proteases. *Journal of Biological Chemistry*, 272(15), pp.9677–9682. Available at: http://www.jbc.org/cgi/doi/10.1074/jbc.272.15.9677 [Accessed June 19, 2014].

Tan, Y. & Kagan, J.C.C., 2014. A cross-disciplinary perspective on the innate immune responses to bacterial lipopolysaccharide. *Molecular Cell*, 54(2), pp.212–223. Available at: http://linkinghub.elsevier.com/retrieve/pii/S1097276514002172 [Accessed April 24, 2014].

Tang, M., Wei, X., Guo, Y., Breslin, P., Zhang, S., Zhang, S., Wei, W., Xia, Z., Diaz, M., Akira, S., et al., 2008. TAK1 is required for the survival of hematopoietic cells and hepatocytes in mice. *The Journal of experimental medicine*, 205(7), pp.1611–9. Available at: http://www.ncbi.nlm.nih.gov/pubmed/18573910.

Taniguchi, T. & Takaoka, a, 2001. A weak signal for strong responses: interferon-alpha/beta revisited. *Nature reviews. Molecular cell biology*, 2(May), pp.378–386.

Tateda, K., Moore, T.A., Newstead, M.W., Tsai, W.A.N.C., Zeng, X., Deng, J.C., Chen, G., Yamaguchi, K., Standiford, T.J. & Tsai, W.A.N.C., 2001. Chemokine-Dependent Neutrophil Recruitment in a Murine Model of Legionella Pneumonia : Potential Role of Neutrophils as Immunoregulatory Cells Chemokine-Dependent Neutrophil Recruitment in a Murine Model of Legionella Pneumonia : Potential Role of Neutrop. *Infection and immunity*, 69(4), pp.2017–2024.

Taylor, R.C., Cullen, S.P. & Martin, S.J., 2008. Apoptosis: controlled demolition at the cellular level. *Nature reviews. Molecular cell biology*, 9(3), pp.231–241.

Tenev, T., Bianchi, K., Darding, M., Broemer, M., Langlais, C., Wallberg, F., Zachariou, A., Lopez, J., MacFarlane, M., Cain, K., et al., 2011. The Ripoptosome, a Signaling Platform that Assembles in Response to Genotoxic Stress and Loss of IAPs. *Molecular Cell*, 43(3), pp.432–448.

Thornberry, N.A. & Molineaux, S.M., 1995. Interleukin-1βconverting enzyme: A novel cysteine protease required for IL-1β production and implicated in programmed cell death. *Protein Science*, 4(1), pp.3–12.

Tiwari, S., Choi, H.-P., Matsuzawa, T., Pypaert, M. & MacMicking, J.D., 2009. Targeting of the GTPase Irgm1 to the phagosomal membrane via PtdIns(3,4)P(2) and PtdIns(3,4,5)P(3) promotes immunity to mycobacteria. *Nature immunology*, 10(8), pp.907–17. Available at: http://dx.doi.org/10.1038/ni.1759.

Tovey, M.G., Streuli, M., Gresser, I., Gugenheim, J., Blanchard, B., Guymarho, J., Vignaux, F. & Gigou, M., 1987. Interferon messenger RNA is produced constitutively in the organs of normal individuals. *Proceedings of the National Academy of Sciences of the United States of America*, 84(14), pp.5038–42. Available at: http://www.pubmedcentral.nih.gov/articlerender.fcgi?artid=305242&tool=pmcentrez&rendertype=abstract.

Traver, M.K., Henry, S.C., Cantillana, V., Oliver, T., Hunn, J.P., Howard, J.C., Beer, S., Pfeffer, K., Coers, J. & Taylor, G. a, 2011. Immunity-related GTPase M (IRGM) proteins influence the localization of guanylate-binding protein 2 (GBP2) by modulating macroautophagy. *The Journal of biological chemistry*, 286(35), pp.30471–80. Available at: http://www.pubmedcentral.nih.gov/articlerender.fcgi?artid=3162407&tool=pmcentrez&rendertype=abstract [Accessed May 27, 2014].

Upton, J.W., Kaiser, W.J. & Mocarski, E.S., 2012. DAI/ZBP1/DLM-1 Complexes with RIP3 to Mediate Virus-Induced Programmed Necrosis that Is Targeted by Murine Cytomegalovirus vIRA. *Cell Host & Microbe*, 11(3), pp.290–297. Available at: http://dx.doi.org/10.1016/j.chom.2012.01.016.

Upton, J.W., Kaiser, W.J. & Mocarski, E.S., 2010. Virus inhibition of RIP3-dependent necrosis. *Cell Host and Microbe*, 7(4), pp.302–313. Available at: http://dx.doi.org/10.1016/j.chom.2010.03.006.

Vanaja, S.K., Rathinam, V.A.K. & Fitzgerald, K.A., 2015. Mechanisms of inflammasome activation: Recent advances and novel insights. *Trends in Cell Biology*, 25(5), pp.308–315. Available at: http://dx.doi.org/10.1016/j.tcb.2014.12.009.

Vance, R.E., 2010. Immunology taught by bacteria. *Journal of clinical immunology*, 30(4), pp.507–11. Available at: http://www.pubmedcentral.nih.gov/articlerender.fcgi?artid=2900594&tool=pmcentrez&rendertype=abstract [Accessed October 1, 2013].

Vanlangenakker, N., Vanden Berghe, T., Bogaert, P., Laukens, B., Zobel, K., Deshayes, K., Vucic, D., Fulda, S., Vandenabeele, P. & Bertrand, M.J.M., 2011. cIAP1 and TAK1 protect cells from TNF-induced necrosis by preventing RIP1/RIP3-dependent reactive oxygen species production. *Cell Death and Differentiation*, 18(4), pp.656–665. Available at: http://www.nature.com/doifinder/10.1038/cdd.2010.138.

van de Veerdonk, F.L., Netea, M.G., Dinarello, C.A. & Joosten, L.A.B., 2011. Inflammasome activation and IL-1β and IL-18 processing during infection. *Trends in immunology*, 32(3), pp.110–6. Available at: http://dx.doi.org/10.1016/j.it.2011.01.003.

Viboud, G.I. & Bliska, J.B., 2005. Yersinia outer proteins: role in modulation of host cell signaling responses and pathogenesis. *Annual review of microbiology*, 59(1), pp.69–89. Available at: http://www.annualreviews.org/doi/10.1146/annurev.micro.59.030804.121320.

Vink, P.M., Smout, W.M., Driessen-Engels, L.J., de Bruin, A.M., Delsing, D., Krajnc-Franken, M.A., Jansen, A.J., Rovers, E.F., van Puijenbroek, A.A., Kaptein, A., et al., 2013. In vivo knockdown of TAK1 accelerates bone marrow proliferation/differentiation and induces systemic inflammation. *PloS one*, 8(3), p.e57348. Available at: http://www.ncbi.nlm.nih.gov/pubmed/23505428.

Vogel, S.N. & Fertsch, D., 1987. Macrophages from endotoxin-hyporesponsive (Lpsd) C3H/HeJ mice are permissive for vesicular stomatitis virus because of reduced levels of endogenous interferon: possible mechanism for natural resistance to virus

infection. *Journal of Virology*, 61(3), pp.812–818. Available at: http://www.ncbi.nlm.nih.gov/pubmed/2433468.

Wallach, D., Kang, T.-B., Dillon, C.P. & Green, D.R., 2016. Programmed necrosis in inflammation: Toward identification of the effector molecules. *Science (New York, N.Y.)*, 352(6281), p.aaf2154. Available at: http://www.ncbi.nlm.nih.gov/pubmed/27034377.

Wandel, M.P., Pathe, C., Werner, E.I., Ellison, C.J., Boyle, K.B., von der Malsburg, A., Rohde, J. & Randow, F., 2017. GBPs Inhibit Motility of Shigella flexneri but Are Targeted for Degradation by the Bacterial Ubiquitin Ligase IpaH9.8. *Cell Host & Microbe*, 22(4), p.507–518.e5. Available at: http://linkinghub.elsevier.com/retrieve/pii/S1931312817303955.

Wang, J., Wu, D., Huang, D. & Lin, W., 2015. TAK1 inhibition-induced RIP1-dependent apoptosis in murine macrophages relies on constitutive TNF-α signaling and ROS production. *Journal of Biomedical Science*, 22(1), pp.1–13. Available at: http://dx.doi.org/10.1186/s12929-015-0182-7%5Cnhttp://dx.doi.org/10.1186/s12929-015-0182-7%5Cnpapers3://publication/doi/10.1186/s12929-015-0182-7.

Wang, S., Miura, M., Jung, Y.K., Zhu, H., Gagliardini, V., Shi, L., Greenberg, A.H. & Yuan, J., 1996. Identification and characterization of Ich-3, a member of the interleukin-1beta converting enzyme (ICE)/Ced-3 family and an upstream regulator of ICE. *The Journal of biological chemistry*, 271(34), pp.20580–7. Available at: http://www.jbc.org/cgi/doi/10.1074/jbc.271.34.20580 [Accessed November 11, 2013].

Wang, S., Miura, M., Jung, Y.K., Zhu, H., Li, E. & Yuan, J., 1998. Murine caspase-11, an ICE-interacting protease, is essential for the activation of ICE. *Cell*, 92(4), pp.501–509.

Wang, Y., Gao, W., Shi, X., Ding, J., Liu, W., He, H., Wang, K. & Shao, F., 2017. Chemotherapy drugs induce pyroptosis through caspase-3 cleavage of a gasdermin. *Nature*, 547(7661), pp.99–103. Available at: http://www.nature.com/doifinder/10.1038/nature22393.

Wang, Y., Ning, X., Gao, P., Wu, S., Sha, M., Lv, M., Zhou, X., Gao, J., Fang, R., Meng, G., et al., 2017. Inflammasome Activation Triggers Caspase-1-Mediated Cleavage of cGAS to Regulate Responses to DNA Virus Infection. *Immunity*, 46(3), pp.393–404. Available at: http://linkinghub.elsevier.com/retrieve/pii/S1074761317300730.

Weng, D., Marty-Roix, R., Ganesan, S., Proulx, M.K., Vladimer, G.I., Kaiser, W.J., Mocarski, E.S., Pouliot, K., Chan, F.K.-M., Kelliher, M.A., et al., 2014. Caspase-8 and RIP kinases regulate bacteria-induced innate immune responses and cell death. *Proceedings of the National Academy of Sciences of the United States of America*, 111(20), pp.7391–6. Available at: http://www.pnas.org/cgi/doi/10.1073/pnas.1403477111 [Accessed September 9, 2014].

West, A.P., Khoury-Hanold, W., Staron, M., Tal, M.C., Pineda, C.M., Lang, S.M., Bestwick, M., Duguay, B.A., Raimundo, N., MacDuff, D.A., et al., 2015.

Mitochondrial DNA stress primes the antiviral innate immune response. *Nature*, 520(7548), pp.553–7. Available at: http://www.pubmedcentral.nih.gov/articlerender.fcgi?artid=4409480&tool=pmcentrez&rendertype=abstract.

Wright, E.K., Goodart, S.A., Growney, J.D., Hadinoto, V., Endrizzi, M.G., Long, E.M., Sadigh, K., Abney, A.L., Bernstein-hanley, I. & Dietrich, W.F., 2003. Naip5 Affects Host Susceptibility to the Intracellular Pathogen Legionella pneumophila. *Current Biology*, 13(2), pp.27–36.

Wu, J. & Chen, Z.J., 2014. Innate Immune Sensing and Signaling of Cytosolic Nucleic Acids. *Annual Review of Immunology*, 32(1), pp.461–488. Available at: http://www.annualreviews.org/doi/10.1146/annurev-immunol-032713-120156.

Wu, J., Powell, F., Larsen, N.A., Lai, Z., Byth, K.F., Read, J., Gu, R.F., Roth, M., Toader, D., Saeh, J.C., et al., 2013. Mechanism and in vitro pharmacology of TAK1 inhibition by (5 Z)-7-oxozeaenol. *ACS Chemical Biology*, 8(3), pp.643–650.

Wu, J., Sun, L., Chen, X., Du, F., Shi, H., Chen, C. & Chen, Z.J., 2013. Cyclic GMP-AMP is an endogenous second messenger in innate immune signaling by cytosolic DNA. *Science (New York, N.Y.)*, 339(6121), pp.826–30. Available at: http://www.ncbi.nlm.nih.gov/pubmed/23258412.

Xiao, T.S. & Fitzgerald, K. a, 2013. The cGAS-STING Pathway for DNA Sensing. *Molecular cell*, 51(2), pp.135–9. Available at: http://www.ncbi.nlm.nih.gov/pubmed/23870141 [Accessed August 6, 2013].

Xie, T., Peng, W., Liu, Y., Yan, C., Maki, J., Degterev, A., Yuan, J. & Shi, Y., 2013. Structural basis of RIP1 inhibition by necrostatins. *Structure*, 21(3), pp.493–499. Available at: http://dx.doi.org/10.1016/j.str.2013.01.016.

Yamamoto, M., Okuyama, M., Ma, J.S., Kimura, T., Kamiyama, N., Saiga, H., Ohshima, J., Sasai, M., Kayama, H., Okamoto, T., et al., 2012. A cluster of interferon-γ-inducible p65 GTPases plays a critical role in host defense against Toxoplasma gondii. *Immunity*, 37(2), pp.302–313. Available at: http://www.ncbi.nlm.nih.gov/pubmed/22795875 [Accessed May 5, 2014].

Yang, J., Zhao, Y. & Shao, F., 2015. Non-canonical activation of inflammatory caspases by cytosolic LPS in innate immunity. *Current Opinion in Immunology*, 32, pp.78–83. Available at: http://dx.doi.org/10.1016/j.coi.2015.01.007.

Yoshida, H., Okabe, Y., Kawane, K., Fukuyama, H. & Nagata, S., 2005. Lethal anemia caused by interferon-β produced in mouse embryos carrying undigested DNA. *Nature Immunology*, 6(1), pp.49–56. Available at: http://www.nature.com/doifinder/10.1038/ni1146.

You, Z., Savitz, S.I., Yang, J., Degterev, A., Yuan, J., Cuny, G.D., Moskowitz, M.A. & Whalen, M.J., 2008. Necrostatin-1 Reduces Histopathology and Improves Functional Outcome after Controlled Cortical Impact in Mice. *Journal of Cerebral Blood Flow & Metabolism*, 28(9), pp.1564–1573. Available at: http://journals.sagepub.com/doi/10.1038/jcbfm.2008.44.

Zanoni, I., Tan, Y., Gioia, M. Di, Broggi, A., Ruan, J., Shi, J., Donado, C.A., Shao, F.,

Wu, H., Springstead, J.R., et al., 2016. An endogenous caspase-11 ligand elicits interleukin-1 release from living dendritic cells. *Science*, 3036(April), pp.1–9.

Zanoni, I., Tan, Y., Gioia, M. Di, Springstead, J.R., Kagan, J.C. & Hyperactivation, I.P., 2017. By Capturing Inflammatory Lipids Released from Dying Cells , the Receptor CD14 Induces By Capturing Inflammatory Lipids Released from Dying Cells , the Receptor CD14 Induces. *Immunity*, 47(4), p.697–709.e3. Available at: https://doi.org/10.1016/j.immuni.2017.09.010.

Zhang, X., Shi, H., Wu, J., Zhang, X., Sun, L., Chen, C. & Chen, Z.J., 2013. Cyclic GMP-AMP containing mixed Phosphodiester linkages is an endogenous high-affinity ligand for STING. *Molecular Cell*, 51(2), pp.226–235. Available at: http://dx.doi.org/10.1016/j.molcel.2013.05.022 [Accessed April 29, 2014].

de Zoete, M.R., Palm, N.W., Zhu, S. & Flavell, R.A., 2014. Inflammasomes. *Cold Spring Harbor Perspectives in Biology*, 6(12), pp.a016287–a016287. Available at: http://cshperspectives.cshlp.org/lookup/doi/10.1101/cshperspect.a016287.

Zurney, J., Howard, K.E. & Sherry, B., 2007. Basal expression levels of IFNAR and Jak-STAT components are determinants of cell-type-specific differences in cardiac antiviral responses. *Journal of virology*, 81(24), pp.13668–13680.